

AD-A131 091

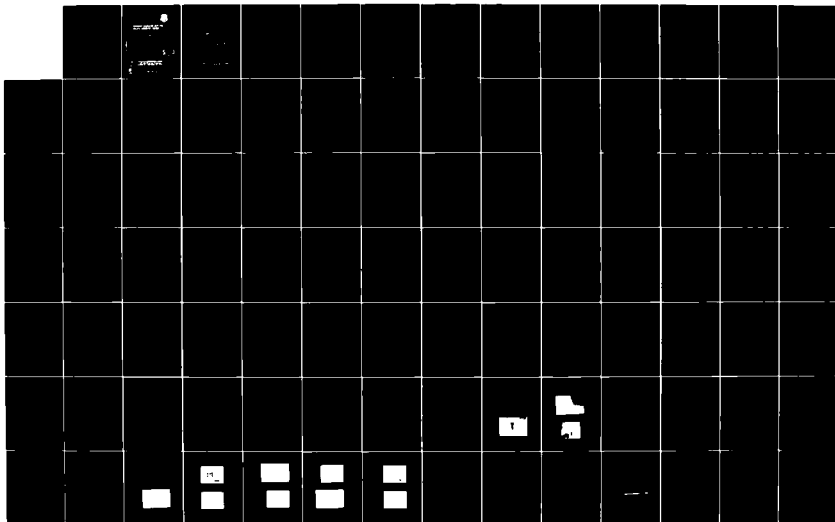
MICROWAVE INTERACTION WITH THIN MULTIPLE CONDUCTIVE  
COATINGS(U) ROME AIR DEVELOPMENT CENTER GRIFFISS AFB NY  
V M MARTIN MAR 83 RADC-TR-83-62

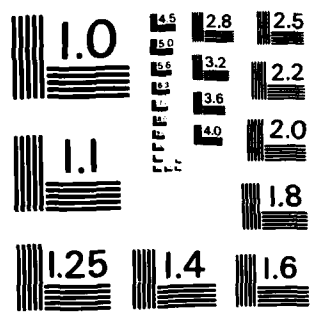
1/3

UNCLASSIFIED

F/G 11/3

NL





MICROCOPY RESOLUTION TEST CHART  
NATIONAL BUREAU OF STANDARDS-1963-A

SCIENCE AND TECHNOLOGY INFORMATION

ADA131091



UNCLASSIFIED

SECURITY CLASSIFICATION OF THIS PAGE (When Data Entered)

REPORT DOCUMENTATION PAGE		READ INSTRUCTIONS BEFORE COMPLETING FORM
1. REPORT NUMBER RADC-TR-83-62	2. GOVT ACCESSION NO. AD-A131091	3. RECIPIENT'S CATALOG NUMBER
4. TITLE (and Subtitle) MICROWAVE INTERACTION WITH THIN MULTIPLE CONDUCTIVE COATINGS		5. TYPE OF REPORT & PERIOD COVERED Final Technical Report Nov 81 - Nov 82
		6. PERFORMING ORG. REPORT NUMBER N/A
7. AUTHOR(s) Victor M. Martin		8. CONTRACT OR GRANT NUMBER(s) N/A
9. PERFORMING ORGANIZATION NAME AND ADDRESS United States Air Force Academy Colorado Springs CO 80840		10. PROGRAM ELEMENT, PROJECT, TASK AREA & WORK UNIT NUMBERS 62702F 23380403
11. CONTROLLING OFFICE NAME AND ADDRESS Rome Air Development Center (RBC) Griffiss AFB NY 13441		12. REPORT DATE March 1983
14. MONITORING AGENCY NAME & ADDRESS (if different from Controlling Office) Same		13. NUMBER OF PAGES 232
		15. SECURITY CLASS. (of this report) UNCLASSIFIED
		15a. DECLASSIFICATION/DOWNGRADING SCHEDULE N/A
16. DISTRIBUTION STATEMENT (of this Report)  Approved for public release; distribution unlimited.		
17. DISTRIBUTION STATEMENT (of the abstract entered in Block 20, if different from Report)  Same		
18. SUPPLEMENTARY NOTES RADC Project Engineer: Jacob Scherer (RBC)		
19. KEY WORDS (Continue on reverse side if necessary and identify by block number) Measurement Techniques                      Surface Currents Electromagnetic Radiation                      Surface Temperature Electromagnetic Compatibility                      Infrared Thermography                      Conductive Coatings		
20. ABSTRACT (Continue on reverse side if necessary and identify by block number) This report presents the analytic solution for the surface temperatures of the first layer of a system of N layers being exposed to microwave radiation. This provides for a correlation between surface temperatures and surface currents present in the system. The surface temperature is to be measured via infrared thermography. Thermography has been available for some time as an aid in determining		

UNCLASSIFIED

SECURITY CLASSIFICATION OF THIS PAGE (When Data Entered)

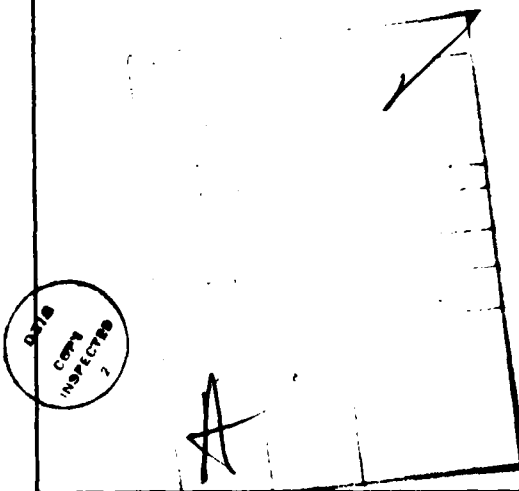
UNCLASSIFIED

SECURITY CLASSIFICATION OF THIS PAGE(When Data Entered)

temperature differentials. Burton, et al, have demonstrated that thermographic techniques can be used qualitatively to detect temperature differentials associated with Joule ( $I^2R$ ) heating from surface currents induced by incident electromagnetic waves on particular shapes. These surface currents result from the interaction of the conducting object with the incident electric field. The tangential component of the electric field with the object surface causes charge to migrate along the surface until electrical equilibrium is established. Thus, the rate of charge migration determines the surface current. Therefore, if the object has some finite resistivity, joule heating will be observed. The heating on the object surface causes surface temperature variations which may be detected with an infrared camera (thermography).

Observing surface heating directly on a highly conductive metallic surface such as aluminum is exceedingly difficult because of the small amount of energy deposited and the large thermal conductivity of the metal. Therefore, an alternative approach is to place a thin resistive coating over the metallic surface. We then observe the heating in the coating which is correlated to surface currents in the metal. We will analyze this situation so that we can design an optimum coating for a given situation and, secondly, so that we can understand the quantitative relationship between surface currents and observed surface temperatures. We will then have an accurate method of measuring surface current amplitudes thermographically.

Thus, the procedure will be to solve the electromagnetic problem for a system of N layers so that we can calculate the absorbed energy in the resistive layer. The thermodynamics is then addressed for the system which yields the coating surface temperature. Experimental verification confirms the validity of the analytic results. Recommendations are then made for various coating schemes.



UNCLASSIFIED

SECURITY CLASSIFICATION OF THIS PAGE(When Data Entered)

## CONTENTS

CHAPTER	
I. INTRODUCTION.....	1
II. ELECTROMAGNETICS IN GENERAL.....	8
III. SINGLE BOUNDARY ANALYSIS.....	12
IV. ELECTROMAGNETIC N-LAYER ANALYSIS.....	29
V. THERMAL ANALYSIS.....	38
VI. EXPERIMENTAL VERIFICATION.....	51
VII. APPLICATION OF MODEL TO TWO-DIMENSIONAL TARGETS.....	64
VIII. RECOMMENDATIONS AND CONCLUSIONS.....	106
BIBLIOGRAPHY.....	140
APPENDIX	
A. ELECTRICAL CONDUCTIVITY MEASUREMENT.....	144
B. ELECTRICAL PERMITTIVITY.....	154
C. COMPUTER PROGRAM (One-B).....	165
D. COMPUTER PROGRAM (Basic).....	175
E. COMPUTER PROGRAM (Signif).....	186
F. COMPUTER PROGRAM (Uo-3D).....	190
G. COMPUTER PROGRAM (Uthick).....	204
H. COMPUTER PROGRAM (Contor).....	216
I. COMPUTER PROGRAM (Epsilon).....	224

TABLES

Table

1. Relative Permittivity for Various Dielectrics..... 154
2. Measured Relative Permittivity at 10 GHz.... 164

## FIGURES

## Figure

1. Plane Wave Interaction with a Single Interface.....	10
2. Plane Wave Interface on a Single Boundary.....	12
3. Reflectance from a Single Plane Interface ( $\sigma=0$ ).....	21
4. Directional Spectral Emissivity at 3 Microns ( $\sigma=0$ ).....	22
5. Reflectance from a Single Plane Interface ( $\sigma=3.00$ mhos/m).....	23
6. Directional Spectral Emissivity at 3 Microns ( $\sigma=3.00$ mhos/m).....	24
7. Reflectance from a Single Plane Interface ( $\sigma=500$ mhos/m).....	25
8. Directional Spectral Emissivity at 3 Microns ( $\sigma=500$ mhos/m).....	26
9. Reflectance from a Single Plane Interface (Copper).....	27
10. Directional Spectral Emissivity at 3 Microns (Copper).....	28
11. N-Layer Electromagnetic Interaction.....	29
12. Auxiliary Matrix for Parallel Polarization ( $k_n = \beta_n \cos \theta_n$ ).....	34
13. Auxiliary Matrix for Perpendicular Polarization ( $k_n = \beta_n \cos \theta_n$ ).....	35
14. Three Layer Electromagnetic Response.....	36
15. Three Layer Thermal Transient Response.....	38

16.	Infrared Versus Convection Comparison.....	42
17.	Infrared Versus Convection Comparison.....	43
18.	Infrared Versus Convection Comparison.....	44
19.	Two Layer Electromagnetic Heating Profiles....	47
20.	Two Layer Electromagnetic Heating Profiles....	48
21.	Two Layer Electromagnetic Heating Profiles....	49
22.	Two Layer Electromagnetic Heating Profiles....	50
23.	Schematic of Convective Exponent Experiment...	53
24.	Results of Convective Exponent Measurements...	55
25.	Schematic of N-Layer Verification.....	57
26.	One Layer Electromagnetic Heating.....	59
27.	One Layer Electromagnetic Heating.....	60
28.	One Layer Electromagnetic Heating.....	61
29.	Two Layer Electromagnetic Heating.....	62
30.	Three Layer Electromagnetic Heating.....	63
31.	Photograph of Monopole and Parabolic Reflector.....	65
32.	Actual Quarter Wave Monopole.....	66
33.	Anechoic Chamber With Electrically Small Target and Infrared Camera in Foreground.....	66
34.	A Uniform Current Sheet Radiator.....	68
35.	$1.0\lambda$ Square Plate Current Distribution.....	71
36.	$.15\lambda$ Square Plate Current Distribution.....	72
37.	Photograph of $1.0\lambda$ Square Plate.....	73
38.	Infrared Photograph of a $1.0\lambda$ Square Plate....	74
39.	Thermal Profile Across the Center of a $1.0\lambda$ Square Plate.....	74

40.	Actual Photograph of a $0.5\lambda$ Square Plate.....	75
41.	Infrared Photograph of a $0.5\lambda$ Square Plate....	75
42.	Thermal Profile Across the Center of a $0.5\lambda$ Square Plate.....	76
43.	Actual Photograph of a $0.25\lambda$ Square Plate.....	76
44.	Infrared Photograph of a $0.25\lambda$ Square Plate...	77
45.	Thermal Profile Across the Center of a $0.25\lambda$ Square Plate.....	77
46.	Current Uniformity on a $.15\lambda$ Plate.....	78
47.	Current at the Center of a Disc as a Function of c.....	79
48.	Cross Section of a Conductive Coating Displaced Away From Conductor Surface.....	81
49.	Parallel Waveguide Sheets.....	82
50.	Photograph of Electrically Large Plate in Place in the Anechoic Chamber.....	85
51.	Photograph of the Single 1.5 cm Hole in the Aluminum Plate.....	85
52.	Photograph of the Double Hole Configuration...	86
53.	Infrared Photograph of Artificially Heated Double Hole Configuration for Size Comparison with Microwave Results.....	86
54.	Infrared Photograph of Single Hole Heating Pattern Resulting from Microwave Radiation ( $1^\circ$ C Scale).....	87
55.	Horizontal Thermal Profile of Single Hole Heating Pattern ( $1^\circ$ C Scale).....	87
56.	Same as Figure 54 Except $2^\circ$ C Scale.....	88
57.	Same as Figure 55 Except $2^\circ$ C Scale.....	88
58.	Infrared Results of Double Hole Microwave Heating Pattern ( $1^\circ$ C Scale).....	89

59.	Horizontal Thermal Profile of Double Hole Heating ( $1^{\circ}$ C Scale).....	89
60.	Same as Figure 58 Except $2^{\circ}$ C Scale.....	90
61.	Same as Figure 59 Except $2^{\circ}$ C Scale.....	90
62.	Irradiated, Finite Size, Conducting Substrate with Hypothetical Surface Current Distribution.....	92
63.	Thermovision Photograph of 1.5 cm Square Sample (No Substrate).....	98
64.	Thermal Profile (Horizontal) through the Center of the 1.5 cm Square Sample ( $2.45$ GHz at $25$ mw/cm <sup>2</sup> ).....	98
65.	Thermovision Photograph of $1.0\lambda$ Square Plate (Horizontal white line indicates area where thermal profile was taken.).....	99
66.	Thermal Profile from $1.0\lambda$ Square Plate with $\Delta T_{\infty}$ Plotted.....	99
67.	Thermovision Photograph of $0.5\lambda$ Square Plate (Horizontal white line indicates area where thermal profile was taken.).....	100
68.	Thermal Profile from $0.5\lambda$ Square Plate with $\Delta T_{\infty}$ Plotted.....	100
69.	Thermovision Photograph of 1.5 cm Square Sample (Copper Substrate).....	101
70.	Thermal Profile (Horizontal) through the Center of the 1.5 cm Square Sample ( $2.45$ GHz at $25$ mw/cm <sup>2</sup> ).....	101
71.	Thermovision Photograph of $1.0\lambda$ Square Plate with a Copper Substrate.....	102
72.	Thermal Profile Corresponding to White Line in Figure 71.....	102
73.	Thermovision Photograph of a $0.5\lambda$ Square Plate with a Copper Substrate.....	103
74.	Thermal Profile Corresponding to White Line in Figure 73.....	103

75.	Carbon/Paraffin/Styrofoam Thermal Contours....	111
76.	Carbon/Paraffin/Styrofoam Thermal Contours....	112
77.	Carbon/Paraffin/Styrofoam/Copper Difference Contours.....	113
78.	Carbon/Paraffin/Styrofoam Thermal Contours....	114
79.	Carbon/Paraffin/Styrofoam/Copper Thermal Contours.....	115
80.	Carbon/Paraffin/Styrofoam/Copper Difference Contours.....	116
81.	Carbon/Paraffin/Styrofoam Thermal Contours....	117
82.	Carbon/Paraffin/Styrofoam/Copper Thermal Contours.....	118
83.	Carbon/Paraffin/Styrofoam/Copper Difference Contours.....	119
84.	Carbon/Paraffin/Neoprene Thermal Contours.....	120
85.	Carbon/Paraffin/Neoprene/Copper Thermal Profiles.....	121
86.	Carbon/Paraffin/Neoprene/Copper Difference Contours.....	122
87.	Carbon/Paraffin/Neoprene Thermal Contours.....	123
88.	Carbon/Paraffin/Neoprene/Copper Thermal Contours.....	124
89.	Carbon/Paraffin/Neoprene/Copper Difference Contours.....	125
90.	Carbon/Paraffin/Neoprene Thermal Contours.....	126
91.	Carbon/Paraffin/Neoprene/Copper Thermal Contours.....	127
92.	Carbon/Paraffin/Neoprene/Copper Difference Contours.....	128
93.	Aquadaq/Plexiglas Thermal Contours.....	129
94.	Aquadaq/Plexiglas/Copper Thermal Contours.....	130

95.	Aquadaq/Plexiglas/Copper Difference Contours..	131
96.	Coating Sample Cross Section.....	145
97.	Drawing of a Typical Disc Sample,.....	146
98.	Square Sample Electrical Connections.....	147
99.	Disc Sample with Clamps Attached.....	148
100.	Schematic of Conductivity Measurements.....	148
101.	Electrical Conductivity Versus Absolute Temperature (Aquadaq Coating).....	150
102.	Electrical Conductivity Versus Carbon/Paraffin Mixing Ratios.....	152
103.	Electrical Conductivity Versus Carbon/Paraffin Mixing Ratios with Empirical Model.....	153
104.	Schematic Arrangement of Permittivity Measurements.....	104
105.	Permittivity Plot for Styrofoam at 10 GHz.....	157
106.	Permittivity Plot for Window Glass at 10 GHz..	158
107.	Permittivity Plot for Paraffin at 10 GHz.....	159
108.	Permittivity Plot for Styrene at 10 GHz....	160
109.	Permittivity Plot for Phenolic at 10 GHz.....	161
110.	Permittivity Plot for Plexiglas at 10 GHz.....	162
111.	Permittivity Plot for Neoprene at 10 GHz.....	163

## CHAPTER I

### INTRODUCTION

This paper deals with the microwave induced heating in thin multiple conductive coatings. An understanding of this phenomenon is needed so an optimum coating may be designed for the thermographic detection of surface currents. This process uses a thermographic camera to detect temperature variations on an object's surface. These temperature variations are caused by joule heating ( $I^2R$ ) due to surface currents. Thus, it is possible to relate surface currents to surface temperature variations. Once this is done the thermographic system can measure surface currents on an entire object very quickly and relatively easily. However, there is still a significant limitation to this type of measurement system. The limitation is that we measure a single scalar quantity (temperature) at each point on the surface; hence, we only obtain the magnitude of the total surface current at that point and have no phase or direction information.

Nonetheless, current amplitude information alone is a valuable piece of information. For example, in the

study of Electromagnetic Pulse (EMP) phenomena we might want to know where the greatest current density amplitudes are located on an aircraft to aid in the proper placement of cable bundles. Or possibly in radar cross section studies, we might want to know where the greatest current densities exist before a design or numerical solution is attempted. And lastly, measured surface current amplitude information would be extremely valuable in the verification of numerous numerical techniques designed to provide amplitude, phase, and direction information. This thesis which relates coating temperature to incident microwave power levels is organized in the following manner.

The second chapter begins with a discussion of electromagnetics in general. It considers the phasor form of Maxwell's equations in a conductive medium and then reviews their simultaneous solution. The result yields the type form the wave must take as it propagates in the medium and discusses some of its characteristics. Particular areas of discussion include attenuation in a medium and the complex form of Snell's law.

The third chapter deals exclusively with the solution of a single boundary electromagnetic problem. The boundary is a semi-infinite plane located at the

$z=0$  interface between air and a conductive medium. The solution is completed for various incident angles and for polarizations both parallel and perpendicular to the plane of incidence. The single boundary problem provides two useful insights to our overall problem. First, it is done in a general manner so the same overall approach is used in the solution to the N-layer system later in chapter four. Second, the results may be used to provide information concerning the theoretical infrared emissivity of the coatings that are to be placed on the various object surfaces. The rate and direction of infrared emission are both directly proportional to this emissivity factor. Therefore, our detection effectiveness is very dependent on surface emissivity. Various plots are presented which illustrate the reflectivity and emissivity for materials with conductivities of 0 to  $5 \times 10^7$  mhos/m.

Chapter four presents a detailed solution for the N-layer electromagnetic interaction problem. The problem considers both parallel and perpendicular polarizations at a particular incident angle. Each layer is considered to have a particular electrical conductivity. The solution is developed in terms of an expanded matrix in a manner similar to that used in chapter three. A computer program is included in appendix D that will do the solution for up to a 10 layer system

and display the results with a Hewlett-Packard 9845B mini-computer. Included is an example of the plot obtained for a three layer system with the layers having conductivities of .5, 1.0, and 1.5 mhos/m respectively. Of note in this development is that there are no approximations used other than assuming semi-infinite slab dimensions.

In the next chapter we tie the electromagnetic interaction to the thermodynamics of the problem. Thus, for a given layer configuration we relate surface temperature to a given microwave input power. Initially in the development, a simplified model is presented that allows us to estimate the transient response of the system. Then somewhat later the steady state thermal characteristics of the system are analyzed. In this analysis we assume there are no heat losses from other than the  $z=0$  interface; that is, we assume one of the layers below the conductive coating to be a perfect insulator. At the  $z=0$  interface we consider both infrared and convective heat losses. The steady state solution to the heat equation yields a transcendental equation that must be solved numerically. A computer program is written that does this solution and plots surface temperature versus electrical conductivity and coating thickness on a three dimensional plot. Plots

are illustrated for typical two and three layer systems.

As in any theoretical development, we must have experimental verification before the results may be used with any confidence. Chapter six provides experimental verification of the computer results for various layer configurations. The three primary sources of error in the experiments resulted from the lack of semi-infinite planes to irradiate with microwaves; thus, samples much smaller than a wavelength were used to avoid resonance problems. Also, the problem of assuming zero heat conduction losses from the  $z=z_n$  interface was partially solved by placing the samples on a styrofoam substrate. Finally, the third major source of error resulted from the convective heat transfer coefficient used which itself was an empirical value. See for example Holman's book, Heat Transfer. Nonetheless, predicted surface temperatures were very close to the measured values.

Chapter seven is a mostly qualitative discussion of the relationship of our one-dimensional model to the more complicated two or even three-dimensional "real world" experiments. In particular, the two areas discussed involve the validity of using a small finite shape in the experimental verification of Chapter VI and the question of "nearest neighbor" significance in the actual measurement of surface currents on electrically large targets. Theoretical

as well as experimental results are presented that help establish the validity and usefulness of our one-dimensional model as applied toward the "real world" situation.

In Chapter VIII recommendations and conclusions are made in regards to what to use as an optimum coating in the thermographic detection of microwave induced surface currents. Basically, there are two situations that must be considered. The first considers geometry only. If we are interested only in the geometrical aspects of a problem such as studying the currents on an entire aircraft, the simpler approach is to build a model of foam and then coat it with a thick (two skin depths) layer of material with a conductivity of from 300 to 750 mhos/m. Hence, the currents we measure are the currents in the coating itself; we simulate a highly conductive object with one of lesser conductivity. The other, and more difficult, situation is one in which the material an object is made matters and cannot be approximated. This situation would occur if several different materials were used in the construction of a particular shape (For example, there might be ferromagnetic materials, copper, aluminum, and composites all located on the underside of an aircraft or spacecraft.). Here we would like to determine how these different materials behave together. Therefore, we

place our coating directly on the object itself. By appropriate design of the coating, we can detect the current distribution under our coating.

Various coating options are described in the final chapter as well as their advantages and disadvantages. The various appendices contain the experimental arrangements for measuring such material characteristics as electrical conductivity and permittivity. Also included are all the major computer programs used in any of the numerical analysis with the 9845B computer. This computer uses a Hewlett-Packard enhanced BASIC language that would be easily modified for use on a computer using either Fortran or Pascal.

Overall then, this paper begins by presenting the development of a one-dimensional model for the electromagnetic interaction with a system of  $N$  layers with differing electrical characteristics. We then use this model in a thermodynamic analysis to arrive at the steady state surface temperature of the system of layers. Thus, we arrive at a model which predicts the equilibrium surface temperature of a system of  $N$  discrete layers in the presence of electromagnetic radiation. This model is verified experimentally and its applicability to two-dimensional targets is discussed. Finally, recommendations are made in regards to particular coating design.

## CHAPTER II

## GENERAL ELECTROMAGNETIC ANALYSIS

In electromagnetic analysis we will study the simple one boundary problem and then progress to multiple boundaries. Throughout this analysis we will assume a time dependence for  $E$  and  $H$  of the form  $e^{-j\omega t}$ . We will first calculate the form the field must take by looking at the solution of Maxwell's equations in a conductive medium.

In a charge free conductor and with the assumed time dependence, Maxwell's equations may be written as follows:

$$\vec{\nabla} \times \vec{E} = j\omega\mu \vec{H} \quad (1)$$

$$\vec{\nabla} \times \vec{H} = (\sigma - j\omega\epsilon) \vec{E} \quad (2)$$

$$\vec{\nabla} \cdot \vec{E} = 0 \quad (3)$$

$$\vec{\nabla} \cdot \vec{H} = 0 \quad (4)$$

Solving equations (1) through (4) simultaneously<sup>10</sup> we can arrive at the vector wave equation

$$\nabla^2 \vec{E} + \beta^2 \vec{E} = 0 \quad (5)$$

where

$\beta^2$  is defined by

$$\beta^2 \equiv \omega^2 \mu \epsilon + j \omega \mu \sigma \quad (6)$$

A wave equation may also be developed for  $\vec{H}$ ; however, its value is readily available through equation (1).

Solving, we have

$$\vec{H} = - \frac{j}{\omega\mu} \nabla \times \vec{E} \quad (7)$$

The solution of (5) is well known<sup>11</sup> and may be written as

$$\vec{E} = \vec{E}_0 e^{j(\vec{\beta} \cdot \vec{r} - \omega t)} \quad (8)$$

where  $\vec{\beta}$  is the wave vector. Thus,

$$\vec{\beta} = \sqrt{\omega^2 \mu \epsilon + j \omega \mu \sigma} \hat{n} \quad (9)$$

with  $\hat{n}$  being in the direction of wave propagation.

Since  $\beta$  is complex, its real and imaginary components may be found by letting  $\beta = \alpha + j\gamma$  where  $\alpha$  and  $\gamma$  are defined to be real. Making the above substitution and equating real and imaginary parts, we arrive at two simultaneous equations given by

$$\alpha^2 - \gamma^2 = \omega^2 \mu \epsilon \quad (10)$$

$$2\alpha\gamma = \omega\mu\sigma \quad (11)$$

Solving (10) and (11) by substitution we find expressions for  $\alpha$  and  $\gamma$  given by

$$\alpha = \omega \sqrt{\frac{\mu\epsilon}{2}} \sqrt{1 + \sqrt{1 + \left(\frac{\sigma}{\omega\epsilon}\right)^2}} \quad (12)$$

$$\gamma = \omega \sqrt{\frac{\mu\epsilon}{2}} \sqrt{-1 + \sqrt{1 + \left(\frac{\sigma}{\omega\epsilon}\right)^2}} \quad (13)$$

For the case of good conductors  $\left(\frac{\sigma}{\omega\epsilon}\right) \gg 1$ ; thus, we have  $\alpha = \gamma = \frac{1}{\delta}$  where  $\delta$  is the characteristic skin depth of the medium in question. It is given by

$$\delta \equiv \sqrt{\frac{2}{\omega\mu\sigma}} \quad (14)$$

From this point on we will omit the  $e^{-j\omega t}$  time dependence, since it will occur in all of our terms, and proceed with the more familiar phasor notation. Thus we will write for the electric field

$$\vec{E} = \vec{E}_0 e^{j\vec{\beta} \cdot \vec{r}} \quad (15)$$

This is a shorthand notation and it is to be understood that the  $e^{-j\omega t}$  is always present even though it is not written.

Lastly, it is advantageous to develop the complex Snell's law. Consider the single interface below separating two conductive materials.

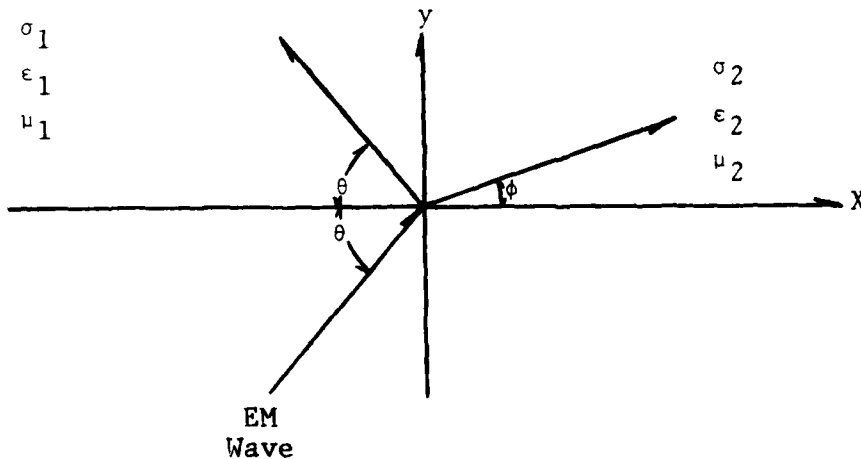


Figure 1: Plane Wave Interaction with a Single Interface

We know the wave phase must be the same on each side of the boundary at any given point on the boundary; otherwise, the wave would "tear" and dispersion would occur. This phase requirement may be satisfied by having<sup>12</sup>

$$\vec{\beta}_1 \cdot \vec{r} = \vec{\beta}_2 \cdot \vec{r} \quad (16)$$

Again referring to the drawing, we have

$$\beta_2(\cos\theta \hat{x} + \sin\theta \hat{y}) \cdot \vec{r} \equiv \beta_2(\cos\phi \hat{x} + \sin\phi \hat{y}) \cdot \vec{r} \quad (17)$$

Since  $\vec{r} = y \hat{y}$  defines the interface, the result is

$$\beta_1 \sin\theta = \beta_2 \sin\phi \quad (18)$$

Thus,  $\sin\phi$  is in general complex and is given by

$$\sin\phi = \frac{\beta_1}{\beta_2} \sin\theta = \frac{\alpha_1 + j\gamma_1}{\alpha_2 + j\gamma_2} \sin\theta \quad (19)$$

We may also write the expression for  $\cos\phi$  by recognizing that for any complex  $z$ ,  $\sin^2 z + \cos^2 z = 1$ <sup>13</sup>; thus,

$$\cos\phi = \sqrt{1 - \frac{\alpha_1^2 - \gamma_1^2 + j 2\alpha_1 \gamma_1}{\alpha_1^2 - \gamma_2^2 + j 2\alpha_2 \gamma_2} \sin^2\theta} \quad (20)$$

We can look at Snell's Law in the case of an air/good conductor interface. If the medium on the left is air,  $\beta_1$  reduces to  $\frac{2\pi}{\lambda}$ , where  $\lambda$  is the free space wavelength. In the good conductor we have

$$\alpha \approx \gamma \approx \frac{1}{\delta}; \text{ then we have } \sin\phi = \left(\frac{2\pi}{\lambda}\right) \left(\frac{1}{\alpha_2 + j\gamma_2}\right) \sin\theta \quad (21)$$

With algebraic manipulation this reduces to

$$\sin\phi = \frac{1}{2c\sqrt{\mu_2\sigma_2}} (1 - j) \sin\theta \quad (22)$$

In the good conductor limit we have therefore,

$$\sin\phi \approx 0 \quad (23)$$

which implies  $\phi \approx 0$

Hence, regardless of the incident angle  $\theta$ , the wave will propagate approximately normal to the surface after entering medium 2.

## CHAPTER III

## SINGLE BOUNDARY ANALYSIS

With the basic equations developed, we can now do the actual field calculation. We will begin with the single boundary which will provide two important pieces of information. First, it will provide needed insight for the solution of the more complex multi-layer problem, and second, it will provide a method of calculating theoretical infrared spectral emissivities. This information will be very valuable in the thermodynamic analysis of the multi-layer problem later in the development.

We begin by considering the diagram below in which we have an incident electromagnetic wave from the left. Parallel incidence is illustrated.

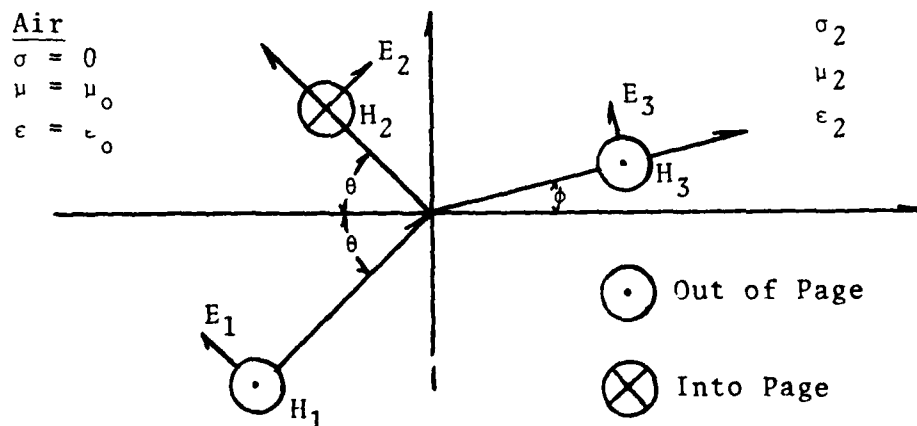


Figure 2: Plane Wave Interface on a Single Boundary

From the previous development we know that

$$\alpha = \omega \sqrt{\frac{\mu_2 \epsilon_2}{2}} \sqrt{1 + \sqrt{1 + \left(\frac{\sigma_2}{\omega \epsilon_2}\right)^2}} \quad (24)$$

$$\gamma = \omega \sqrt{\frac{\mu_2 \epsilon_2}{2}} \sqrt{-1 + \sqrt{1 + \left(\frac{\sigma_2}{\omega \epsilon_2}\right)^2}} \quad (25)$$

$$\beta_2 = \alpha + j \gamma \quad \beta_0 \equiv \frac{2\pi}{\lambda} \quad (26)$$

$$\sin \phi = \beta_0 \left( \frac{\alpha - j\gamma}{\alpha^2 + \gamma^2} \right) \sin \theta \quad (27)$$

$$\cos \theta = \sqrt{1 - \beta_0^2 \frac{\sin^2 \theta (\alpha^2 - \gamma^2 - j 2\alpha\gamma)}{(\alpha^2 + \gamma^2)^2}} \quad (28)$$

We will need the real and imaginary parts of  $\cos \phi$  later so it is advantageous to calculate them now. We begin by letting  $\cos \phi = x + j y$  where  $x$  and  $y$  are defined to be real. Thus,

$$\cos^2 \phi = x^2 - y^2 + j 2xy \quad (29)$$

Equating real and imaginary parts, we obtain two simultaneous equations:

$$x^2 - y^2 = 1 - \beta_0^2 \frac{\sin^2 \theta (\alpha^2 - \gamma^2)}{(\alpha^2 + \gamma^2)^2} \quad (30)$$

$$xy = \beta_0^2 \frac{\sin^2 \theta \alpha \gamma}{(\alpha^2 + \gamma^2)^2} \quad (31)$$

Solving (30) and (31) by substitution, yields the following

$$x = \sqrt{P + \sqrt{P^2 + Q^2}} \quad (32)$$

$$y = \sqrt{-P + \sqrt{P^2 + Q^2}} \quad (33)$$

where

$$P \equiv \frac{1}{2} - \beta_o^2 \frac{\sin^2 \theta (\alpha^2 - \gamma^2)}{2(\alpha^2 + \gamma^2)^2} \quad (34)$$

$$Q \equiv \beta_o^2 \frac{\sin^2 \theta \alpha \gamma}{(\alpha^2 + \gamma^2)^2} \quad (35)$$

In the good conductor limit where  $(\frac{\sigma}{\omega \epsilon}) \gg 1$  these reduce to

$$x = \sqrt{\frac{1}{2} + \frac{1}{2} \sqrt{1 + \frac{1}{4} (\beta_o \delta \sin \theta)^4}} \quad (36)$$

$$y = \sqrt{-\frac{1}{2} + \frac{1}{2} \sqrt{1 + \frac{1}{4} (\beta_o \delta \sin \theta)^4}} \quad (37)$$

For example if the incident frequency is 2.5 GHz and  $\sigma = 10$  mhos/m we have  $\cos \phi \approx 1.00002 + j(.007)$  which indicates that  $\phi$  may be considered to be approximately zero for values of  $\sigma > 10$ . In some numerical calculations this could vastly shorten the computer time.

By considering the geometry of the problem, we may write the wave vectors as follows:

$$\vec{\beta}_1 = \beta_o (\sin \theta \hat{x} + \cos \theta \hat{z}) \quad (38)$$

$$\vec{\beta}_2 = \beta_o (\sin \theta \hat{x} - \cos \theta \hat{z}) \quad (39)$$

$$\vec{\beta}_3 = \beta_2 (\sin \phi \hat{x} + \cos \phi \hat{z}) \quad (40)$$

Since we are considering an infinite plane, we are interested only in the  $z$  dependence of the fields; thus we may take  $\vec{r} = z \hat{z}$ . We have

$$\vec{\beta}_1 \cdot \vec{r} = \beta_o z \cos \theta \quad (41)$$

$$\vec{\beta}_2 \cdot \vec{r} = -\beta_o z \cos \theta \quad (42)$$

$$\vec{\beta}_3 \cdot \vec{r} = (\alpha + j\gamma) z \cos\phi \quad (43)$$

At this point we divide the problem into two parts since we must consider parallel and perpendicular polarization of the E vector separately.

### E Parallel

If  $\vec{E}$  is parallel to the plane of incidence we may write the vector fields with reference to the diagram. We have

$$\vec{E}_1 = E_1 e^{j\beta_0 z \cos\theta} (\cos\theta \hat{x} - \sin\theta \hat{z}) \quad (44)$$

$$\vec{H}_1 = \frac{\beta_0}{\omega\mu} E_1 e^{j\beta_0 z \cos\theta} \hat{y} \quad (45)$$

$$\vec{E}_2 = E_2 e^{-j\beta_0 z \cos\theta} (\cos\theta \hat{x} + \sin\theta \hat{z}) \quad (46)$$

$$\vec{H}_2 = -\frac{\beta_0}{\omega\mu} E_2 e^{-j\beta_0 z \cos\theta} \hat{y} \quad (47)$$

$$\vec{E}_3 = E_3 e^{j\beta_2 z \cos\phi} (\cos\phi \hat{x} - \sin\phi \hat{z}) \quad (48)$$

$$\vec{H}_3 = \frac{\beta_2}{\omega\mu_2} E_3 e^{j\beta_2 z \cos\phi} \hat{y} \quad (49)$$

To satisfy the boundary conditions at  $z = 0$ , we equate the tangential field components of E and H there; thus, we have

$$E_1 \cos\theta + E_2 \cos\theta = E_3 \cos\phi \quad (50)$$

$$\frac{\beta_0}{\omega\mu} E_1 - \frac{\beta_0}{\omega\mu} E_2 = \frac{\beta_2}{\omega\mu_2} E_3 \quad (51)$$

Since we know the value of  $E_1$ , (50) and (51) may be rearranged and written in matrix form as follows <sup>14</sup>

$$\begin{bmatrix} \cos \theta & -\cos \phi \\ \frac{\beta_0}{\mu} & \frac{\beta_2}{\mu_2} \end{bmatrix} \times \begin{bmatrix} E_2 \\ E_3 \end{bmatrix} = \begin{bmatrix} -E_1 \cos \theta \\ \frac{\beta_0}{\mu} E_1 \end{bmatrix} \quad (52)$$

Equation (52) may now be solved to yield values of  $E_2$  and  $E_3$ . Before solving (52) we will derive the solution for perpendicular incidence and then develop a common method of solution.

### E Perpendicular

We may proceed directly to the field equations; they are given by

$$\vec{E}_1 = E_1 e^{j \beta_0 z \cos \theta} \hat{y} \quad (53)$$

$$\vec{H}_1 = \frac{\beta_0 E_1}{\omega \mu} e^{j \beta_0 z \cos \theta} (-\cos \theta \hat{x} + \sin \theta \hat{z}) \quad (54)$$

$$\vec{E}_2 = E_2 e^{-j \beta_0 z \cos \theta} \hat{y} \quad (55)$$

$$\vec{H}_2 = \frac{\beta_0}{\omega \mu} E_2 e^{-j \beta_0 z \cos \theta} (\cos \theta \hat{x} + \sin \theta \hat{z}) \quad (56)$$

$$\vec{E}_3 = E_3 e^{j \beta_2 z \cos \phi} \hat{y} \quad (57)$$

$$\vec{H}_3 = \frac{\beta_2}{\omega \mu_2} E_3 e^{j \beta_2 z \cos \phi} (-\cos \phi \hat{x} + \sin \phi \hat{z}) \quad (58)$$

As before, we apply the boundary conditions at the  $z = 0$  interface which yields

$$E_1 + E_2 = E_3 \quad (59)$$

$$- \frac{\beta_0 \cos \theta}{\omega \mu} E_1 + \frac{\beta_0 \cos \theta}{\omega \mu} E_2 = - \frac{\beta_2 \cos \phi}{\omega \mu_2} E_3 \quad (60)$$

Again these equations simplify and may be put into matrix form.

$$\begin{bmatrix} 1 & -1 \\ \frac{\beta_0}{\mu} \cos \theta & \frac{\beta_2}{\mu_2} \cos \phi \end{bmatrix} \begin{bmatrix} E_2 \\ E_3 \end{bmatrix} = \begin{bmatrix} -E_1 \\ \frac{\beta_0}{\mu} \cos \theta \end{bmatrix} \quad (61)$$

#### Analytic Solution

Equations (52) and (61) may be solved directly with little difficulty; however, since we are developing a general technique for a multi-layer system, it is worthwhile to do the solution numerically. The technique is relatively straight forward in that the coefficient matrices are loaded into a computer along with the constant vector. For example, if we have the matrix equation  $Ax = B$ , we would load the auxiliary matrix

$$\begin{bmatrix} a_{11} & \cdots & a_{1n} & | & b_1 \\ \vdots & a_{22} & \vdots & | & \vdots \\ a_{n1} & \cdots & a_{nn} & | & b_n \end{bmatrix} \quad (62)$$

into the computer. It would be an  $N \times N + 1$  dimensional

matrix. We then do a Gauss-Jordan row reduction to put the A portion into identity format. The B column will now correspond to the solution vector of x. This is relatively easy to program unless A happens to be complex. In this case the complex equation  $Ax = B$  may be expanded into its real and imaginary parts to yield a matrix equation of only real terms which may be handled in a straight forward manner. For example if the set of equations,

$$a_{11} x_1 + a_{12} x_2 = b_1 \quad (63)$$

$$a_{21} x_1 + a_{22} x_2 = b_2 \quad (64)$$

is complex, we may in complex notation write a complex matrix equation as

$$\begin{bmatrix} a_{11} & a_{12} \\ a_{21} & a_{22} \end{bmatrix} x \begin{bmatrix} x_1 \\ x_2 \end{bmatrix} = \begin{bmatrix} b_1 \\ b_2 \end{bmatrix} \quad (65)$$

Likewise we may write (63) and (64) in an expanded format in terms of its real and imaginary parts. If we let R and I designate Real and Imaginary respectively, we have

$$\begin{aligned} (Ra_{11} + jIa_{11})(Rx_1 + jIx_1) + (Ra_{12} + jIa_{12})(Rx_2 + jIx_2) = \\ Rb_1 + jIb_1 \end{aligned} \quad (66)$$

$$(Ra_{21} + jIa_{21})(Rx_1 + jIx_1) + (Ra_{22} + jIa_{22})(Rx_2 + jIx_2) = Rb_2 + jIb_2 \quad (67)$$

Equating real and imaginary parts in (66) and (67) we have

$$Ra_{11} Rx_1 - Ia_{11} Ix_1 + Ra_{12} Rx_2 - Ia_{12} Ix_2 = Rb_1 \quad (68)$$

$$Ia_{11} Rx_1 + Ra_{11} Ix_1 + Ia_{12} Rx_2 + Ra_{12} Ix_2 = Ib_1 \quad (69)$$

$$Ra_{21} Rx_1 - Ia_{21} Ix_1 + Ra_{22} Rx_2 - Ia_{22} Ix_2 = Rb_2 \quad (70)$$

$$Ia_{21} Rx_1 + Ra_{21} Ix_1 + Ia_{22} Rx_2 + Ra_{22} Ix_2 = Ib_2 \quad (71)$$

or in matrix format we have a matrix of real terms only written as follows <sup>15</sup>:

$$\begin{bmatrix} Ra_{11} & -Ia_{11} & Ra_{12} & -Ia_{12} \\ Ia_{11} & Ra_{11} & Ia_{12} & Ra_{12} \\ Ra_{21} & -Ia_{21} & Ra_{22} & -Ia_{22} \\ Ia_{21} & Ra_{21} & Ia_{22} & Ra_{22} \end{bmatrix} \begin{bmatrix} Rx_1 \\ Ix_1 \\ Rx_2 \\ Ix_2 \end{bmatrix} = \begin{bmatrix} Rb_1 \\ Ib_1 \\ Rb_2 \\ Ib_2 \end{bmatrix} \quad (72)$$

Thus, to numerically solve a 2 x 2 complex matrix a computer must reduce a 4 x 4 matrix, and in general to solve an N x N complex matrix we must generate a 2N x 2N real matrix.

There are some advantages to this approach in that after the reduction is complete we have all our variables written in real and imaginary format. Also, the expanded matrix is easy to generate if one partitions the original complex matrix and then notes that

each complex element goes into a 2 x 2 matrix that is nearly semetric except for one sign.

### Numeric Solution

The numeric solution takes the material characteristics ( $\sigma_2, \mu_2, \epsilon_2$ ) and then constructs the expanded auxiliary matrix, Para (I,J) and Perp (I,J) corresponding to the Parallel or Perpendicular solutions respectively. The program then does a Gauss-Jordan elimination for each of these as it iterates through  $1^\circ$  increments from 0 to  $90^\circ$ . For each iteration a reflectivity coefficient is calculated and stored. After the routine is complete the reflectivity coefficients are plotted as a function of  $\theta$  for both parallel and perpendicular polarizations on the same plot. Additionally a plot of spectral emissivity (absorbance) is calculated. For the emissivity,  $\lambda$  is set equal to 3  $\mu\text{m}$  and is calculated as  $\epsilon = (1 - \text{Reflectivity})$ . The result is then plotted as  $\epsilon$  versus  $\theta$ . The program written for a Hewlett-Packard 9845B computer is listed in appendix C. Figures 3 through 10 are the microwave reflectance and emissivity plots for a dielectric and a conductor with conductivities of 0, 3, 500, and  $5 \times 10^7$  mhos/meter respectively.

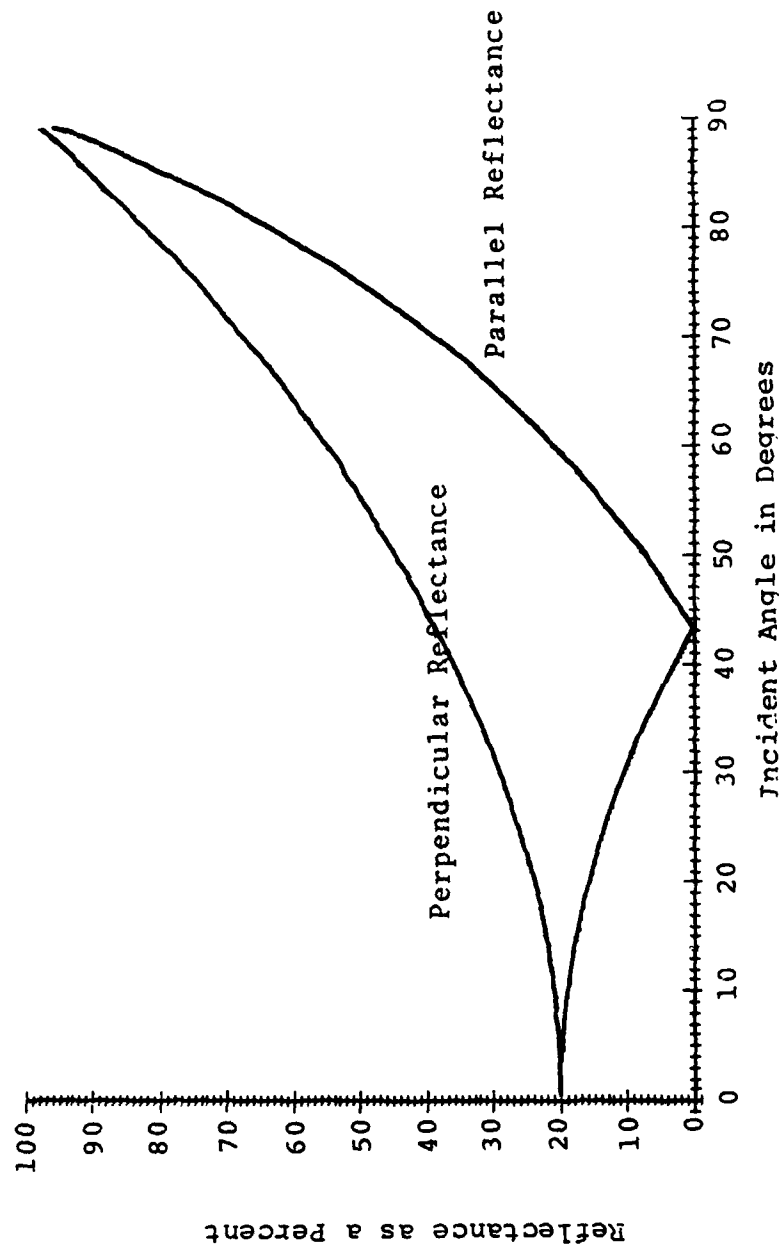


Figure 3: Reflectance from a Single Plane Interface ( $\sigma=0$ )

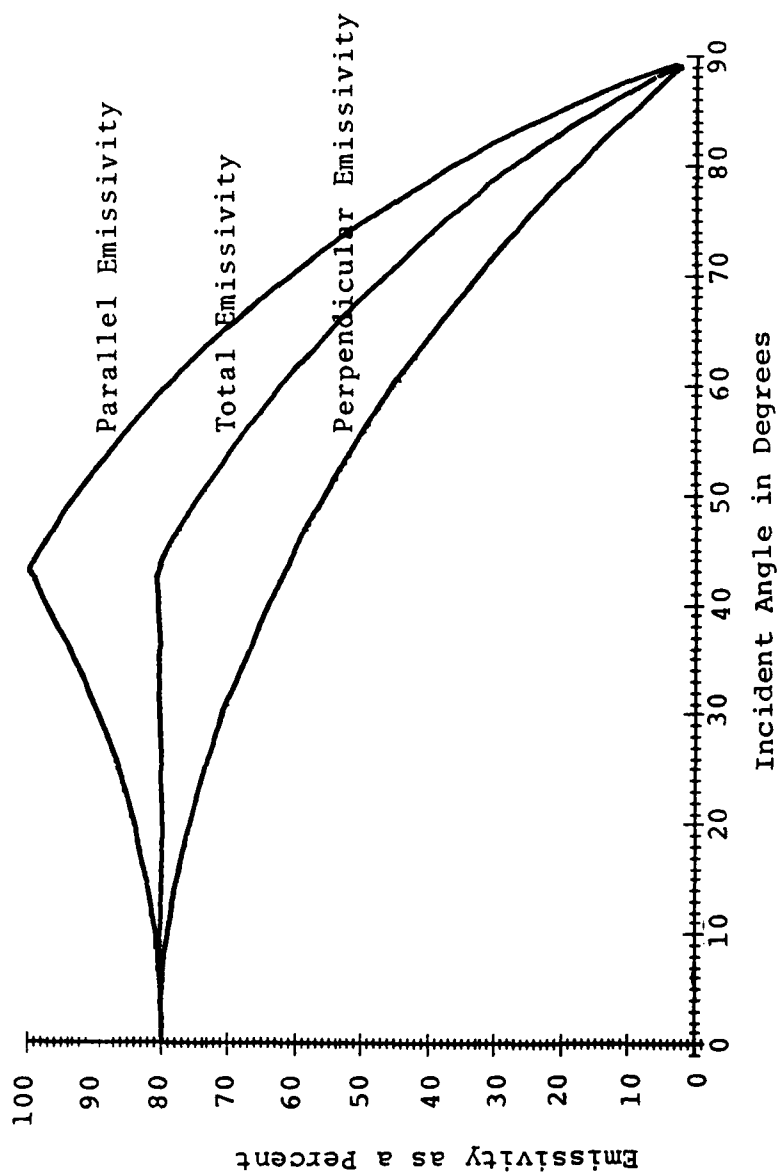


Figure 4: Directional Spectral Emissivity at 3 Microns ( $\sigma=0$ )

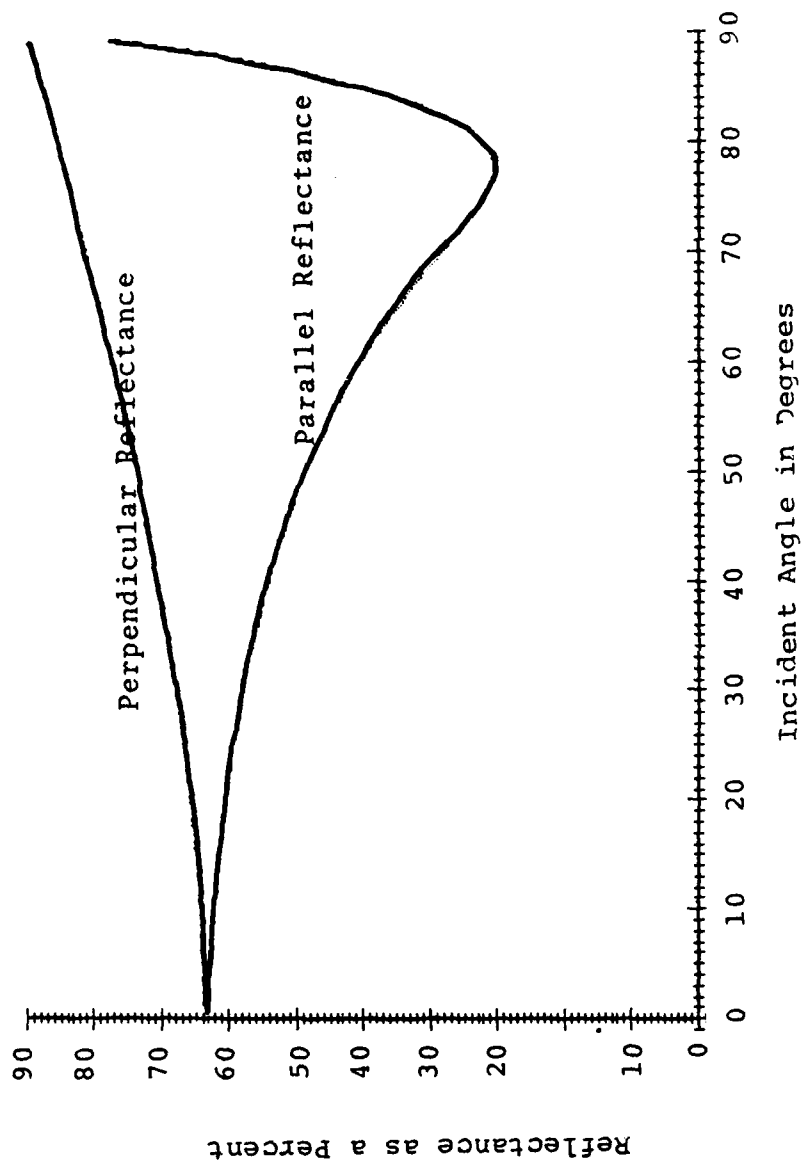


Figure 5: Reflectance from a Single Plane Interface ( $\sigma=3.00$  mhos/m)

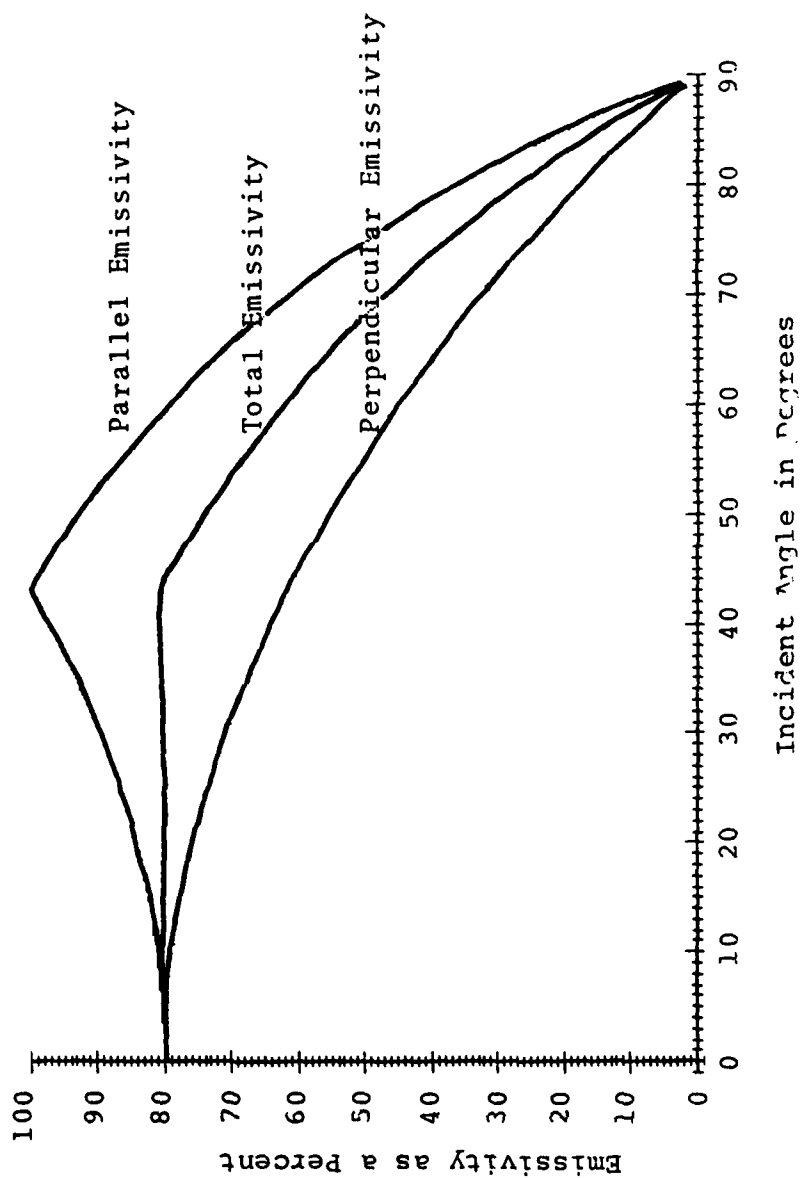


Figure 6: Directional Spectral Emissivity at 3 Microns ( $\sigma=3$  mhos/m)

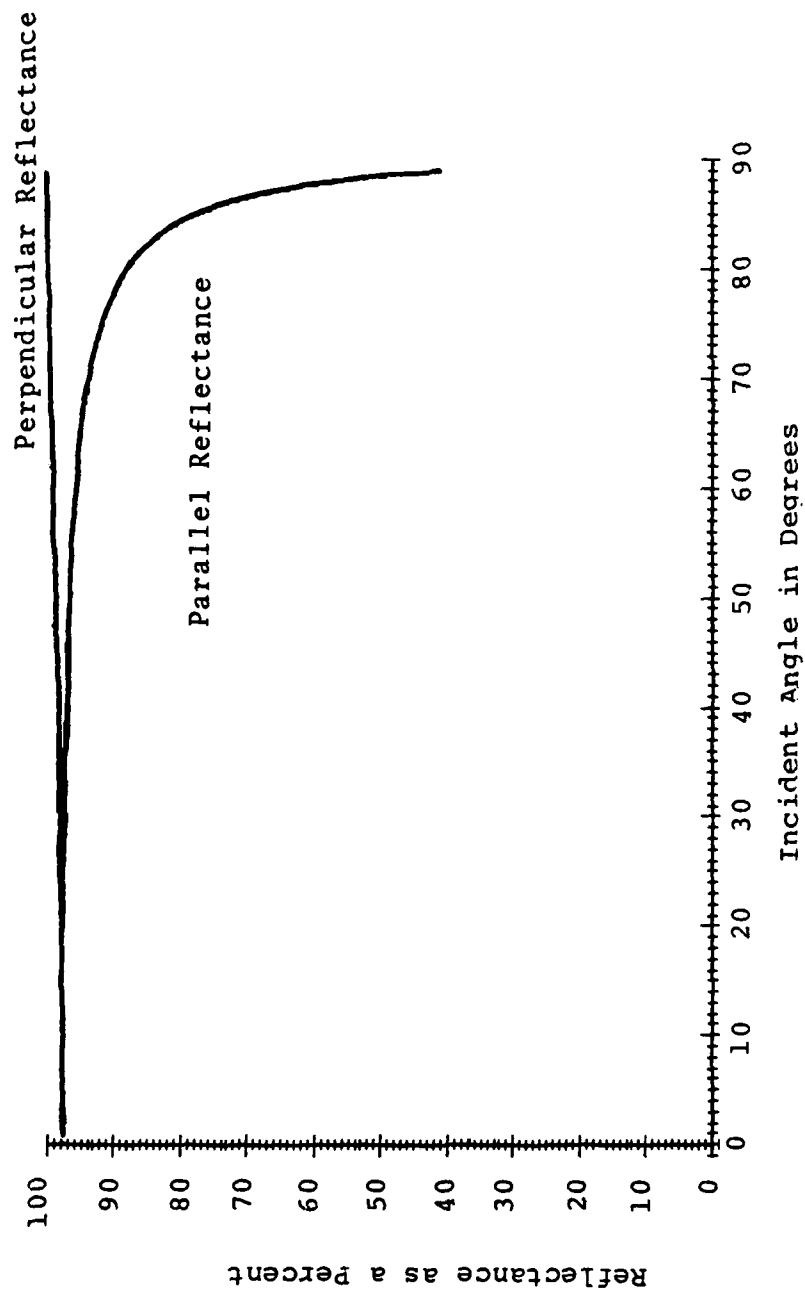


Figure 7: Reflectance from a Single Plane Interface ( $\sigma=500$  mhos/m)

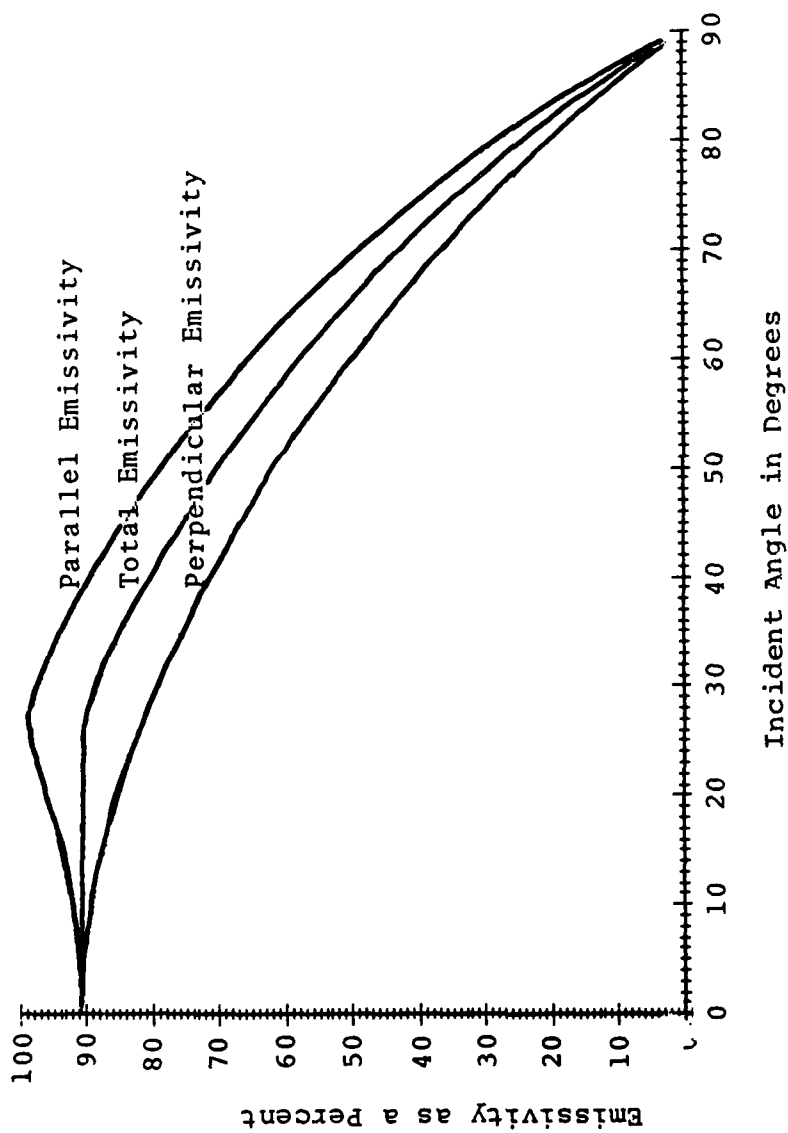


Figure 8: Directional Spectral Emissivity at 3 Microns ( $\sigma=500$  mhos/m)

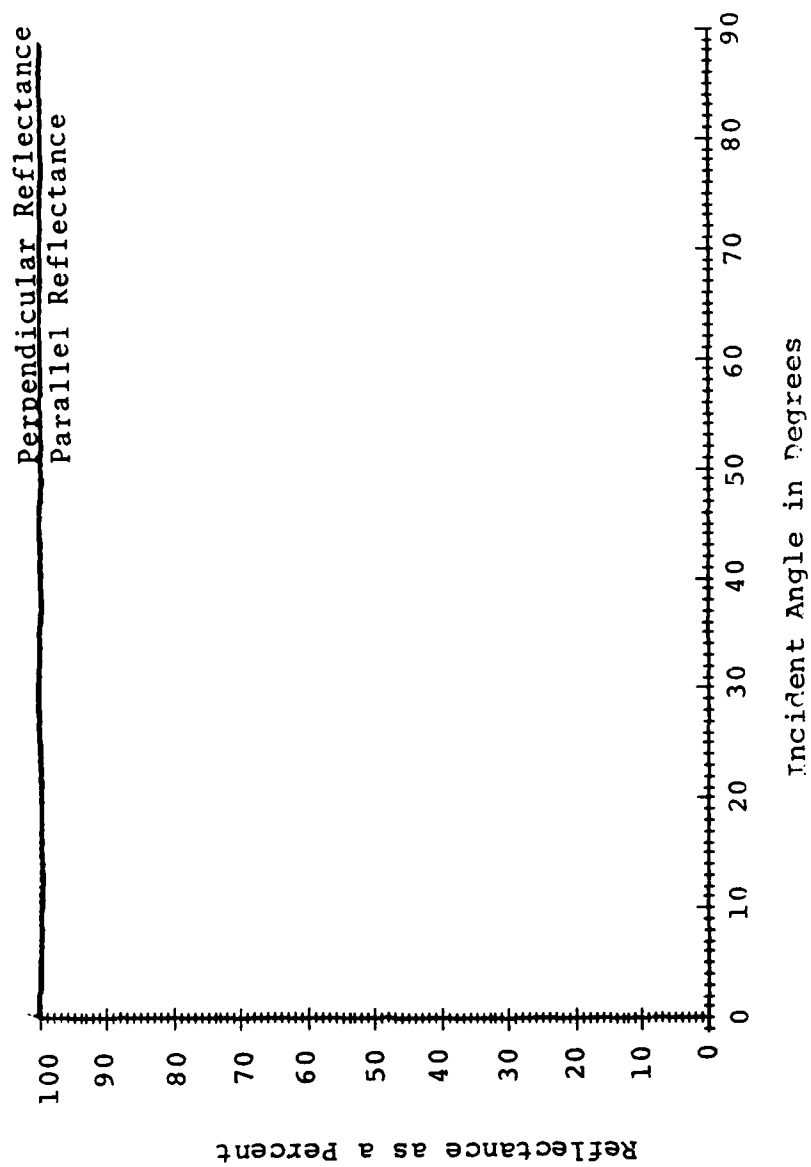


Figure 9: Reflectance from a Single Plane Interface (Copper)

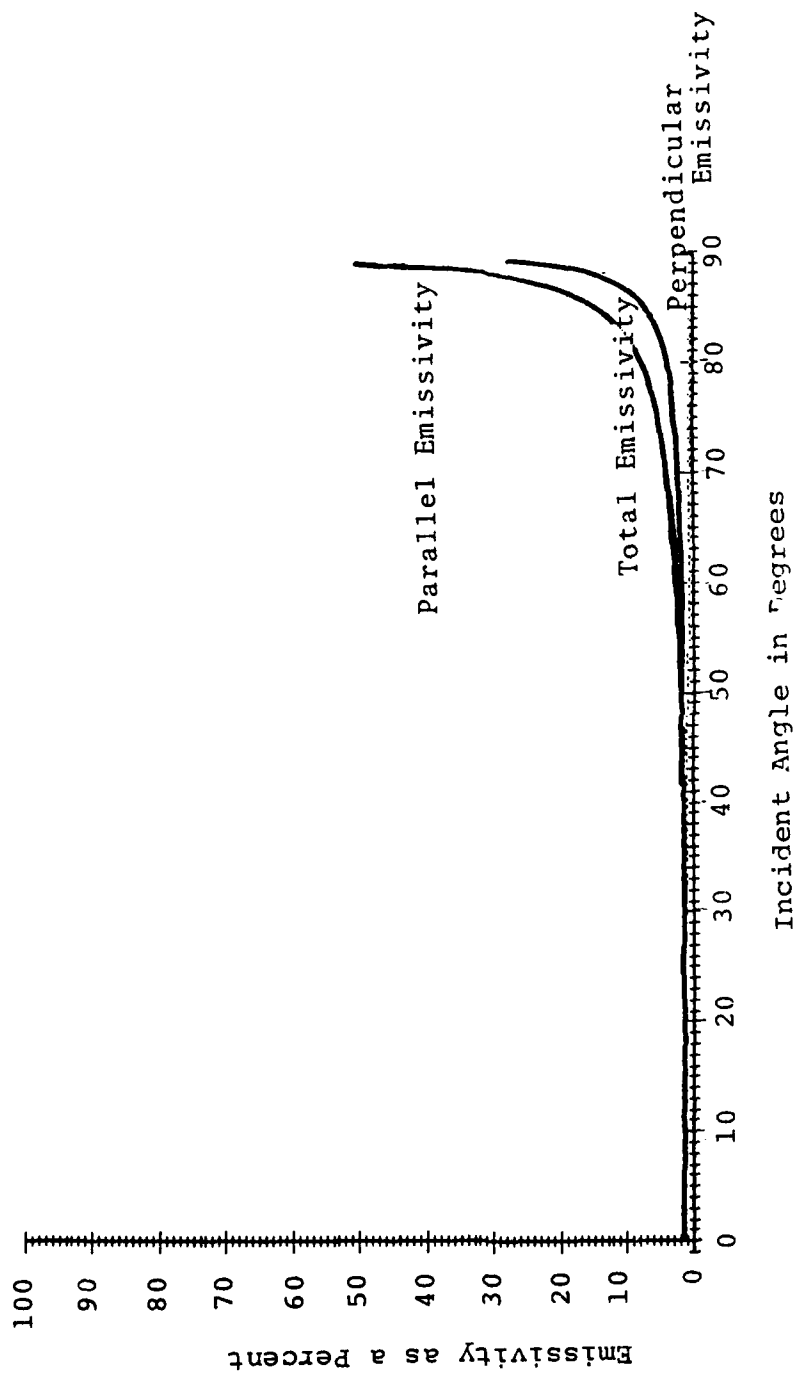


Figure 10: Directional Spectral Emissivity at 3 Microns (Copper)

## CHAPTER IV

## ELECTROMAGNETIC N-LAYER ANALYSIS

We now consider the problem of N-layers with air on each side. See the diagram below.

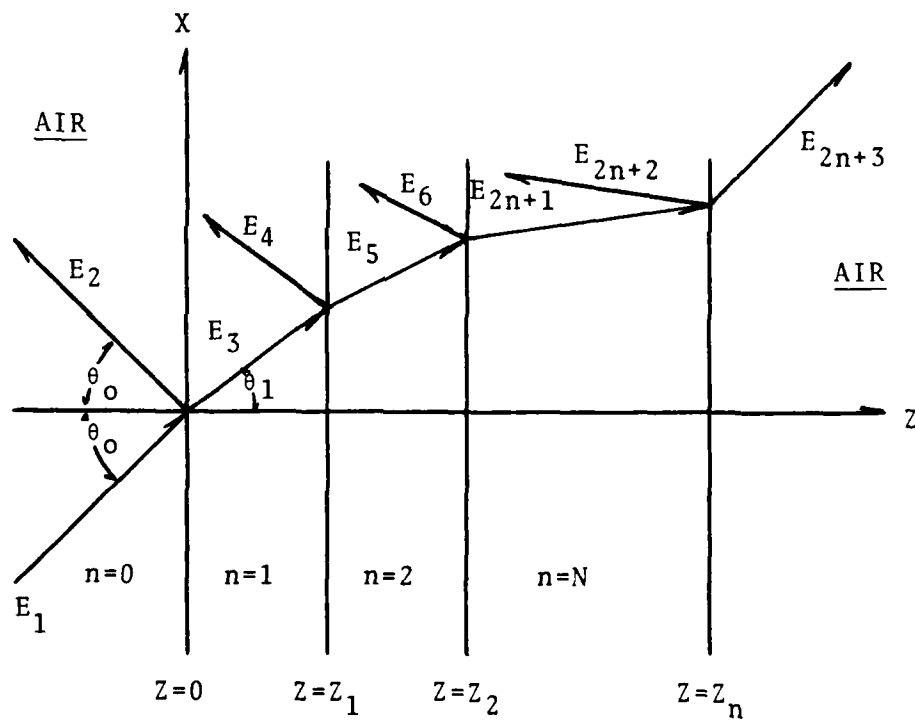


Figure 11: N-Layer Electromagnetic Interaction

Since we have N separate layers,  $E_{2n+1}$  defines the electric field of the wave traveling to the right in material n and  $E_{2n+2}$  defines the wave traveling to the left. As in the single boundary case, we may write the field components in each layer as follows:

E Parallel

$$\vec{E}_1 = E_1 e^{j\beta_0 z \cos\theta_0} (\cos\theta_0 \hat{x} - \sin\theta_0 \hat{z}) \quad (73)$$

$$\vec{H}_1 = \frac{\beta_0}{\omega\mu} E_1 e^{j\beta_0 z \cos\theta_0} \hat{y} \quad (74)$$

$$\vec{E}_2 = E_2 e^{-j\beta_0 z \cos\theta_0} (\cos\theta_0 \hat{x} + \sin\theta_0 \hat{z}) \quad (75)$$

$$\vec{H}_2 = -\frac{\beta_0}{\omega\mu} E_2 e^{-j\beta_0 z \cos\theta_0} \hat{y} \quad (76)$$

$$\vec{E}_3 = E_3 e^{j\beta_1 z \cos\theta_1} (\cos\theta_1 \hat{x} - \sin\theta_1 \hat{z}) \quad (77)$$

$$\vec{H}_3 = \frac{\beta_1}{\omega\mu_1} E_3 e^{j\beta_1 z \cos\theta_1} \hat{y} \quad (78)$$

$$\vec{E}_4 = E_4 e^{-j\beta_1 z \cos\theta_1} (\cos\theta_1 \hat{x} + \sin\theta_1 \hat{z}) \quad (79)$$

$$\vec{H}_4 = -\frac{\beta_1}{\omega\mu_1} E_4 e^{-j\beta_1 z \cos\theta_1} \hat{y} \quad (80)$$

$$\vdots$$

$$\vec{E}_{2n+1} = E_{2n+1} e^{j\beta_n z \cos\theta_n} (\cos\theta_n \hat{x} - \sin\theta_n \hat{z}) \quad (81)$$

$$\vec{H}_{2n+1} = \frac{\beta_n}{\omega\mu_n} E_{2n+1} e^{j\beta_n z \cos\theta_n} \hat{y} \quad (82)$$

$$\vec{E}_{2n+2} = E_{2n+2} e^{-j\beta_n z \cos\theta_n} (\cos\theta_n \hat{x} + \sin\theta_n \hat{z}) \quad (83)$$

$$\vec{H}_{2n+2} = -\frac{\beta_n}{\omega\mu_n} E_{2n+2} e^{-j\beta_n z \cos\theta_n} \hat{y} \quad (84)$$

$$\vec{E}_{2n+3} = E_{2n+3} e^{j\beta_0 z \cos\theta_0} (\cos\theta_0 \hat{x} - \sin\theta_0 \hat{z}) \quad (85)$$

$$\vec{H}_{2n+3} = \frac{\beta_0}{\omega\mu} E_{2n+3} e^{j\beta_0 z \cos\theta_0} \hat{y} \quad (86)$$

E Perpendicular

$$\vec{E}_1 = E_1 e^{j\beta_0 z} \cos\theta_0 \hat{y} \quad (87)$$

$$\vec{H}_1 = \frac{\beta_0}{\omega\mu} E_1 e^{j\beta_0 z} \cos\theta_0 (-\cos\theta_0 \hat{x} + \sin\theta_0 \hat{z}) \quad (88)$$

$$\vec{E}_2 = E_2 e^{-j\beta_0 z} \cos\theta_0 \hat{y} \quad (89)$$

$$\vec{H}_2 = \frac{\beta_0}{\omega\mu} E_2 e^{-j\beta_0 z} \cos\theta_0 (\cos\theta_0 \hat{x} + \sin\theta_0 \hat{z}) \quad (90)$$

$$\vec{E}_3 = E_3 e^{j\beta_1 z} \cos\theta_1 \hat{y} \quad (91)$$

$$\vec{H}_3 = \frac{\beta_1}{\omega\mu_1} E_3 e^{j\beta_1 z} \cos\theta_1 (-\cos\theta_1 \hat{x} + \sin\theta_1 \hat{z}) \quad (92)$$

$$\vec{E}_4 = E_4 e^{-j\beta_1 z} \cos\theta_1 \hat{y} \quad (93)$$

$$\vec{H}_4 = \frac{\beta_1}{\omega\mu_1} E_4 e^{-j\beta_1 z} \cos\theta_1 (\cos\theta_1 \hat{x} + \sin\theta_1 \hat{z}) \quad (94)$$

$$\vdots$$

$$\vec{E}_{2n+1} = E_{2n+1} e^{j\beta_n z} \cos\theta_n \hat{y} \quad (95)$$

$$\vec{H}_{2n+1} = \frac{\beta_n}{\omega\mu_n} E_{2n+1} e^{j\beta_n z} \cos\theta_n (-\cos\theta_n \hat{x} + \sin\theta_n \hat{z}) \quad (96)$$

$$\vec{E}_{2n+2} = E_{2n+2} e^{-j\beta_n z} \cos\theta_n \hat{y} \quad (97)$$

$$\vec{H}_{2n+2} = \frac{\beta_n}{\omega\mu_n} E_{2n+2} e^{-j\beta_n z} \cos\theta_n (\cos\theta_n \hat{x} + \sin\theta_n \hat{z}) \quad (98)$$

$$\vec{E}_{2n+3} = E_{2n+3} e^{j\beta_0 z} \cos\theta_0 \hat{y} \quad (99)$$

$$\vec{H}_{2n+3} = \frac{\beta_0}{\omega\mu} E_{2n+3} e^{j\beta_0 z} \cos\theta_0 (-\cos\theta_0 \hat{x} + \sin\theta_0 \hat{z}) \quad (100)$$

Application of the tangential boundary conditions at the interface yields the following:

E Parallel

$z = 0$ :

$$E_1 \cos \theta_0 + E_2 \cos \theta_0 = E_3 \cos \theta_1 + E_4 \cos \theta_1 \quad (101)$$

$$E_1 \frac{\beta_0}{\mu} - E_2 \frac{\beta_0}{\mu} = E_3 \frac{\beta_1}{\mu_1} - E_4 \frac{\beta_1}{\mu_1} \quad (102)$$

$z = z_1$ :

$$E_3 \cos \theta_1 e^{j\beta_1 z_1 \cos \theta_1} + E_4 \cos \theta_1 e^{-j\beta_1 z_1 \cos \theta_1} = E_5 \cos \theta_2 e^{j\beta_2 z_1 \cos \theta_2} + E_6 \cos \theta_2 e^{-j\beta_2 z_1 \cos \theta_2} \quad (103)$$

$$E_3 \frac{\beta_1}{\mu_1} e^{j\beta_1 z_1 \cos \theta_1} - E_4 \frac{\beta_1}{\mu_1} e^{-j\beta_1 z_1 \cos \theta_1} = E_5 \frac{\beta_2}{\mu_2} e^{j\beta_2 z_1 \cos \theta_2} - E_6 \frac{\beta_2}{\mu_2} e^{-j\beta_2 z_1 \cos \theta_2} \quad (104)$$

$\vdots$   
 $z = z_n$ :

$$E_{2n+1} \cos \theta_n e^{j\beta_n z_n \cos \theta_n} + E_{2n+2} \cos \theta_n e^{-j\beta_n z_n \cos \theta_n} = E_{2n+3} \cos \theta_0 e^{j\beta_0 z_n \cos \theta_0} \quad (105)$$

$$E_{2n+1} \frac{\beta_n}{\mu_n} e^{j\beta_n z_n \cos \theta_n} - E_{2n+2} \frac{\beta_n}{\mu_n} e^{-j\beta_n z_n \cos \theta_n} = E_{2n+3} \frac{\beta_0}{\mu} e^{j\beta_0 z_n \cos \theta_n} \quad (106)$$

E Perpendicular

$$z = 0:$$

$$E_1 + E_2 = E_3 + E_4 \quad (107)$$

$$-E_1 \frac{\beta_0 \cos \theta_0}{\mu} + E_2 \frac{\beta_0 \cos \theta_0}{\mu} = -E_3 \frac{\beta_1 \cos \theta_1}{\mu_1} + E_4 \frac{\beta_1 \cos \theta_1}{\mu_1} \quad (108)$$

$$z = z_1:$$

$$E_3 e^{j\beta_1 z_1 \cos \theta_1} + E_4 e^{-j\beta_1 z_1 \cos \theta_1} = \quad (109)$$

$$E_5 e^{j\beta_2 z_1 \cos \theta_2} + E_6 e^{-j\beta_2 z_1 \cos \theta_2}$$

$$-E_3 \frac{\beta_1}{\mu_1} \cos \theta_1 e^{j\beta_1 z_1 \cos \theta_1} + E_4 \frac{\beta_1}{\mu_1} \cos \theta_1 e^{-j\beta_1 z_1 \cos \theta_1} = \quad (110)$$

$$-E_5 \frac{\beta_2}{\mu_2} \cos \theta_2 e^{j\beta_2 z_1 \cos \theta_2} + E_6 \frac{\beta_2}{\mu_2} \cos \theta_2 e^{-j\beta_2 z_1 \cos \theta_2}$$

$$z = z_n:$$

$$E_{2n+1} e^{j\beta_n z_n \cos \theta_n} + E_{2n+2} e^{-j\beta_n z_n \cos \theta_n} = E_{2n+3} e^{j\beta_0 z_n \cos \theta_0} \quad (111)$$

$$-E_{2n+1} \frac{\beta_n \cos \theta_n}{\mu_n} e^{j\beta_n z_n \cos \theta_n} + E_{2n+2} \frac{\beta_n \cos \theta_n}{\mu_n} e^{-j\beta_n z_n \cos \theta_n} = \quad (112)$$

$$-E_{2n+3} \frac{\beta_0 \cos \theta_0}{\mu_0} e^{j\beta_0 z_n \cos \theta_0}$$

Thus, we have generated  $N$  equations with  $N$  unknowns for both parallel and perpendicular incidence. These equations may easily be consolidated into matrix format; see Figures 12 and 13. Figure 14 is an example plot of a three layer system with layer conductivities of .5, 1, and

$\frac{k_0}{\beta_0}$	$-\frac{k_1}{\beta_1}$	$-\frac{k_1}{\beta_1}$	$\frac{k_1}{\beta_1} e^{-jz_1 k_1}$	$-\frac{k_1}{\beta_1} e^{-jz_1 k_1}$	0	0	...	0	0	0	$\frac{k_0}{\beta_0}$
$\frac{\beta_0}{\mu}$	$-\frac{\beta_1}{\mu_1}$	$-\frac{\beta_1}{\mu_1}$	$\frac{\beta_1}{\mu_1} e^{-jz_1 k_1}$	$-\frac{\beta_1}{\mu_1} e^{-jz_1 k_1}$	0	0	...	0	0	0	$\frac{\beta_0}{\mu}$
0	$\frac{k_1}{\beta_1} e^{-jz_1 k_1}$	$\frac{k_1}{\beta_1} e^{-jz_1 k_1}$	$\frac{k_1}{\beta_1} e^{-jz_1 k_1}$	$-\frac{k_2}{\beta_2} e^{-jz_1 k_2}$	$-\frac{k_2}{\beta_2} e^{-jz_1 k_2}$	$-\frac{k_2}{\beta_2} e^{-jz_1 k_2}$	...	0	0	0	0
0	$\frac{\beta_1}{\mu_1} e^{-jz_1 k_1}$	$\frac{\beta_1}{\mu_1} e^{-jz_1 k_1}$	$-\frac{\beta_1}{\mu_1} e^{-jz_1 k_1}$	$-\frac{\beta_2}{\mu_2} e^{-jz_1 k_2}$	$\frac{\beta_2}{\mu_2} e^{-jz_1 k_2}$	$\frac{\beta_2}{\mu_2} e^{-jz_1 k_2}$	...	.	.	.	0
0	0	0	0	$\frac{k_2}{\beta_2} e^{-jz_2 k_2}$	$\frac{k_2}{\beta_2} e^{-jz_2 k_2}$	$\frac{k_2}{\beta_2} e^{-jz_2 k_2}$	...	0	0	0	0
.	.	.	.	$\frac{\beta_2}{\mu_2} e^{-jz_2 k_2}$	$-\frac{\beta_2}{\mu_2} e^{-jz_2 k_2}$	$-\frac{\beta_2}{\mu_2} e^{-jz_2 k_2}$	...	0	0	0	0
.	.	.	.	.	.	.	...	0	0	0	0
0	0	0	0	0	0	0	...	$\frac{k_n}{\beta_n} e^{-jz_n k_n}$	$\frac{k_n}{\beta_n} e^{-jz_n k_n}$	$\frac{k_0}{\beta_0} e^{-jz_n k_0}$	0
0	0	0	0	0	0	0	...	$\frac{\beta_n}{\mu_n} e^{-jz_n k_n}$	$\frac{\beta_n}{\mu_n} e^{-jz_n k_n}$	$\frac{\beta_0}{\mu_0} e^{-jz_n k_0}$	0

Figure 12: Auxiliary Matrix for Parallel Polarization ( $k_n = \beta_n \cos \theta_n$ )



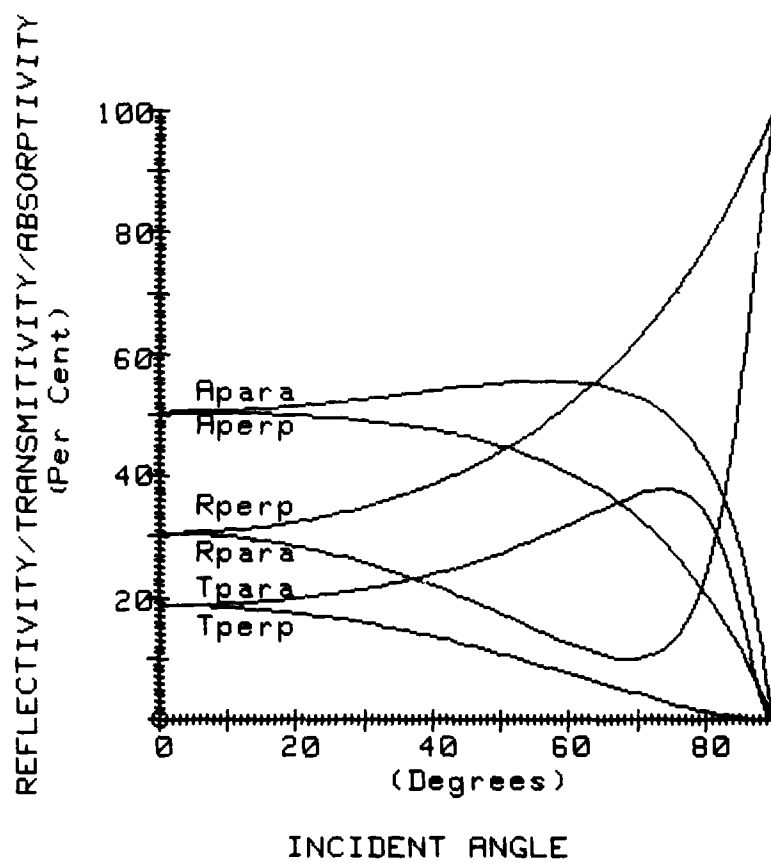


Figure 14: Three Layer Electromagnetic Response

1.5 mho/m respectively. See Appendix D for a listing of the computer program written for a Hewlett-Packard 9845B computer; it will handle up to 10 layers.

It should be pointed out that this is not the first time the electromagnetic N-layer problem has been solved. Hansen <sup>16</sup> develops a procedure in which explicit equations are derived for the mean-square electric fields induced by plane electromagnetic radiation in a single boundary, single layer, and N-layer system. His approach is to allow for a complex permittivity in the energy absorption process rather than using Ohm's law explicitly in the solution of Maxwell's equations. It is for this reason and as a result of the desire to present a more straight forward approach, that the preceding chapter was developed. Additionally, interested readers may also refer to Wait <sup>17</sup> for an in-depth discussion of electromagnetic absorption by stratified media. Most of Wait's discussion is directed at the electromagnetic interaction occurring at the surface of a stratified earth.

## CHAPTER V

## THERMAL ANALYSIS

The simplest analysis is one that assumes a steady state situation with no heat losses at the  $z=z_n$  interface. In practice this is not a bad assumption since our Nth layer may be made of a low thermal conductivity material such as one of the many foams available. Also, it has been demonstrated that for relatively thin layers (thickness less than one millimeter) steady state is reached very quickly (in most cases less than five minutes for  $10 \text{ mW/cm}^2$  incident power).

A rough estimate for the transient response of the system may be made as follows. Consider the semi-infinite slab insulated at  $z=L$  as shown in Figure 15 below.

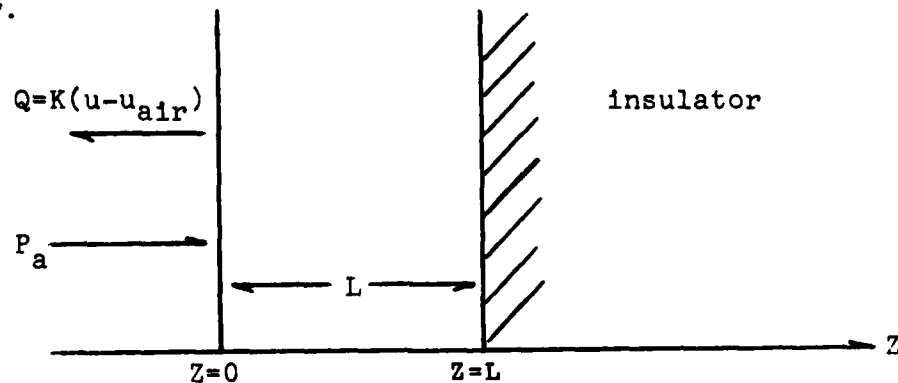


Figure 15: Three Layer Thermal Transient Response

$P_a$  = total absorbed power ( $\text{watt/m}^2$ )

$Q$  = total heat loss (Newton cooling)

$u$  = temperature of the layer (K) which is assumed uniform throughout

If  $u$  is assumed constant throughout our thin layer (this assumes the thermal conductivity,  $\kappa$ , is large or the thickness,  $L$ , is small or both for the layer), we may write the energy equation for the system as follows:

$$P_a \Delta t = K(U - U_{\text{air}}) \Delta t + \rho c \Delta u L \quad (113)$$

where  $\Delta t$  = time (s)

$$K = \text{constant (J/s-m}^2\text{-K)}$$

$$\rho = \text{mass density (Kg/m}^3\text{)}$$

$$c = \text{specific heat (J/Kg-K)}$$

Solving for  $\Delta u / \Delta t$ , we have

$$\frac{\Delta u}{\Delta t} = \frac{1}{\rho c L} P_a - K(U - U_{\text{air}}) \quad (114)$$

Taking the limit as  $\Delta t \rightarrow 0$ , we have

$$\frac{du}{dt} = \frac{1}{\rho c L} P_a - K(U - U_{\text{air}}) \quad (115)$$

This is a linear homogenous differential equation which has a solution given by

$$U = U_{\text{air}} + \frac{P_a}{K} (1 - e^{-\frac{K}{\rho c L} t}) \quad (116)$$

Thus, we may calculate a time constant  $\tau$  given by

$$\tau = \frac{\rho c L}{K} \quad (117)$$

For example, a thin layer of water 100 microns thick has a time constant of approximately 210 sec or about 3.5 minutes which is in agreement with our experimental observation. Finally, a thin system made up of  $N$  layers would yield a heat term given as  $\Delta u \sum_{i=1}^N \rho_i c_i L_i$  if the

layers are heated at a relatively constant rate (same  $u$  throughout); hence the time constant for the layered system may be approximated by

$$\tau \approx \frac{1}{K} \sum_{i=1}^N \rho_i c_i L_i \quad (118)$$

It is important to point out that the above development assumed a linear heat loss at the  $z=0$  surface. In fact, this term consists of a convective term and a radiative (infrared) term which is in no way linear for large temperature increases (large  $P_a$ ). However, the steady state surface temperature may still be calculated using numerical techniques for this non-linear case.

We begin the steady state solution as before by writing the energy equation for the system; thus, we have absorbed power,  $P_a$ , equal to convective losses,  $Q_{con}$ , plus infrared losses,  $Q_{ir}$ . For the two loss terms we have<sup>18,19,20</sup>

$$Q_{con} = h (U_o - U_{air})$$

and

$$Q_{ir} = F_e \gamma (U_o^4 - U_{air}^4)$$

where

$h$  = convective heat transfer coefficient (watt/m<sup>2</sup>-K)

$U_o$  = steady state surface temperature (K)

$U_{air}$  = ambient air temperature (K)

$F_e$  = surface emissivity

$\gamma$  = Stefan-Boltzman constant (5.67x10<sup>-8</sup> watt/m<sup>2</sup>-K<sup>4</sup>)

It has been shown that  $h$  for a vertical flat plate may be approximated by <sup>21</sup>

$$h \approx \frac{1.42 (U_o - U_{air})^\delta}{H^\delta}$$

where  $H$  is the plate height and  $\delta$  is a number that falls in the range  $.1 < \delta < .6$ . The number,  $\delta$ , is a function of such things as atmospheric pressure, humidity, etc. Furthermore,  $P_a$  is simply the incident power minus the reflected and transmitted power; therefore, we may write,

$$\frac{1}{2} \sqrt{\frac{\epsilon_o}{\mu_o}} (E_1^2 - E_2^2 - E_{2n+3}^2) = \frac{1.42}{H^\delta} (U_o - U_{air})^{1+\delta} + F_{e\gamma} (U_o^4 - U_{air}^4) \quad (119)$$

It is important to note that it is necessary to consider both convection and infrared radiation in the temperature range near 20C as indicated in Figures 16 through 18. This figure illustrates the ratio of  $Q_{ir}/Q_{con}$  for a surface temperature increase of 10C with an ambient air temperature of 20C. This ratio is nominally between 1 and 2 over this range indicating that both processes are significant in the energy loss transport and therefore each must be considered.

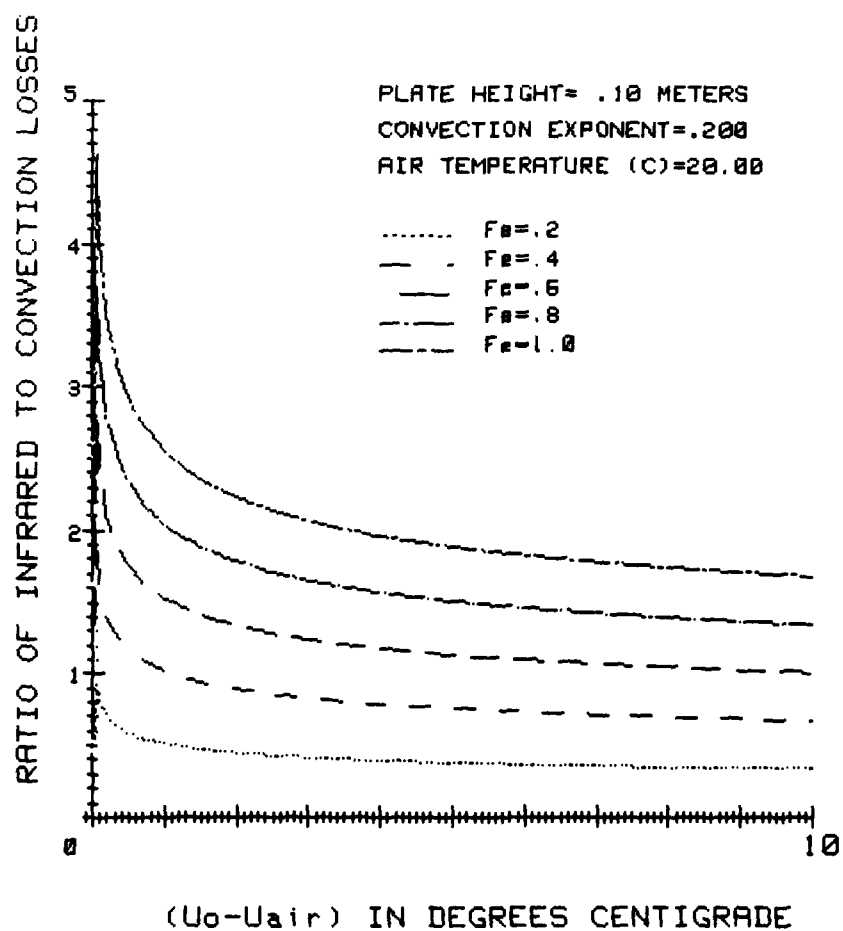


Figure 16: Infrared Versus Convection Comparison

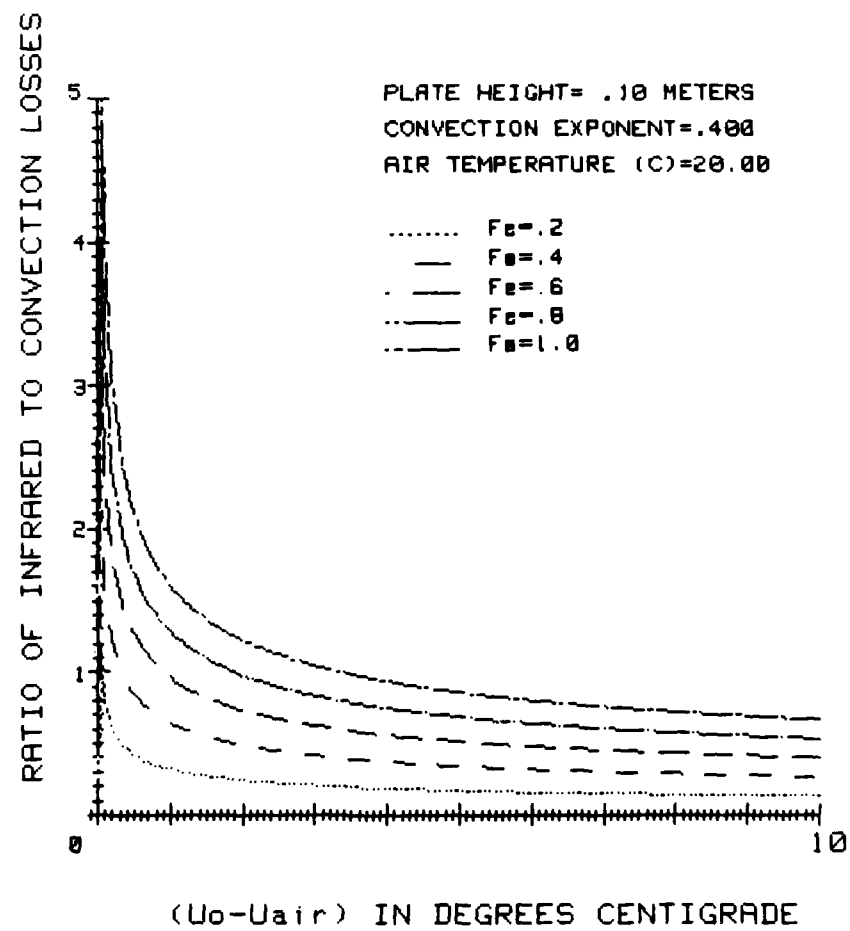


Figure 17: Infrared Versus Convection Comparison

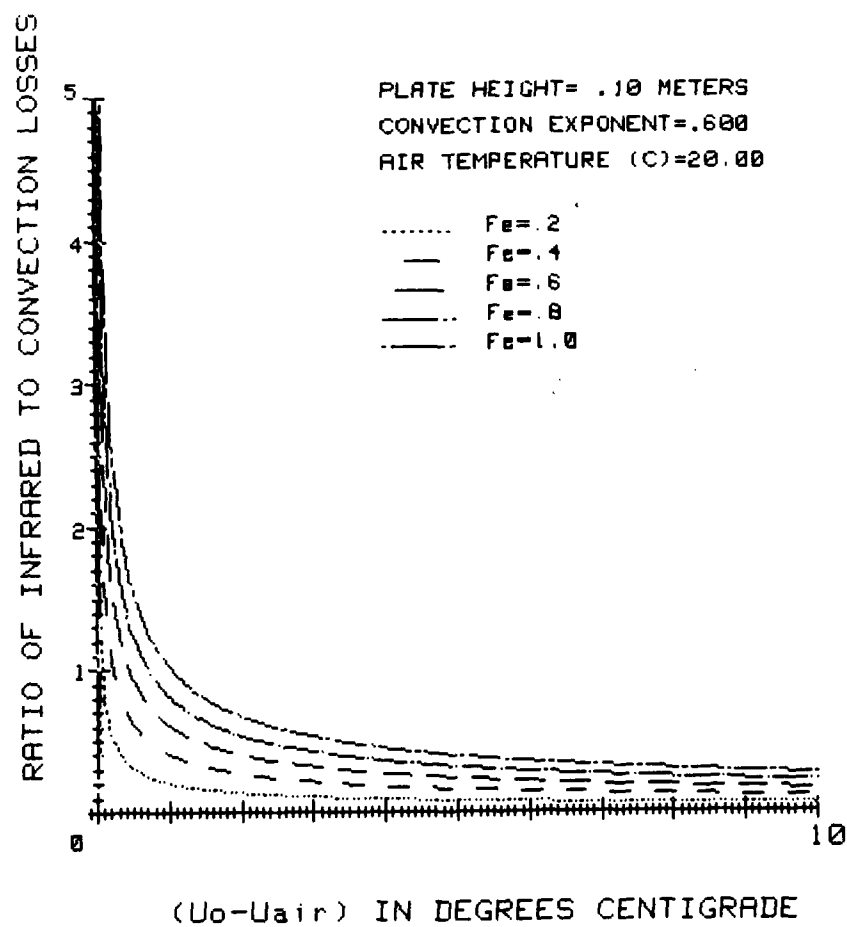


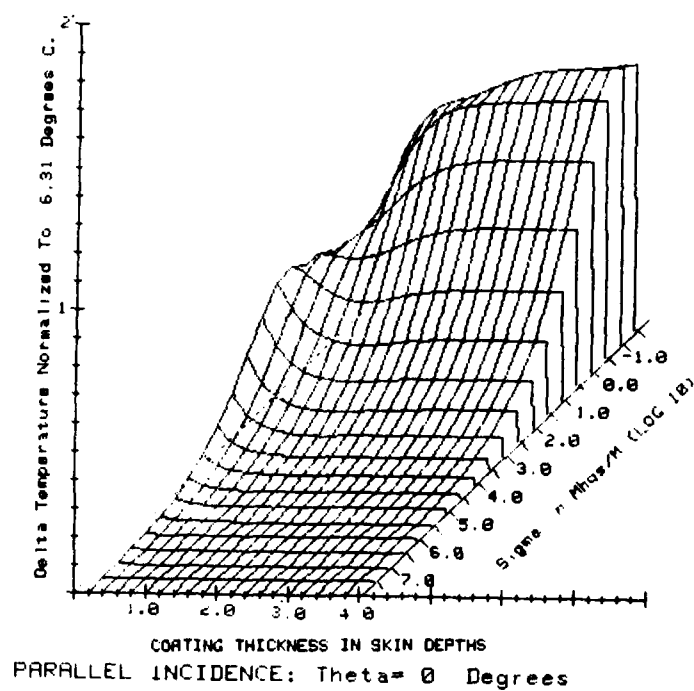
Figure 18: Infrared Versus Convection Comparison

Even though equation 119 is relatively simple in appearance, it is important to recognize that  $U_0$  is in fact a function of several variables. These variables include the layer thicknesses, relative permittivities, relative permeabilities, electrical conductivities, surface emissivity, convection exponent, convection coefficient, sample height, incident microwave power level, microwave frequency, and microwave incident angle. Thus, in general  $U_0$  is a function of  $4N+7$  variables where  $N$  is the number of layers considered. Even for the case of  $N=1$ , we see that  $U_0$  must be considered in 11 space in order to analyze all the variables and their interaction at once. Clearly, we can visually represent 3 space but not 11; therefore, in order to graphically display the interactions of the more dynamic variables--the ones over which we have direct control--we fix the values of such things as incident angle, power level, convection exponent, etc., and allow only coating thickness and coating electrical conductivity to vary which then yield our equilibrium surface temperature,  $U_0$ . Topologically then, by allowing only two of the variables to vary we are in effect looking only at a particular plane in  $4N+7$  space.<sup>22</sup> As was indicated earlier, this is sufficient for our analysis since we are observing the more easily manipulated variables in

the actual design of a particular coating.

Equation 119 is readily solved numerically using a Newton algorithm. This equation is solved for the N-layer system and is represented on a three dimensional plot. The axis variables are layer number 1's electrical conductivity, layer number 1's thickness, and differential surface temperature increase. Figures 19 to 22 are representative plots of a typical 2 layer system at various incident angles and polarizations.

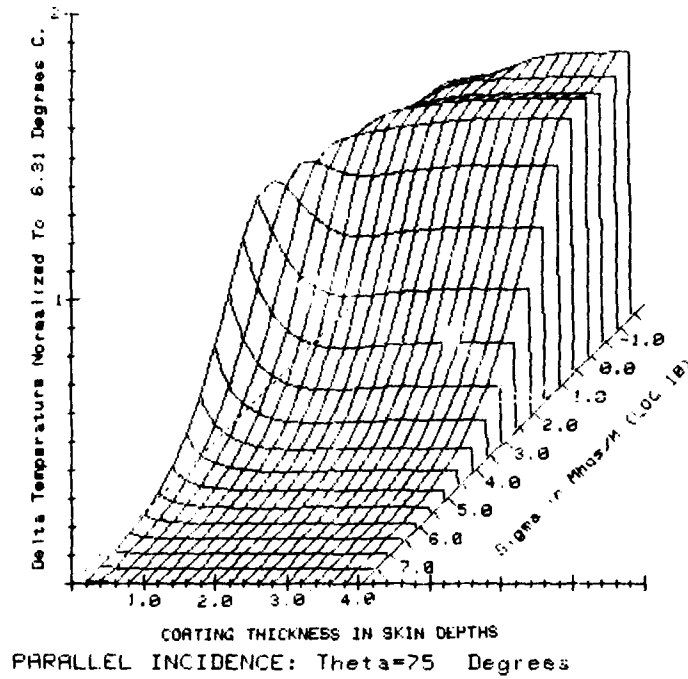
Later in the experimental verification in Chapter VI, it will be important to realize that a given coating will be considered as a function of incident power level only. The coating and all its particular characteristics are already fixed; they cannot be varied without constructing an entirely new coating configuration. Thus, we will calculate equilibrium temperature as a function of incident power level using equation 119 and then compare these values to the actual measured values. Topologically then, we will be considering single lines in  $4N+7$  space.



Number of Layers= 2      Power in W/cm<sup>2</sup>=10      Freq. in GHz=2.45  
 Air Temp -C=19.7      Convective E p= .48      Emissivity= .90      Plate Height -M= .100

Sigma(1)=3.16E-02      Mu(1)= 1.0      Epsilon(1)=1.30      Thickness(1)=2.29E-01  
 Sigma(2)=0.00E+00      Mu(2)= 1.0      Epsilon(2)=2.40      Thickness(2)=1.25E-02

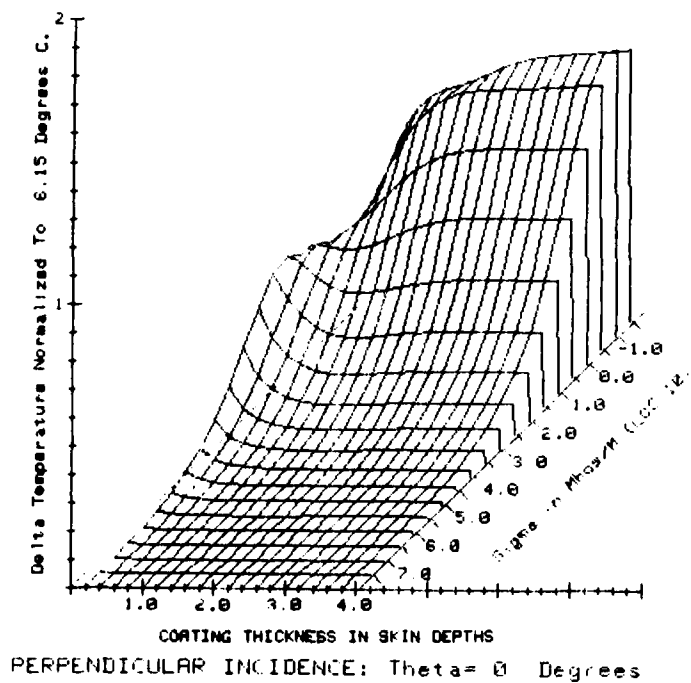
Figure 19: Two Layer Electromagnetic Heating Profiles



Number of Layers= 2      Power in W Cm<sup>-2</sup>=10      Freq. in GHz=2.45  
 Air Temp (C)=19.7      Convective Exp= .48      Emissivity=.90      Plate Height (M)= .100

Sigma(1)=3.16E-02      Mu(1)= 1.0      Epsilon(1)=1.30      Thickness(1)=2.29E-01  
 Sigma(2)=0.00E+00      Mu(2)= 1.0      Epsilon(2)=2.40      Thickness(2)=1.25E-02

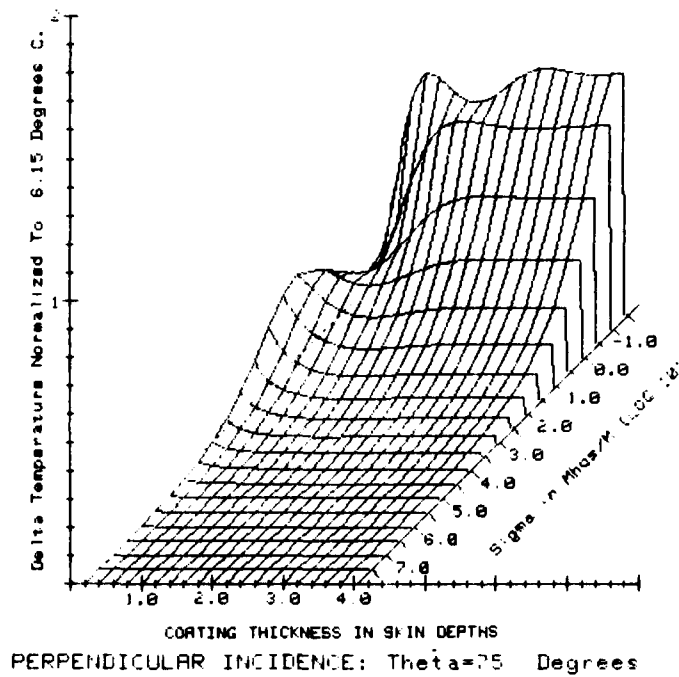
Figure 20: Two Layer Electromagnetic Heating Profiles



Number of Layers= 2      Power in W/Cm 2=10      Freq. in GHz=2.45  
 Air Temp (C)=19.7    Convective Exp= .48    Emissivity= .90    Plate Height in= .100

Sigma(1)=8.16E-02    Mu(1)= 1.0    Epsilon(1)=1.30    Thickness(1)=2.49E-01  
 Sigma(2)=0.00E+00    Mu(2)= 1.0    Epsilon(2)=2.40    Thickness(2)=1.25E-02

Figure 21: Two Layer Electromagnetic Heating Profiles



Number of Layers= 2      Power in W/Cm 2=10      Freq. in GHz=2.45  
 Air Temp (C)=19.7    Convective E p= .48    Emissivity= .90    Plate Height in M= .100

Sigma(1)=3.16E-02    Mu(1)= 1.0    Epsilon(1)=1.30    Thickness(1)=2.29E-01  
 Sigma(2)=0.00E+00    Mu(2)= 1.0    Epsilon(2)=2.40    Thickness(2)=1.25E-02

Figure 22: Two Layer Electromagnetic Heating Profiles

## CHAPTER VI

## EXPERIMENTAL VERIFICATION

The coupling of the electromagnetic solution with the thermodynamic solution for a system of  $N$  layers yields a theoretically valuable tool for predicting the surface temperatures of a layered system. However, before this development can be used with any certainty, we must experimentally verify the accuracy of the predicted results. The overall verification was a three step process. We first measured the convective heat transfer exponent,  $\delta$ , and then examined five different conductive samples as they were exposed to various microwave power levels ranging from 10 to 40 mW/cm<sup>2</sup>. Irradiation frequency was fixed at 2.54 GHz. An appropriate convective heat transfer coefficient was then chosen that would allow the best possible fit between experimental and theoretical data.

The convective heat transfer exponent was measured in the following manner. A constant power was generated within a thin conductive coating (aquadaq) by keeping a constant direct current voltage applied accross the sample. This sample was insulated with two inches of styrofoam insulation on the sides and back so that we

could closely approximate our model which assumed no conductive heat losses. The sample was allowed to reach steady state conditions before the surface temperature was measured. Surface temperature measurements were made with an infrared camera capable of measuring temperature variations to within one tenth degree Centigrade. We then calculated an absorbed power density given by

$$P_a = VI/A \quad (123)$$

where

V = applied voltage across sample (volts)

I = current through the sample (amperes)

A = area of the sample (meters squared)

This absorbed power must be dissipated via surface convection and infrared radiation; therefore, as in the development in Chapter 5, we equated the power gains to the power losses which resulted in

$$VI/A = \frac{1.42}{H^\delta} (U_o - U_{air})^{1+\delta} + F_e \gamma (U_o^4 - U_{air}^4) \quad (124)$$

Surface emissivities have been measured by other researchers<sup>23,24</sup> and are thus known quantities. If we assume the convective coefficient (1.42) remains relatively constant, the only variable remaining is the convective exponent which may be calculated. Its value is given by

$$\delta = \frac{1}{\ln\left(\frac{U_o - U_{air}}{H}\right)} \ln \left[ \frac{1}{1.42 (U_o - U_{air})} \left( \frac{VI}{A} - F_e \gamma (U_o^4 - U_{air}^4) \right) \right] \quad (125)$$

Figure 23 illustrates the general layout of the experiment.

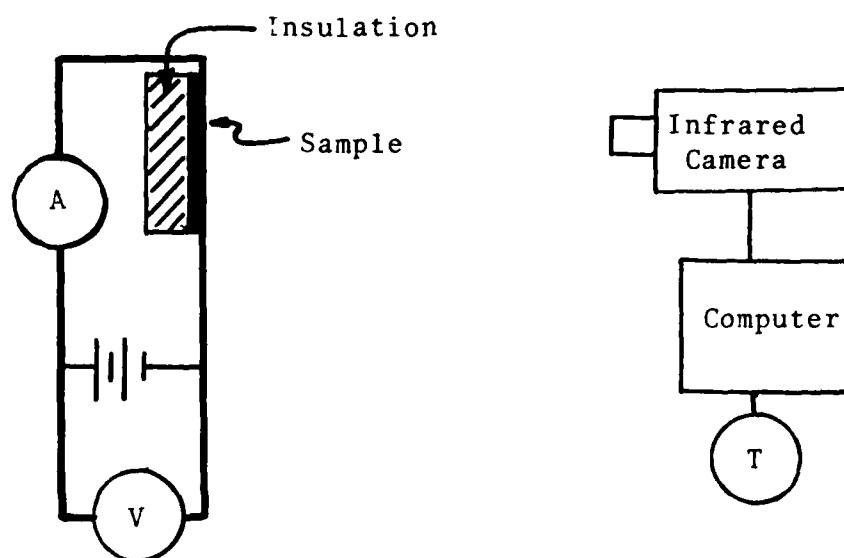


Figure 23: Schematic of Convective Exponent Experiment

Test equipment used in the experiment consisted of the following:

<u>Nomenclature</u>	<u>Identification</u>
Power Supply	Regulated D.C. Power Supply 0-50 VDC, 0-1.5A Kepco Manufacturing Co. Flushing, New York
Ammeter	Digital Multimeter Model 3466A Hewlett-Packard Mfg. Co. Colorado Springs, CO

Voltmeter

Digital Multimeter  
Model 3466A  
Hewlett-Packard Mfg. Co.  
Colorado Springs, CO

Infrared Camera

Thermovision Model 680  
AGA Manufacturing Co.  
Secaucus, New Jersey

The sample measured consisted of a 10 cm square of conductive coating 59 microns in thickness and mounted vertically. Room temperature was maintained at  $20.5 \pm 1$  C throughout the experiment. Five different direct current power levels were observed to determine the linearity of the convection exponent with temperature. Figure 24 illustrates the experimental results in which the average value of the convective exponent was determined to be 0.53. Having a value for the convection exponent, we then verified the N-layer electromagnetic interaction.

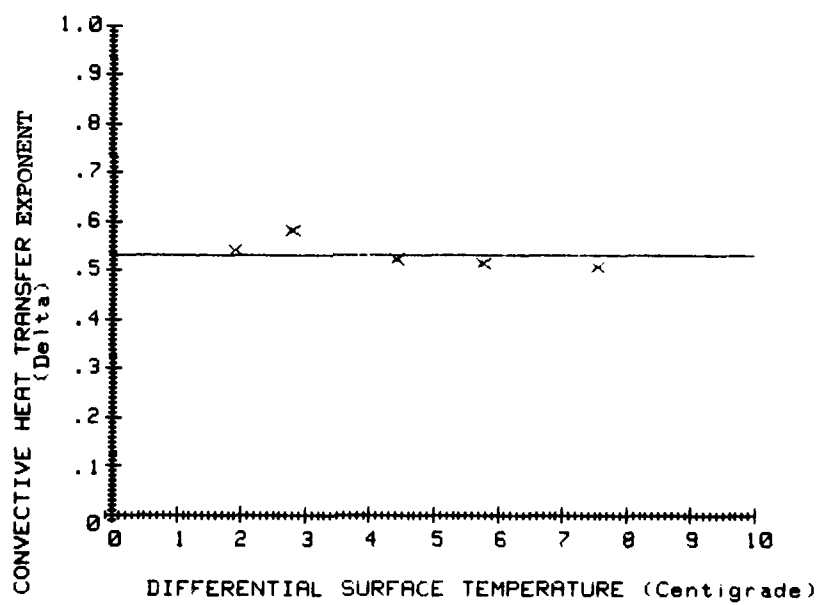


Figure 24: Results of Convective Exponent Measurements

There are two major shortfalls of the N-layer model which have a drastic impact on the verification. The first of these is the semi-infinite plane assumption. We obviously cannot construct a semi-infinite layered system in the laboratory and irradiate it uniformly with a plane electromagnetic wave; therefore, the approach is to use a very small (much less than a wavelength) multilayered sample. By avoiding resonant shapes and sizes the sample will experience a relatively uniform electric field across the surface and the observed surface temperature will approximate that observed on a semi-infinite sheet.

Secondly, from the thermodynamics point of view, we assumed the conductive coating would be placed on a perfect insulator and thus no thermal conduction would occur. Obviously, perfect thermal insulators do not exist either; hence, we have another source of error. To minimize the thermal conduction losses, samples were placed on styrofoam blocks with a minimum of two inches of insulation on all but the front surface. Styrofoam proved to be well suited for this purpose since it is an excellent insulator and has a measured electrical permittivity of approximately 1.1 (10 GHz). Electrically, therefore, the foam was virtually invisible while thermally it provided the desired insulation. The samples consisted of 1, 2, and 3 layer configurations all

cut to be 1.5 cm square. In addition to the equipment already listed, the following instruments were also used:

<u>Nomenclature</u>	<u>Identification</u>
Microwave Generator	Microwave Generator 2.45 GHz, 0-200 Watt Kiva Instrument Co. Rockville, Maryland
Power Meter	Radiation Hazard Meter (RAHAM), Model 481 General Microwave Farmingdale, New York

Figure 25 illustrates the physical arrangement of the experiment.

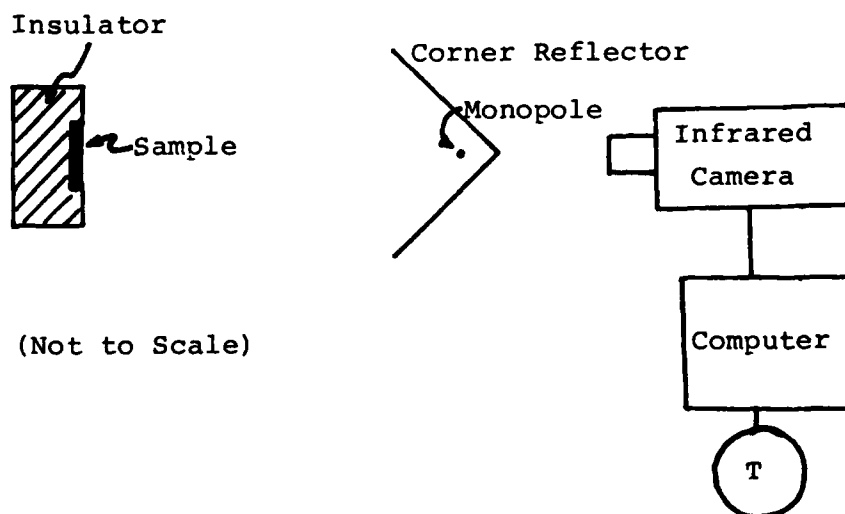


Figure 25: Schematic of N-Layer Verification

The procedure itself was relatively straight forward. The microwave power meter was used to measure the free field power level of the 2.45 GHz radiation. After the power was adjusted to the proper value the layered sample was placed at the point where the power was measured. The samples were then allowed to reach thermal equilibrium prior to measuring their surface temperatures with the infrared camera. In most cases thermal equilibrium was reached in less than 10 minutes; however, the samples were irradiated at least 20 minutes each. Each sample was exposed to power levels of 10, 15, 20, 30, and 40  $\text{mW/cm}^2$ . The measured temperature for each is plotted versus input power in figures 26 to 30. Calculated values are also plotted on the same graph for comparison purposes. The single greatest variation occurred for the two layer aquadaq/plexiglas combination. In this case the average deviation from theoretical values was about 33 percent. The other four samples yielded much better results of typically less than 20 percent variation. To obtain the theoretical values shown we had to use a convective coefficient of 15 rather than the 1.42 used in the theoretical discussion in Chapter V thus indicating that convection is much more significant than originally assumed.

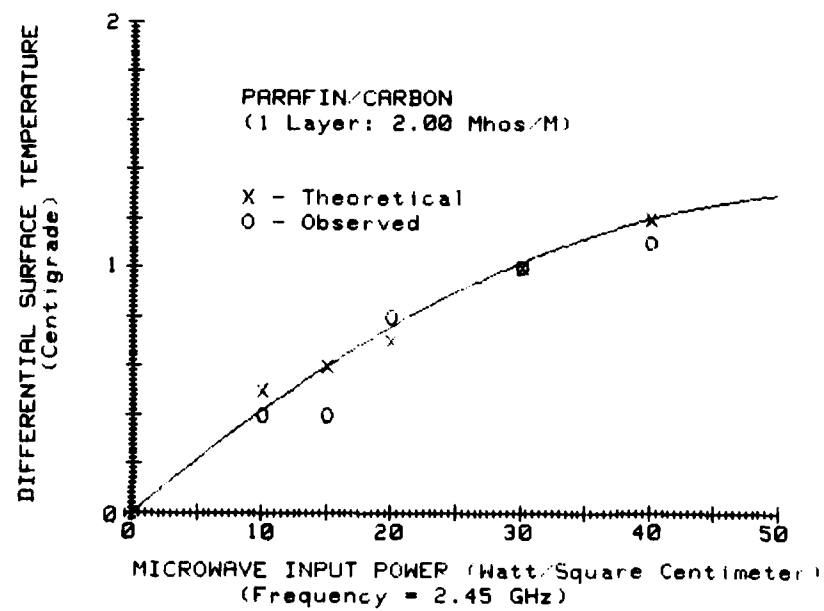


Figure 26: One Layer Electromagnetic Heating

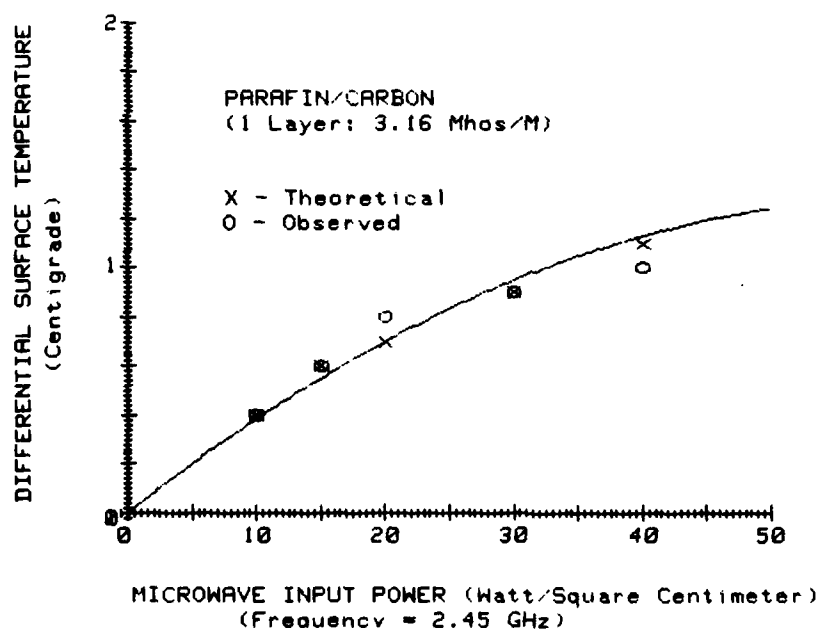


Figure 27: One Layer Electromagnetic Heating

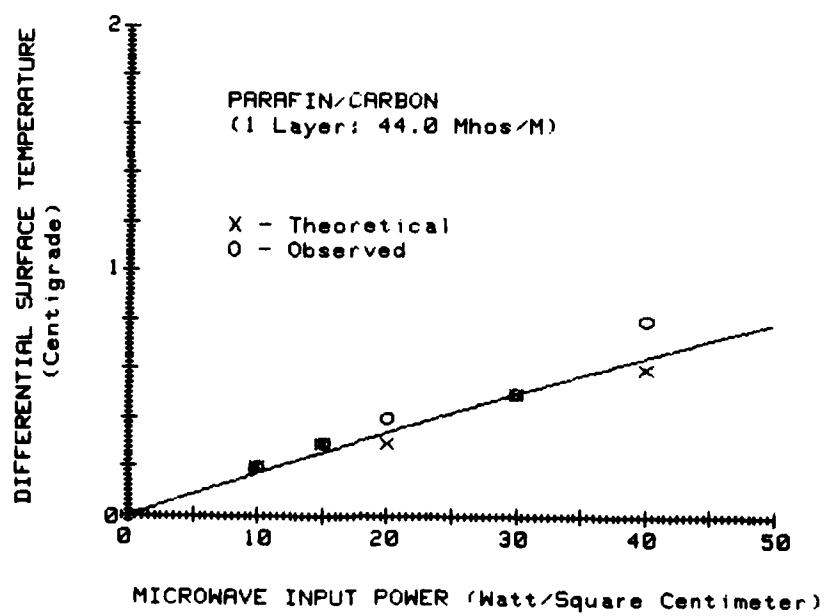


Figure 28: One Layer Electromagnetic Heating

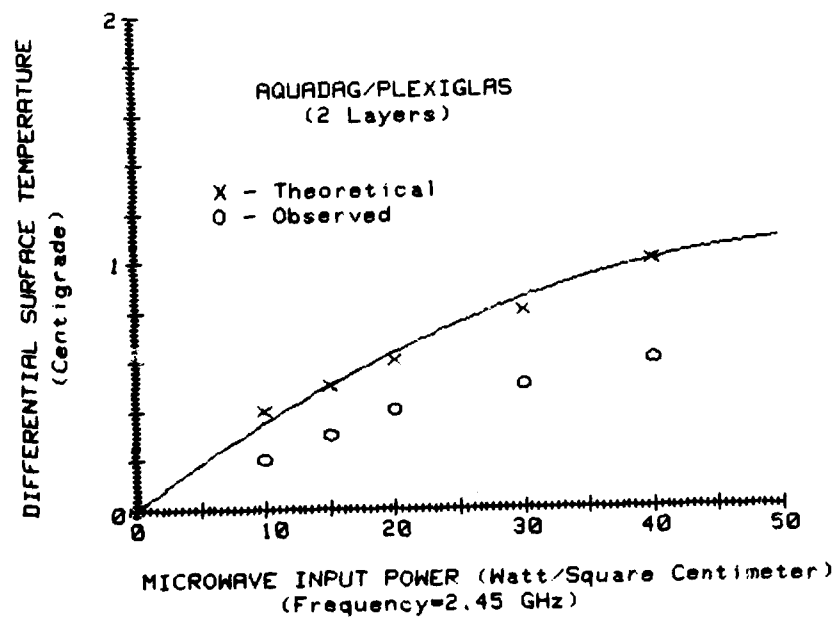


Figure 29: Two Layer Electromagnetic Heating

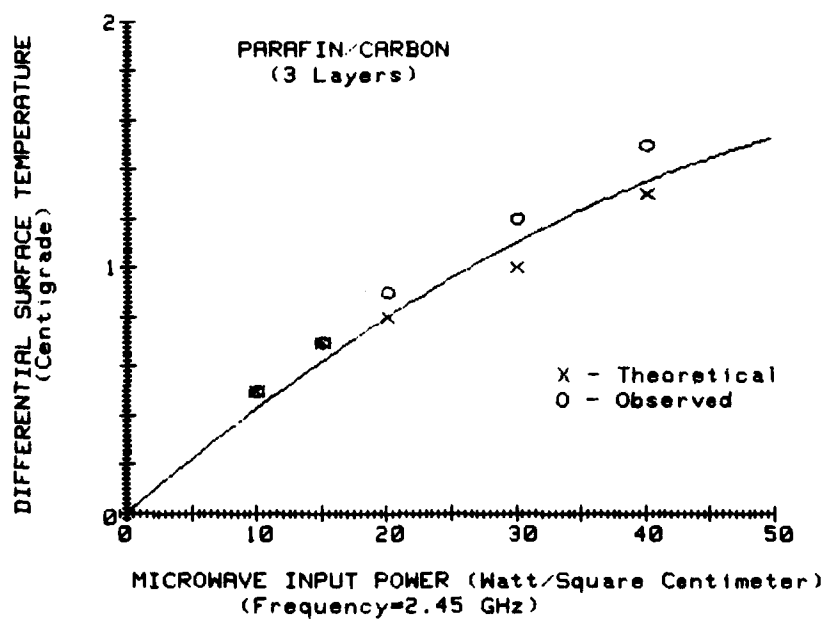


Figure 30: Three Layer Electromagnetic Heating

## CHAPTER VII

## APPLICATION OF MODEL TO TWO-DIMENSIONAL TARGETS

As was pointed out earlier in the initial development of our coating model, a possible limitation to its use results from the one-dimensional analysis itself. This chapter discusses the problem of applying the one-dimensional coating model to the more "real world" two-dimensional problem. In particular, the experimental verification itself uses an electrically small two-dimensional square sample to approximate the current present in the semi-infinite one-dimensional case. Also, the question of "nearest neighbor" influence is important when considering electrically large samples. That is, when we observe a temperature at a point on the surface of a coated shape, how well does that relate to the currents present directly under it? Clearly, the currents in the neighborhood of this point must contribute something to the coating temperature but the question is, "how significant is their influence?" In order to qualitatively address each of these situations, we will first consider the electrically small sample as applied to the verification experiment and later discuss the "nearest neighbor" considerations in regards to electrically large models.

As was indicated earlier in Chapter VI, the verification process for the semi-infinite one-dimensional model is a difficult

one. Physically, we were constrained in size by an anechoic chamber with a maximum usable width of approximately one meter. In the far field we had an area of approximately 20 x 15 cm in which the microwave power density was relatively uniform. Electrically we could achieve a power density of  $20 \text{ mW/cm}^2$  in the above area at a frequency of 2.45 GHz. The radiation pattern was formed by use of a quarter wave monopole in conjunction with a parabolic reflector over an aluminum ground plane. See figures 31, 32, and 33 below.

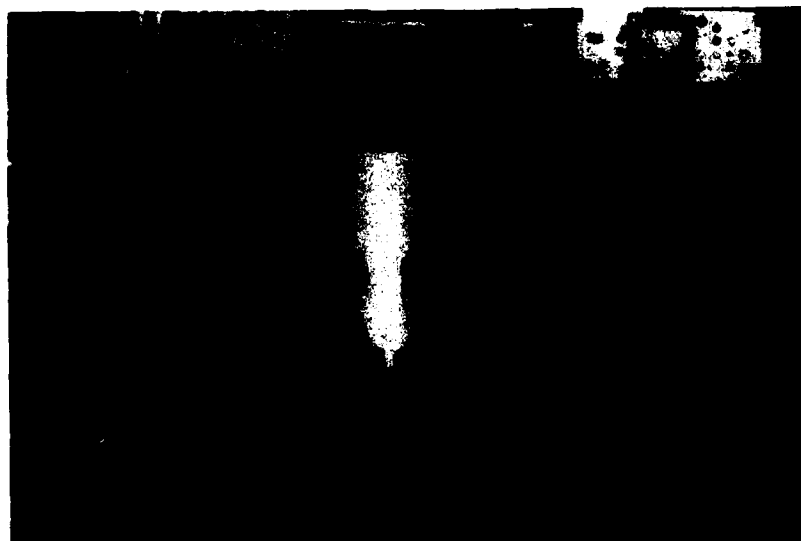


Figure 31: Photograph of Monopole and Parabolic Reflector



Figure 32: Actual Quarter Wave Monopole

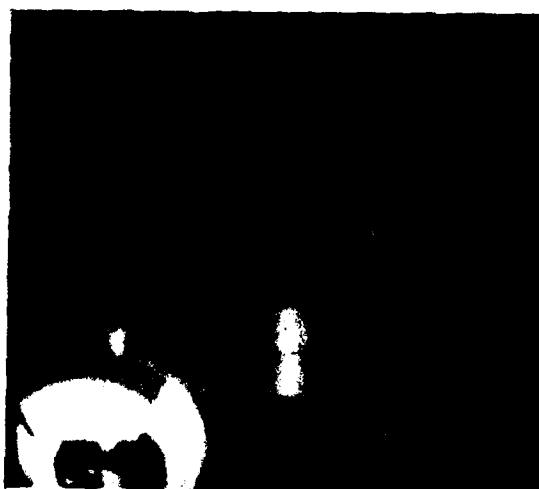


Figure 33: Anechoic Chamber With Electrically Small Target and Infrared Camera in Foreground

The verification problem is such that it could proceed in either of two ways. The first was to construct several electrically very large samples that by nature of their size would approximate the semi-infinite condition of our model. There are several problems associated with this approach. Large coated targets are considerably difficult to construct since they must have completely uniform conductive coatings over their surfaces. The problem is even more difficult with two or three composite layers. The largest problem, however, results from the nature of the anechoic chamber itself. That is, if we placed a large target completely across the chamber, nearly all of the incident microwave field would be back scattered into the parabolic emitter which in effect would turn our anechoic chamber into some type of tuned cavity. Thus, we would know nothing about the fields present at the coating. The back scatter problem could be reduced or eliminated by removing the parabolic reflector and substituting anechoic absorbers but then our incident field strength would have suffered drastically. Therefore, because of the mechanical and electrical difficulties inherent with the large model approximation, it appears more desirable to use an electrically small model to approximate the semi-infinite results.

The electrically small sample has several advantages. First, it is much easier to fabricate and characterize electrically. In fact we can measure the coating thickness directly

using a good micrometer since the micrometer jaws nearly completely cover the sample's face. The back scatter problem is practically nonexistent. Similar to developments elsewhere, if we consider a sample which is electrically small and assume the incident field induces a relatively uniform surface current across the sample faces then we may treat it as a Huygen's source (We will discuss the uniformity assumption more later.)<sup>25</sup>. See figure 34 below.

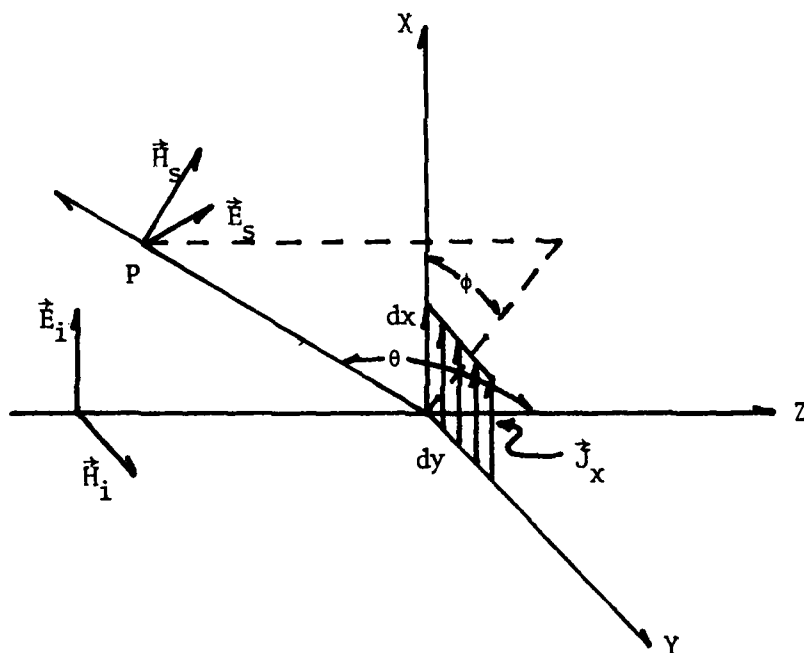


Figure 34: A Uniform Current Sheet Radiator

If we further assume the induced current is not only uniform but also the same as that induced on an infinite conductor and that contour charge is negligible, then we have  $J_x = |\vec{H}_i|$ . The radiation field is  $\vec{E}_s = -j\omega\vec{A}$  <sup>25</sup> (126)

where

$$\vec{A} = A_x \hat{x} = \mu \frac{(\int J_x dy) dx e^{-j\beta r}}{4\pi r} \hat{x} \quad (127)$$

$$E_s^\theta = -j\omega A_x \cos\phi \cos\theta \quad (128)$$

$$E_s^\phi = j\omega A_x \sin\phi \quad (129)$$

Therefore, the approximate magnitude of the backscattered field on the z axis and polarized in the x direction ( $\theta = 0$ ,  $\phi = 0$ ) would be

$$|E_s|_0 = \omega \left( \frac{E_i}{4\pi c} \frac{dy dx}{r} \right) \quad (130)$$

Assuming that this field is redirected by the parabolic reflector with some gain G, the redirected field strength at the target would be

$$|E_t| = \frac{\omega G E_i}{8\pi c} \frac{dy dx}{r} \quad (131)$$

The percentage of re-reflected to incident power at the target face would be

$$\frac{|E_t|^2}{|E_i|^2} = \left[ \frac{\omega G}{8\pi c} \frac{dy dx}{r} \right]^2 \times 100 \quad (132)$$

For

$$\omega = 2\pi \times 2.45 \times 10^9 \text{ Hz}$$

$$dy = dx = .015 \text{ m}$$

$$G \approx 20$$

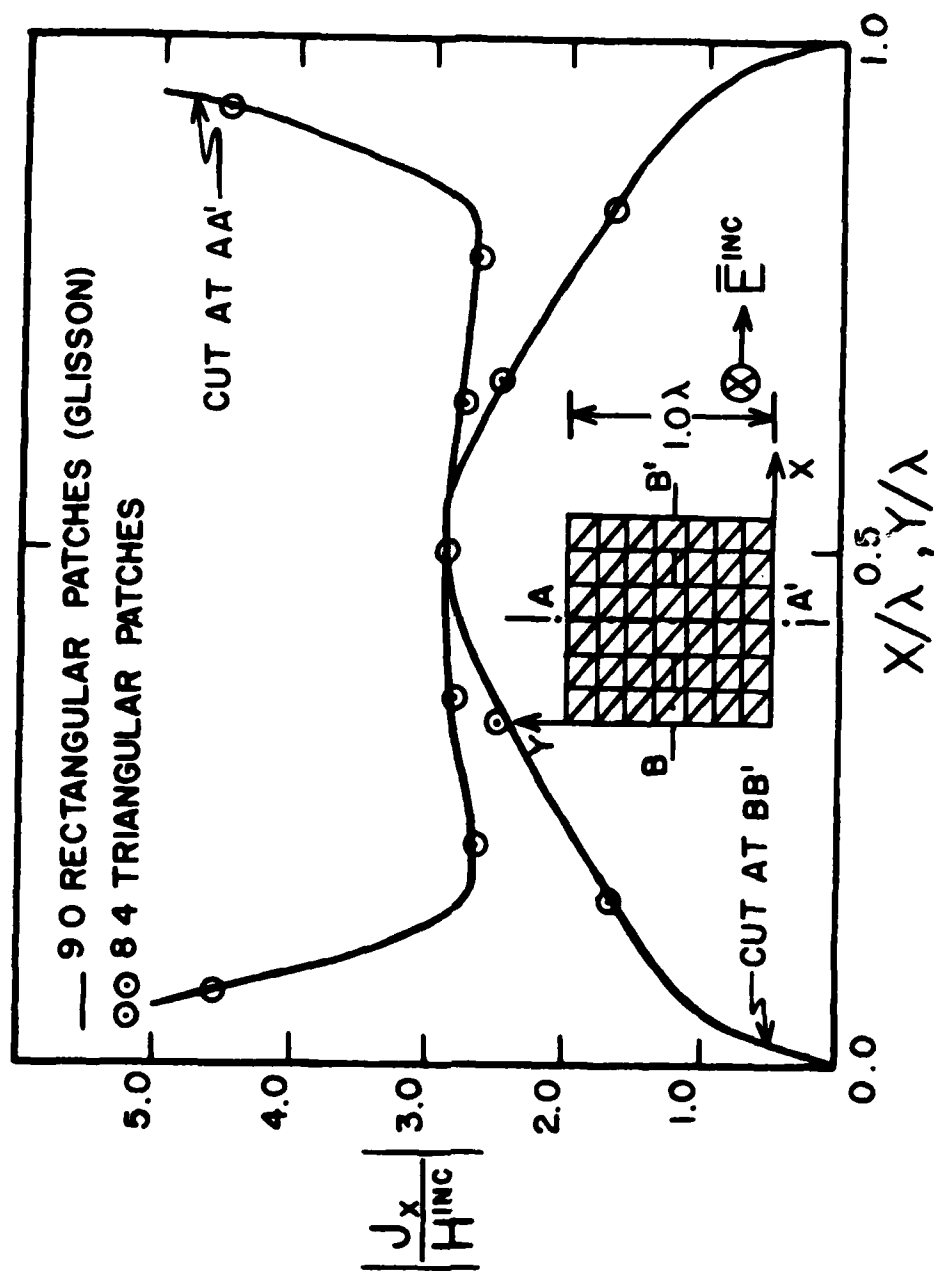
$$r = 1.3 \text{ m}$$

$$c = 3 \times 10^8 \text{ m/s}$$

$$\text{we have } \frac{|E_t|^2}{|E_i|^2} \approx 5 \times 10^{-3} \% \quad (133)$$

In other words, our small sample size interferes with the incident field only a small amount. One obvious advantage of this is that we can measure and characterize the microwave fields within the anechoic chamber with no targets present and then be sure that this characterization changes very little with the addition of a small object.

Two other considerations that must be addressed before the small sample may be used with confidence concern the surface current uniformity and magnitude on such targets. Considerable insight is provided to both of these questions in an article by Wilton, et al, in which a method of moment solution is considered for various size flat conducting plates. See figures 35 and 36 below for a profile of surface currents on a  $1.0\lambda$  and  $0.15\lambda$  square plate<sup>26</sup>.

Figure 35:  $1.0\lambda$  Square Plate Current Distribution

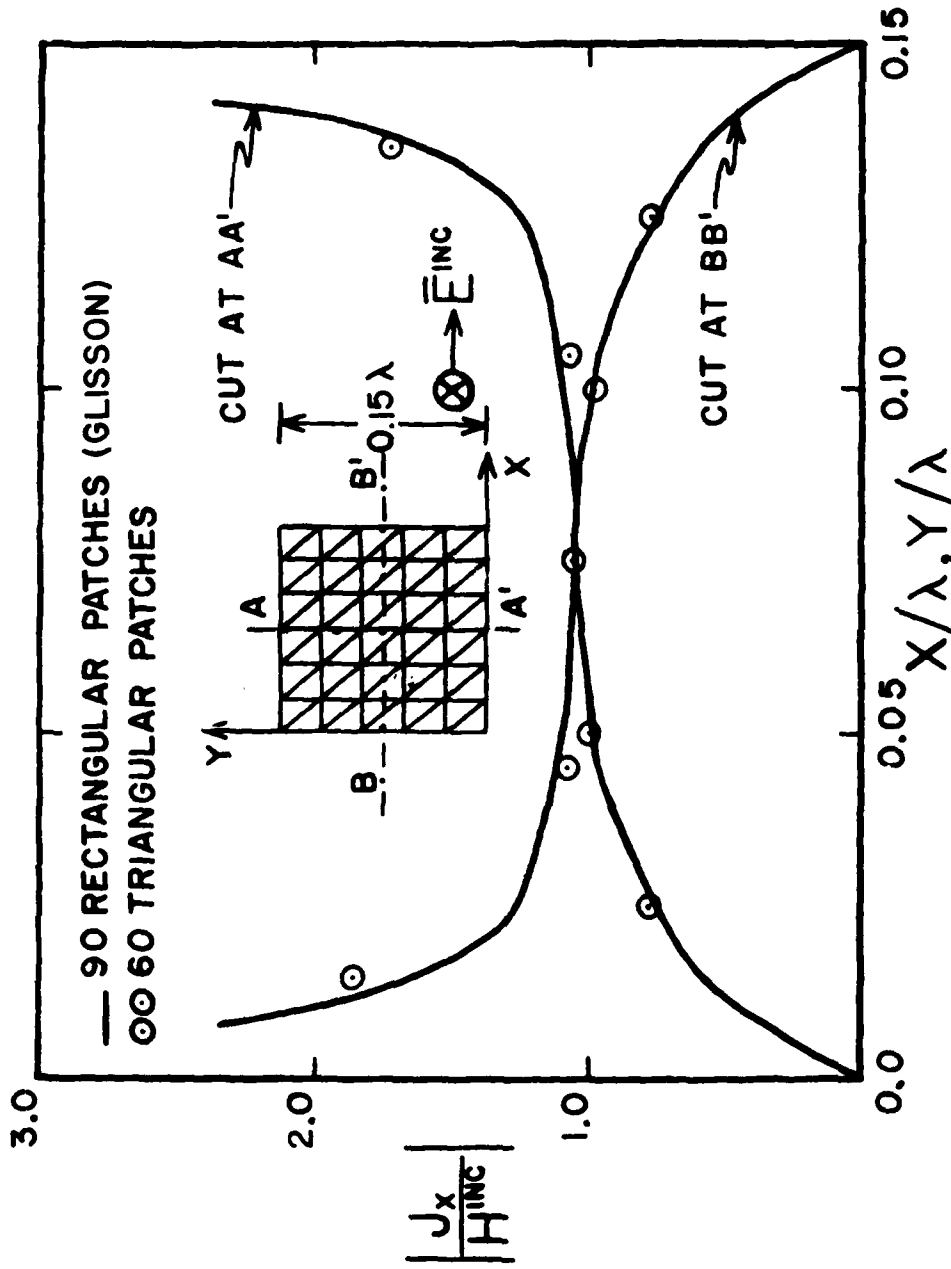


Figure 36: .15λ Square Plate Current Distribution

The important aspects to note are the magnitude of  $J$  as the plate size decreases and also the more uniform current distribution as the plate size reduces. In an experiment to observe these effects more graphically,  $1.0\lambda$ ,  $0.5\lambda$ , and  $0.25\lambda$  square plates were irradiated with normally incident microwaves at a power level of  $20 \text{ mW/cm}^2$ . See figures 37 to 45.



Figure 37: Photograph of  $1.0\lambda$  Square Plate

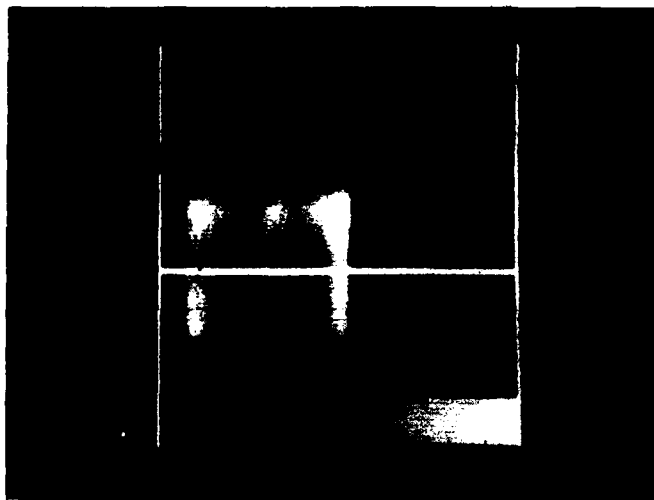


Figure 38: Infrared Photograph of a  $1.0\lambda$  Square Plate

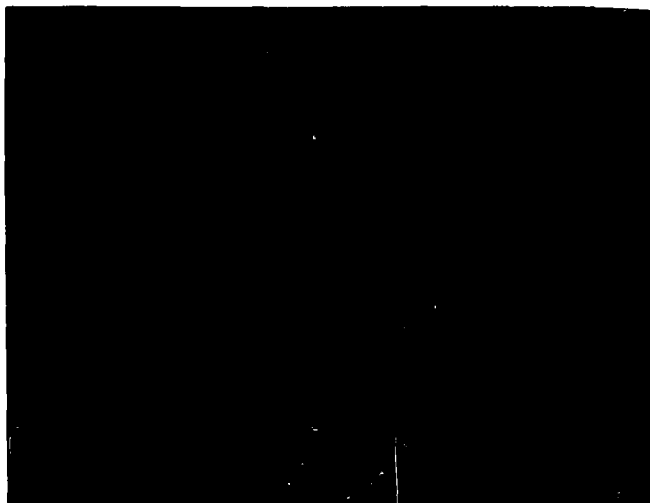


Figure 39: Thermal Profile Across the Center of a  $1.0\lambda$  Square Plate

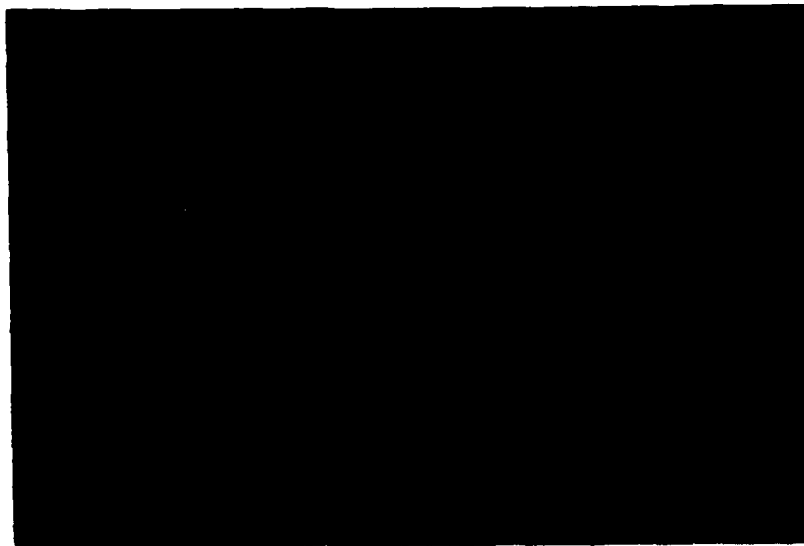


Figure 40: Actual Photograph of a  $0.5\lambda$  Square Plate



Figure 41: Infrared Photograph of a  $0.5\lambda$  Square Plate

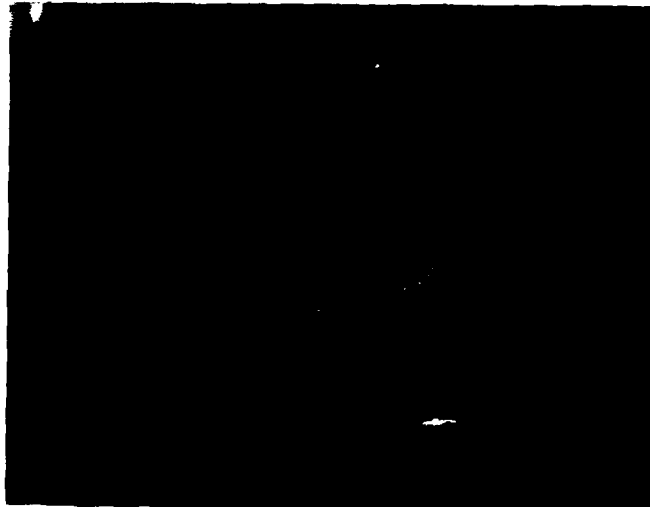


Figure 42: Thermal Profile Across the Center of a  $0.5\lambda$  Square Plate



Figure 43: Actual Photograph of a  $0.25\lambda$  Square Plate

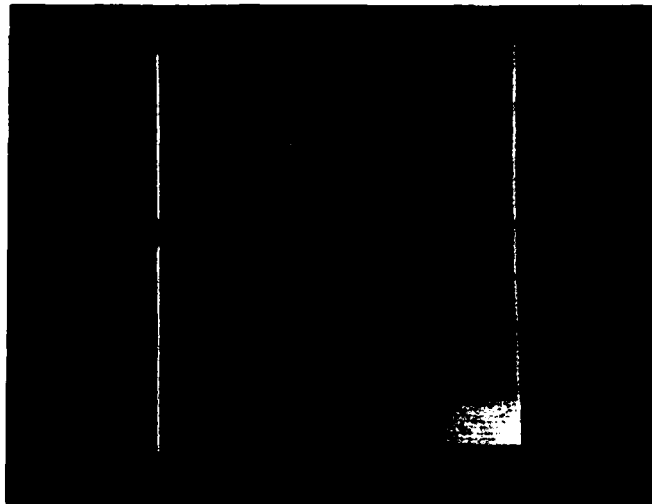


Figure 44: Infrared Photograph of a  $0.25\lambda$  Square Plate

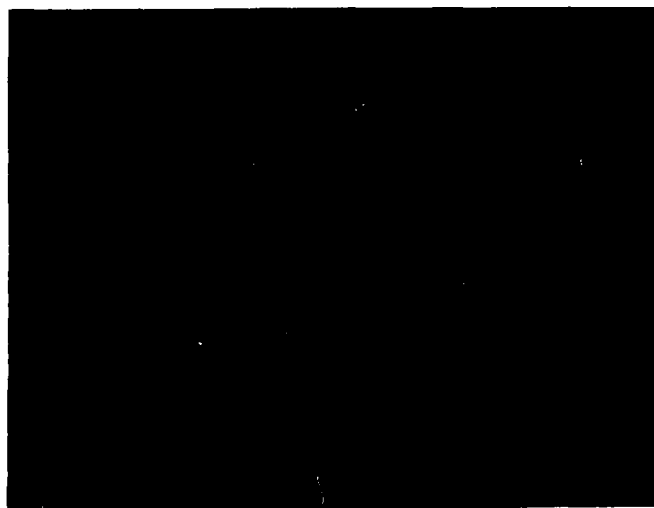


Figure 45: Thermal Profile Across the Center of a  $0.25\lambda$  Square Plate

The lighter areas correspond to greater surface currents. A single temperature profile was taken across the middle of each target to allow comparison with the method of moments results by Wilton. Notice the great similarity between the  $1.0\lambda$  experimental plate and theoretical results. To consider the question of uniformity more graphically, Figure 46 is a plot of a  $.15\lambda$  square plate in which the shading depicts those areas in which the surface current varied less than 20% from that which would be observed on an infinite conducting sheet. This information is graphically taken from the plot of Wilton, Figure 36.

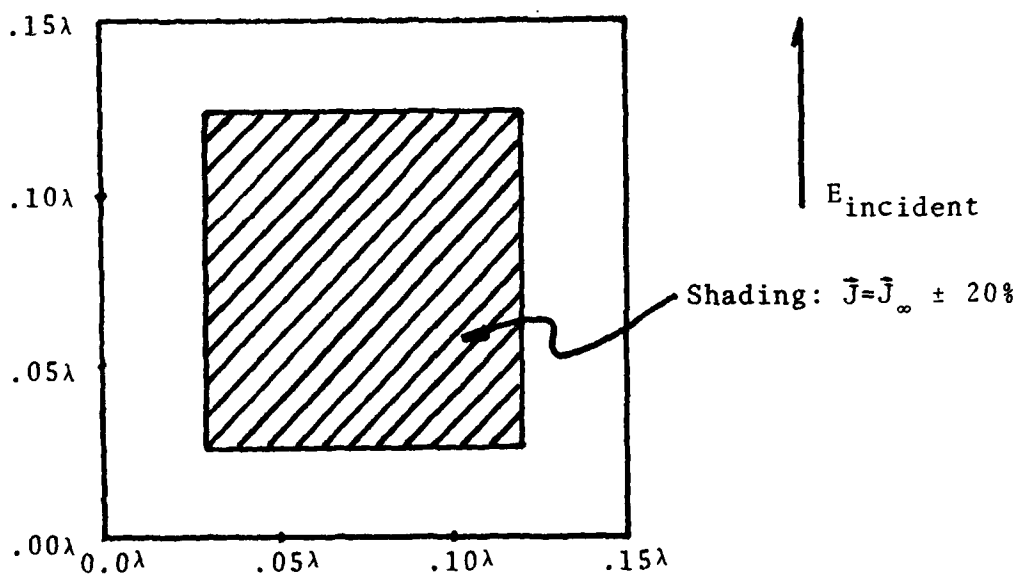


Figure 46: Current Uniformity on a  $.15\lambda$  Plate

Therefore, by observing the temperature at the center of our small sample, we are reasonably assured that our results are similar to what would be observed on a semi-infinite plate.

In the experimental verification small square samples were used which facilitated the above discussion; however, this is not an absolute requirement. Andrejewski<sup>27</sup> has computed the surface current at the center of a disc as a function of  $c$  where  $c \equiv 2\pi(\frac{a}{\lambda})$  with "a" being the radius of a sample disc. See figure 47<sup>28</sup> for a plot of his results.

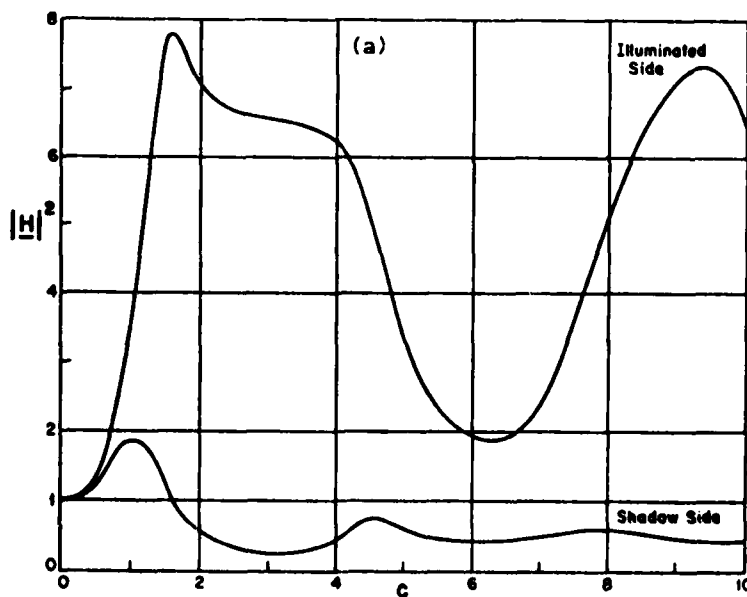


Figure 47: Current at the Center of a Disc as a Function of  $c$

As in the case of the small square, notice that as  $c$  gets small the field at the center of the disc approaches the semi-infinite plane value (  $|\vec{H}|=1$  ). In fact for a disc 1.5 cm in diameter the predicted surface current value at the center is within 10% of the value experienced by a semi-infinite conducting sheet. Therefore, it seems reasonable that we may use small discs as well as squares in the verification process with no loss in validity. For a more complete discussion of theoretical solutions of the disc one may refer to any of several good references. 28,29,30

All the discussion to this point has been limited to the small samples used in the verification process. We have developed a model and have shown that it is valid in regards to whether or not a particular coating configuration will heat properly when exposed to microwave radiation. One final question which is relevant when considering electrically large samples is the question of "nearest neighbor" influence. That is, how well can our coating model predict surface currents below it?

Recall that in general our coating will be displaced from the surface of the object we are observing. Although, this displacement is necessary in order to observe heating, it is an overall detriment to the resolving power of the coating. We may begin to understand this problem more if we recognize that in order for a particular current element to interact with the coating, that current element must emit an electromagnetic wave which in turn must travel to the coating. See Figure 48.

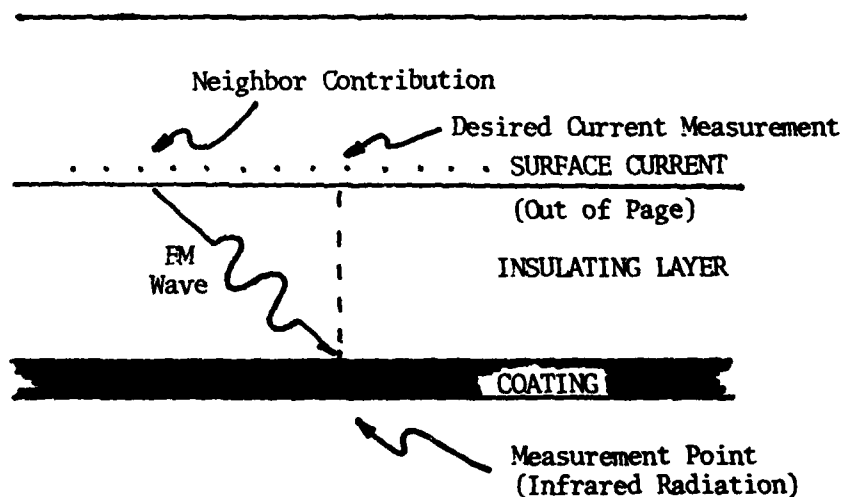


Figure 48: Cross Section of a Conductive Coating Displaced Away From Conductor Surface

The question then is how far away from the measurement point can this neighbor contribution be? We may receive some insight to the problem by considering the typical waveguide solution<sup>31</sup> to two semi-infinite planes separated by a distance "a". See figure 49 below.

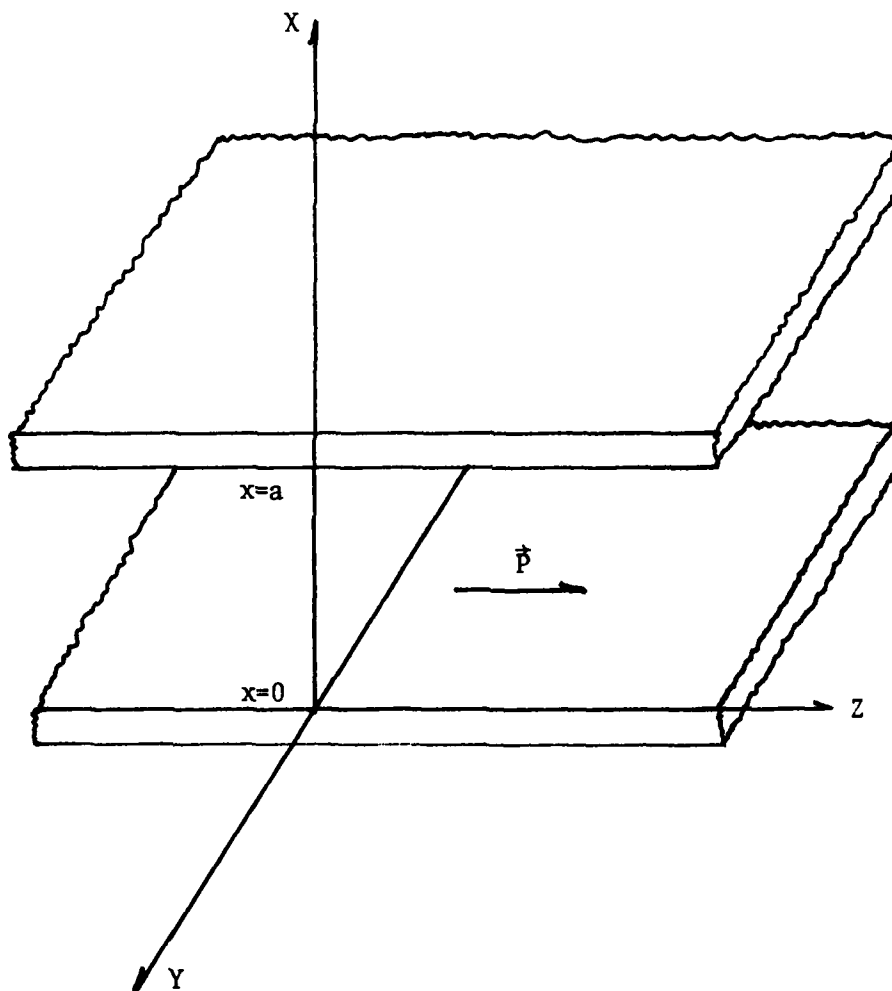


Figure 49: Parallel Waveguide Sheets

Assuming wave propagation in the  $z$  direction and a TE mode, the solution is given as <sup>11</sup>

$$E_y = C_1 \sin \left( \frac{m\pi}{a} x \right) e^{-\bar{\gamma}z} \quad (134)$$

$$m = 1, 2, 3, \dots \quad (135)$$

$$\bar{\gamma} = \sqrt{\left( \frac{m\pi}{a} \right)^2 - \omega^2 \mu \epsilon} \quad (136)$$

We see that  $\bar{\gamma}$  will either be pure imaginary or real depending on the argument under the radical. If  $\bar{\gamma}$  is real, the wave will attenuate exponentially which is what we desire in order to reduce the nearest neighbor effect. We may solve for a minimum value of  $a$  in which this will occur. Forcing the argument to be greater than zero and solving for  $a$ , we find that attenuation will occur as long as

$$a < \frac{\lambda m}{2\sqrt{\epsilon_r \mu_r}} \quad (137)$$

If we assume the simplest propagation mode ( $m = 1$ ) and a foam insulating layer ( $\epsilon_r \approx \mu_r \approx 1$ ), then we have lateral attenuation as long as the insulator is less than  $\frac{\lambda}{2}$  thick. Obviously the attenuation will be stronger as the layer gets thinner. The distance at which an attenuated wave has reduced to a value  $\frac{1}{e}$  of its initial value is given by

$$z = \frac{1}{\sqrt{\left( \frac{m\pi}{a} \right)^2 - \omega^2 \mu \epsilon}} \quad (138)$$

In the regime where we must operate in order to have significant lateral attenuation and thus little nearest neighbor influence, we have

$$\left(\frac{m\pi}{\lambda}\right)^2 \gg \omega^2 \mu \epsilon \quad (139)$$

Therefore,

$$z \approx \frac{a}{m\pi} \quad (140)$$

In other words, we would not expect to see significant nearest neighbor influence at distances much over  $a/\pi$  for the worse case of  $m=1$ .

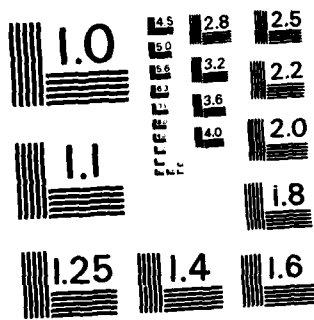
An experiment was conducted in order to further understand the significance of the nearest neighbor problems. A large aluminum conductor was covered with a layer of foam 5.1 mm in thickness. The foam was subsequently coated with an aquadaq coating approximately 15 microns in thickness and electrical conductivity of approximately 315 mhos/m. As the large target was irradiated, 1.5 cm diameter holes were placed in the aluminum at closer and closer intervals. The holes behind the coating were observed as hot spots. A point was finally reached at which time the two spots had begun to merge. At this point the centers of the holes were 2.0 cm apart. See figures 50 to 61 for thermovision photographs and thermal profiles of the results.

MICROWAVE INTERACTION WITH THIN MULTIPLE CONDUCTIVE  
COATINGS(U) ROME AIR DEVELOPMENT CENTER GRIFFISS AFB NY  
V M MARTIN MAR 83 RADC-TR-83-62

UNCLASSIFIED

F/G 11/3

NL



MICROCOPY RESOLUTION TEST CHART  
NATIONAL BUREAU OF STANDARDS-1963-A



Figure 50: Photograph of Electrically Large Plate in Place in the Anechoic Chamber

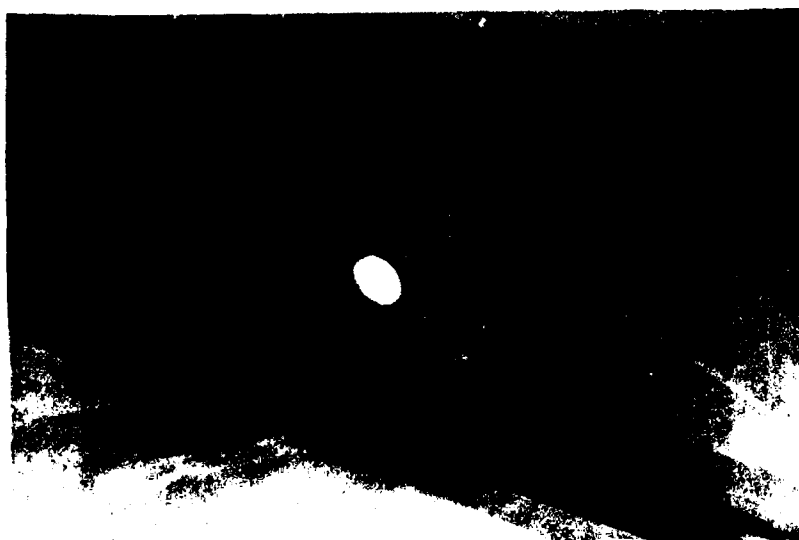


Figure 51: Photograph of the Single 1.5 cm Hole in the Aluminum Plate



Figure 52: Photograph of the Double Hole Configuration

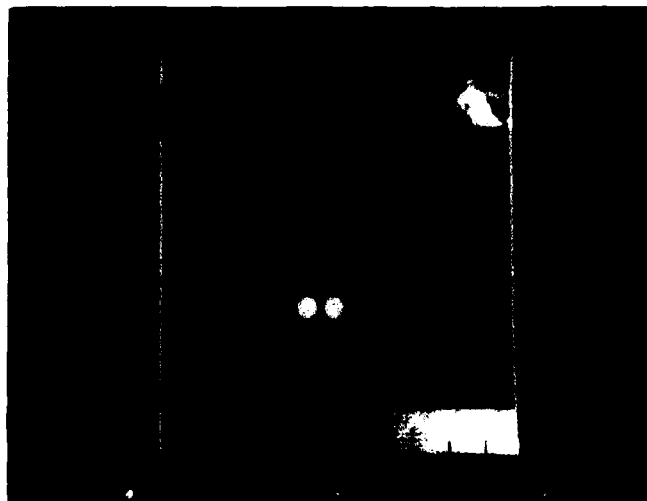


Figure 53: Infrared Photograph of Artificially Heated Double Hole Configuration for Size Comparison with Microwave Results



Figure 54: Infrared Photograph of Single Hole Heating Pattern  
Resulting from Microwave Radiation ( $1^{\circ}$  C Scale)



Figure 55: Horizontal Thermal Profile of Single Hole Heating  
Pattern ( $1^{\circ}$  C Scale)

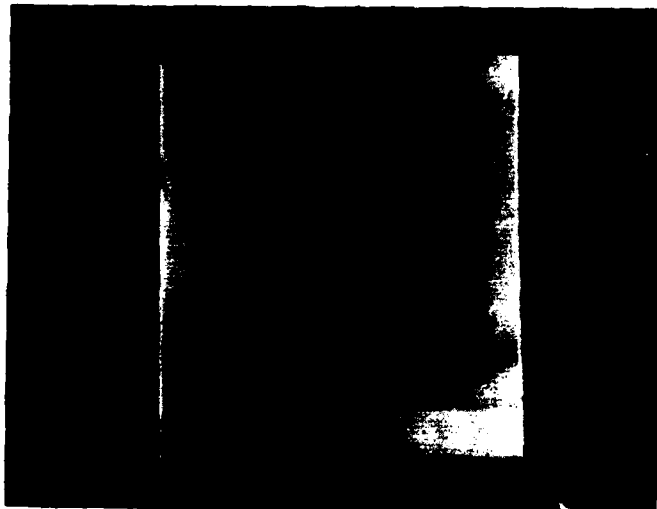


Figure 56: Same as Figure 54 Except  $2^{\circ}$  C Scale



Figure 57: Same as Figure 55 Except  $2^{\circ}$  C Scale

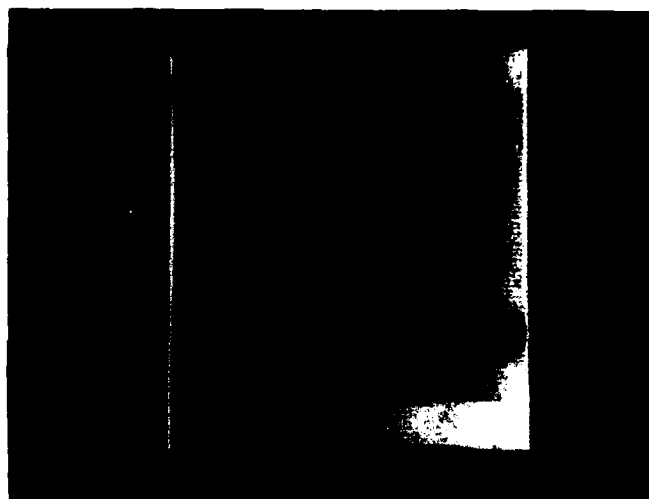


Figure 58: Infrared Results of Double Hole Microwave Heating  
Pattern ( $1^{\circ}$  C Scale)



Figure 59: Horizontal Thermal Profile of Double Hole Heating  
( $1^{\circ}$  C Scale)



Figure 60: Same as Figure 58 Except  $2^{\circ}$  C Scale



Figure 61: Same as Figure 59 Except  $2^{\circ}$  C Scale

A  $z$  calculated for the simplest ( $m=1$ ) mode in this configuration is approximately .2 cm. Note that we may still observe separation of the two holes on the thermovision photographs and at that point the actual metal separating the holes was .5 cm. It is of note also, that the particular infrared camera/object separation distance for this experiment only provided a .17 cm camera resolution.

As a final note, it should be obvious that electrically large, finite dimensional, targets exhibit large variations in surface current density (See figures 35, 38, and 39 for examples.). It is possible to gain some insight into how these variations relate to the one-dimensional model by considering the following. Suppose that we have a two-dimensional problem in which there are surface current variations in the  $x$  direction of a substrate as a result of its finite size. See Figure 62.

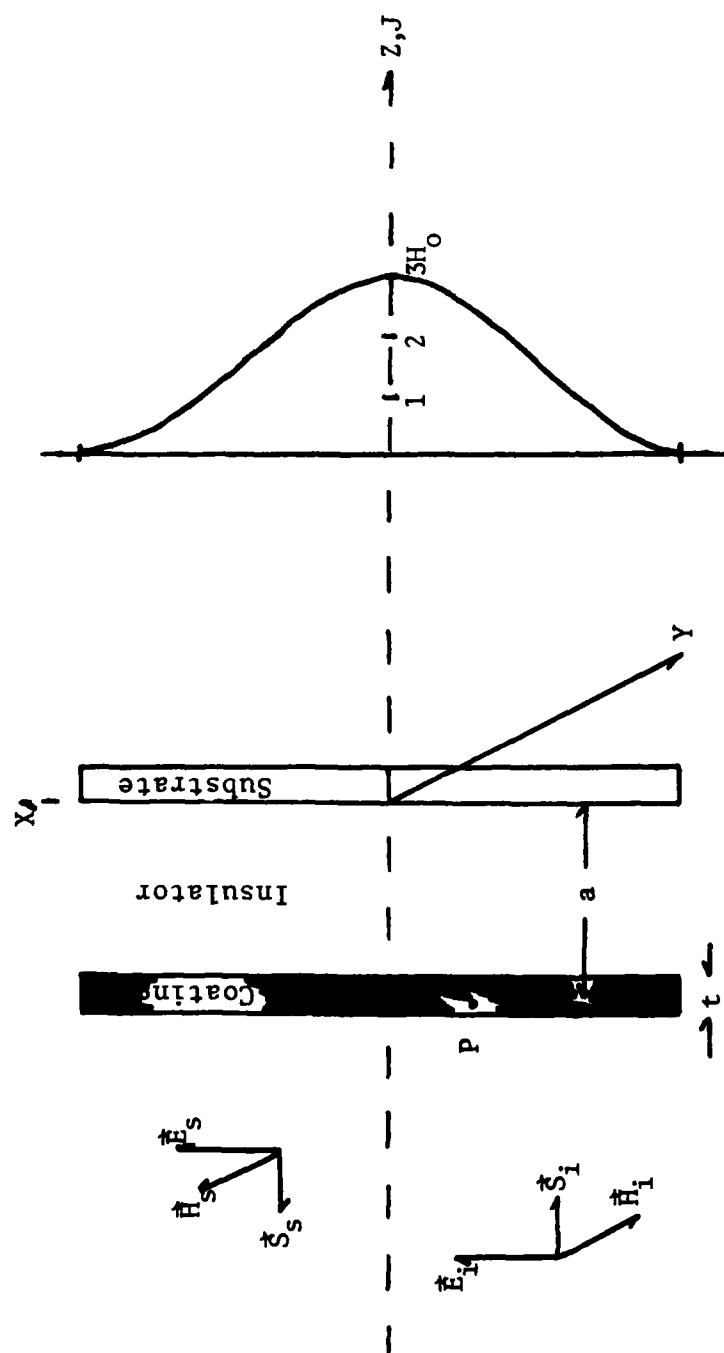


Figure 62: Irradiated, Finite Size, Conducting Substrate with Hypothetical Surface Current Distribution

Clearly, if the substrate were infinite in the x-y plane, the value of  $J$  would be a constant given by  $|\vec{H}_1|$ . However, as a result of its finite size in the x direction and the imposition of boundary conditions, we actually have a current distribution varying spatially in the x direction and supposed to be that illustrated in Figure 62. In this example only, the surface current is confined to the range  $0 < J < 3H_1$ .

We know that the total electric field in the coating will be the vector sum of the incident field plus the scattered field from the current element beneath the measurement point, P. The question of nearest neighbor contribution to the field at P has already been discussed. It was shown that most of the scattered field at P resulted from current distributions within a circular radius of approximately  $a/\pi$ . Therefore, if  $a$  is small, we may assume the radiating source to be located directly behind P. We have

$$\vec{E}_c = \vec{E}_i + \vec{E}_s \quad (141)$$

where  $\vec{E}_c$  is the field in the coating,  $\vec{E}_i$  is the incident field, and  $\vec{E}_s$  is the scattered field. We may define a fourth field,  $\vec{E}_\infty$ , as the scattered field from an infinite substrate and  $\vec{E}_p$  as a perturbing field that when combined with  $\vec{E}_\infty$  would yield the actual scattered field from the finite size substrate. Thus,

$$\vec{E}_s = \vec{E}_\infty + \vec{E}_p \quad (142)$$

Substituting equation 142 into equation 141 we have,

$$\vec{E}_c = \vec{E}_i + \vec{E}_\infty + \vec{E}_p \quad (143)$$

Recalling the development in Chapter V, we may write an expression

for the deposited power density in the coating,  $Q_c$ , as follows:

$$Q_c = \vec{J}_c \cdot \vec{E}_c = \sigma \vec{E}_c \cdot \vec{E}_c \quad (144)$$

Taking the dot product of  $\vec{E}_c$  with itself, we have

$$Q_c = \sigma \{ E_1^2 + E_\infty^2 + E_p^2 + 2(\vec{E}_1 \cdot \vec{E}_\infty + \vec{E}_1 \cdot \vec{E}_p + \vec{E}_\infty \cdot \vec{E}_p) \} \quad (145)$$

Rearranging, we have

$$Q_c = \sigma \{ E_1^2 + E_\infty^2 + 2\vec{E}_1 \cdot \vec{E}_\infty + (E_p^2 + 2(\vec{E}_1 \cdot \vec{E}_p + \vec{E}_\infty \cdot \vec{E}_p)) \} \quad (146)$$

Clearly, by considering temperature regimes in which no changes of state occur for our coating and by remembering the conservation of energy, we may infer that the temperature of the coating is a continuous, increasing function of  $Q_c$ ; that is,

$$\Delta T = f(Q_c, H) \quad (147)$$

where  $H$  consists of several thermodynamic variables such as surface emissivity, sample height, orientation, roughness, etc..

The important point, however, is that for each increment we increase  $Q_c$ ,  $\Delta T$  will also increase. If we consider a simple case in which the power loss,  $Q_L$ , may be expressed in terms of Newton's law of cooling, we have

$$Q_L = g(H) \Delta T \quad (148)$$

where  $g(H)$  is some function of the thermodynamic variables listed above; for a given coating/substrate configuration it is assumed that  $g(H)$  will be relatively constant independent of temperature. For example, infrared emissivity is a function of coating electrical conductivity; electrical conductivity was measured versus temperature for an aquadaq coating in Appendix A and found to vary less than 0.3% over the temperature

ranges of interest. It can be shown that the emissivity would vary even less than the conductivity; thus, it is assumed to be constant. We may now write the conservation of energy equation for the coating/substrate system in dynamic equilibrium; we have

$$Q_L = Q_C(z=-a)t \quad (149)$$

where  $t$  is the coating thickness. In equation 149 we have assumed that the coating in this example is so thin that the power deposition is uniform throughout and is only a function of the coating separation from the substrate. Substituting equation 148 into equation 149, we find

$$\Delta T = \frac{t}{g(H)} Q_C(z=-a) \quad (150)$$

This is the sought after result; the differential surface temperature is directly proportional to the deposited power density. The importance of this arises from the composition of  $Q_C$ . The first part of equation 146,  $(E_1^2 + E_\infty^2 + 2\vec{E}_1 \cdot \vec{E}_\infty)$ , is what we might call the first order terms which result from a purely one-dimensional analysis of the problem (The coating/substrate combination is infinite in the x-y plane.). The remainder of equation 146,  $(E_p^2 + 2\vec{E}_p \cdot (\vec{E}_1 + \vec{E}_\infty))$ , may be interpreted as the higher order contributions resulting from the imposed boundary conditions in a finite case. Thus, the differential temperatures we observe on our coating surface may be thought of as the sum of temperatures we would observe on an infinite configuration plus any changes that would occur as a result of observing a finite size; that is,

$$\Delta T = \Delta T_\infty + \Delta T_p \quad (151)$$

In equation 151 bear in mind that  $\Delta T_p$  may have a negative value since only  $\Delta T$  is required to be greater than zero by the law of conservation of energy.  $\Delta T_p$  is the term that results from the interference of our perturbing field,  $E_p$ , with the total field that would be present in the case of an infinite coating/substrate configuration,  $(\vec{E}_i + \vec{E}_\infty)$ . Also,  $\Delta T$  typically is not directly proportional to the absorbed power density but rather approximates a square law to a large degree. This non-linearity is no problem since the infrared data is generally entered directly into a computer and may, therefore, be corrected for in a relatively straight forward manner.

The importance of all this is that in analyzing the current distribution on a finite plate via the coating temperature distribution we may wish to consider only the non-steady state term,  $\Delta T_p$ . That is, in the process of completing an infrared measurement we may wish to scale the results by some additive constant in order to correlate the infrared results with a single probe measurement on a particular surface and thereby "calibrate" the infrared results for all other points on that surface.

Since we have shown earlier that small samples may be used to approximate the one dimensional infinite plane, it seems reasonable then to assume that we can use small samples to measure  $\Delta T_\infty$  directly. A series of flat plate experiments were performed in which this was done. First, a small 1.5 cm square was irradiated with microwaves at a frequency of 2.45 GHz and a

power of  $25 \text{ mW/cm}^2$ . This is the same sized sample used in the verification experiments. Therefore, by measuring the equilibrium temperatures on the surface of the small sample we have obtained  $\Delta T_{\infty}$  for that particular coating configuration. Next, a  $1.0\lambda$  square plate was irradiated in order to illustrate the process. An infrared photograph was made along with a single thermal profile.  $\Delta T_p$  may be obtained by subtracting  $\Delta T_{\infty}$  from the total temperature measured by the thermovision.  $\Delta T_{\infty}$  was drawn on the profile photograph to illustrate the magnitude involved. Figures 63 to 68 were made from a coating of 15 microns of aquadaq (315 mhos/m) placed on 5.1 mm of foam insulator. Figures 69 through 74 were made using an aquadaq coating 15 microns thick and placed on 10.2 mm of foam insulation. Additionally, Figures 69 through 74 included a copper substrate whereas the earlier photographs contained no substrate.

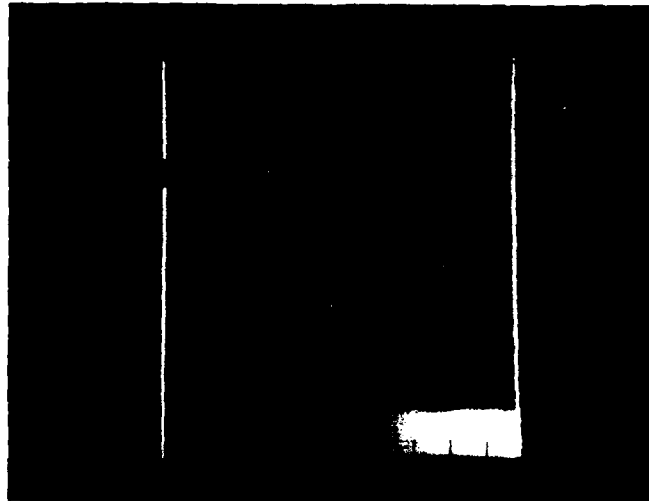


Figure 63: Thermovision Photograph of 1.5 cm Square Sample  
(No Substrate)

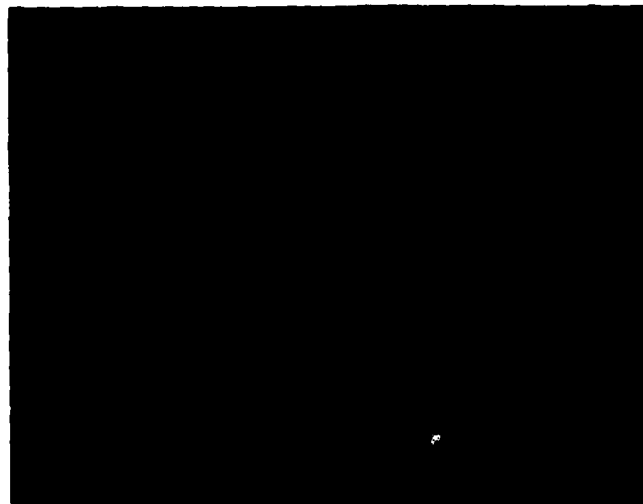


Figure 64: Thermal Profile (Horizontal) through the Center of  
the 1.5 cm Square Sample (2.45 GHz at 25 mw/cm<sup>2</sup>)

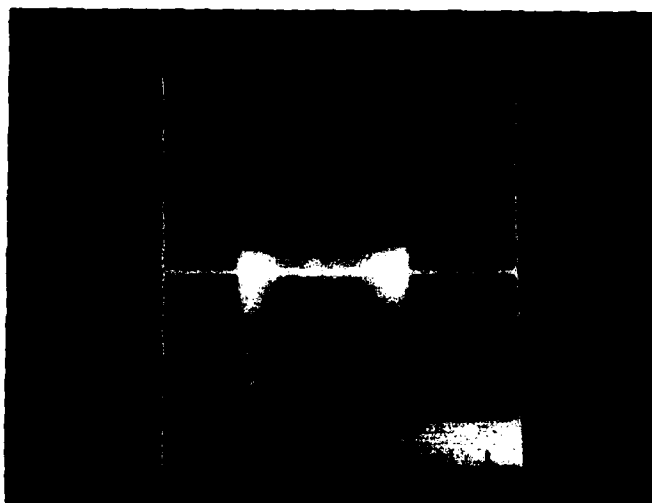


Figure 65: Thermovision Photograph of 1.0λ Square Plate (Horizontal white line indicates area where thermal profile was taken.)



Figure 66: Thermal Profile from 1.0λ Square Plate with  $\Delta T_{\infty}$  Plotted

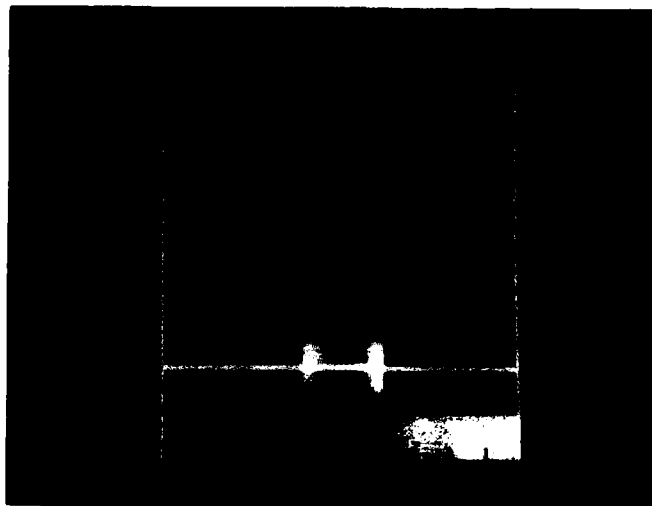


Figure 67: Thermovision Photograph of  $0.5\lambda$  Square Plate (Horizontal white line indicates area where thermal profile was taken.)



Figure 68: Thermal Profile from  $0.5\lambda$  Square Plate with  $\Delta T_{\infty}$  Plotted

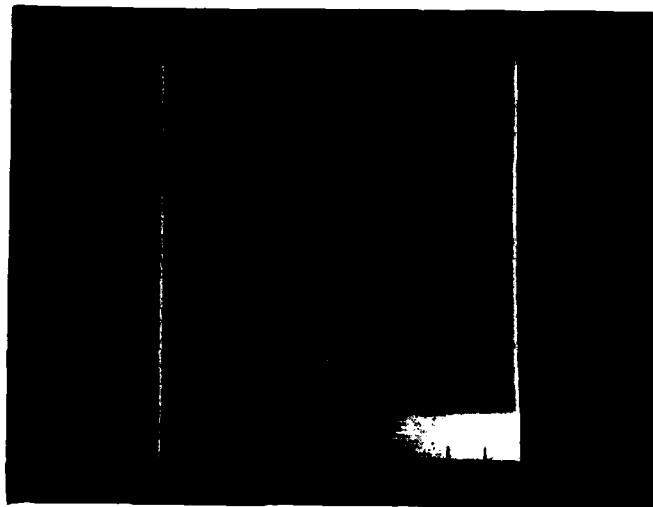


Figure 69: Thermovision Photograph of 1.5 cm Square Sample (Copper Substrate)



Figure 70: Thermal Profile (Horizontal) through the Center of the 1.5 cm Square Sample (2.45 GHz at 25 mW/cm<sup>2</sup>)

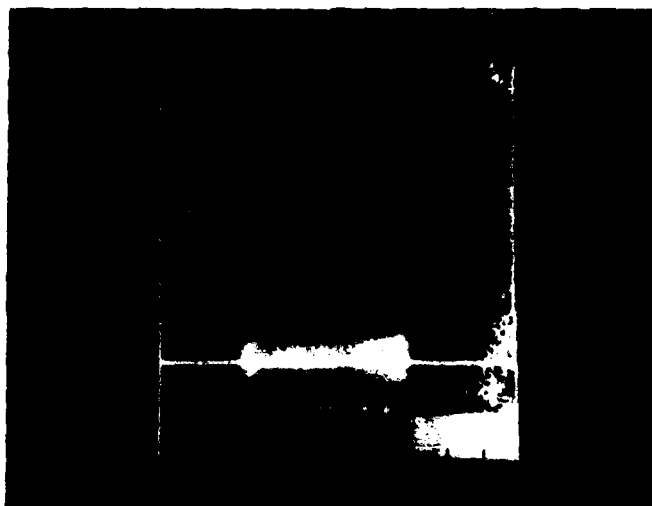


Figure 71: Thermovision Photograph of 1.0λ Square Plate with a Copper Substrate



Figure 72: Thermal Profile Corresponding to White Line in Figure 71

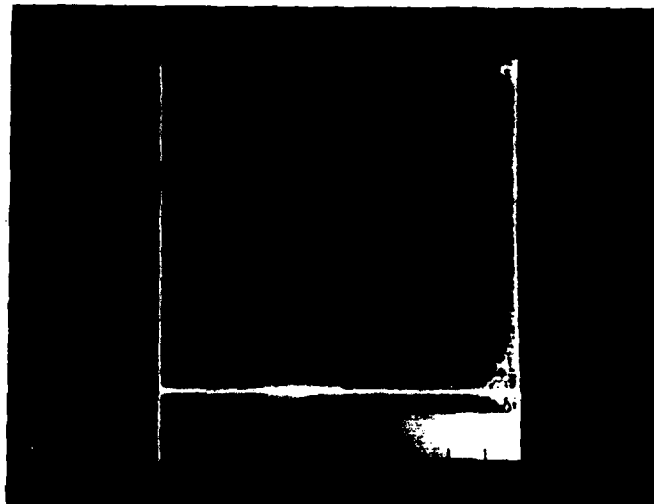


Figure 73: Thermovision Photograph of a  $0.5\lambda$  Square Plate with a Copper Substrate



Figure 74: Thermal Profile Corresponding to White Line in Figure 73

In passing it should be pointed out that the preceding results are consistent with the theoretical analysis typically employed in the development of holography<sup>36</sup>. This is to be expected since the coating is simply recording the interference patterns resulting from the combined effects of the incident and scattered fields from the substrate surface. This would be the arrangement for a typical Gabor hologram<sup>37</sup>. As is the case of an optical hologram, we have both phase and amplitude information stored in the thermogram of the surface coating. Clearly, the points on a thermal profile lying below  $\Delta T_\infty$  indicate that  $\vec{E}_p$  must be out of phase with  $(\vec{E}_i + \vec{E}_\infty)$  which would yield a negative value for the dot product in equation 146. It is not as easy to assess phase information for the  $\Delta T$ 's above  $\Delta T_\infty$ . These areas may correspond to  $\vec{E}_p$ 's out of phase with  $(\vec{E}_i + \vec{E}_\infty)$  but much greater in magnitude such that  $\vec{E}_p$  itself is the primary heating source. Continued research in this area may finally provide much needed information in regards to surface current phase. Fast Fourier Transform (FFT) techniques and optical reduction of the coating interference patterns into optical wavelengths for subsequent laser illumination are both techniques that may provide the desired phase information.<sup>38</sup>

This was not an attempt to quantitatively determine the resolving power of any particular coating. That effort is better left as a topic for further study on its own merit in another dissertation. However, it does illustrate that there

are no far reaching 'nearest neighbor' effects. We observed no shadows or false apertures as might be expected if there were some other propagation mode present. Thus, the end result of this series of experiments is a qualitative understanding of the nearest neighbor interaction in electrically large targets plus an assurance that the one dimensional model may be used with confidence in the design of a particular coating.

## CHAPTER VIII

## RECOMMENDATIONS AND CONCLUSIONS

This paper provides a method of selecting an optimum coating for use in the thermographic detection of microwave induced surface currents. Optimum in this sense implies two things. First, we needed a coating that would heat to at least 1 degree Centigrade above ambient temperature to achieve 10 levels of resolution on the infrared system. This is directed by the accuracy of the thermographic camera which can resolve temperatures to within  $0.1^{\circ}$  C. Secondly, we needed a coating that would heat to an acceptable level but minimally interfere with the fields present. This second requirement stems from the necessity of minimizing the effect any measurement device would have with the quantity being measured.

In attaining an optimum coating there were other constraints that we had to adhere to in order to have a realizable system. First, the coating should not contain ferrites, non-isotropic, or permeable materials. This requirement was established to ensure that the coating itself did not introduce possible intermodulation distortions resulting from non-linear materials.

Secondly, it was desired that the coating be easily fabricated for application to a variety of possible shapes. And thirdly, it had to be non-toxic to avoid possible health problems.

From an engineering point of view, there are only a finite number of variables that may be controlled to achieve the desired results. The material characteristics are limited to coating electrical conductivity and the insulating layer permittivity. Since we do not allow the use of ferrous materials in either, the relative permeability is approximately 1. The easiest factor to control, and the most effective, is the individual layer thickness.

Before explaining the coating development, it is appropriate to point out the two different uses of the coatings. The first involves a situation in which only the shape of a particular object is important in an electromagnetic interaction problem. To determine the current distribution in this problem, the simplest and most effective technique is to construct a model of the object from a foam material (low thermal mass) and then coat it with a thick (2-3 skin depths) coating of high electrical conductivity (300-500 mhos/m) material. Thus, we simulate a highly conductive object which may be made of something such as aluminum with one of lesser conductivity. Senior, et al <sup>32</sup> have demonstrated

that the modeling would not be one-to-one for small conductivities but Sega has demonstrated that for reasonable conductivities (greater than 300 mhos/m) the comparison may be close<sup>33</sup>. A possible application of such a scheme might be to determine the current distributions on an aircraft, ship, or spacecraft to facilitate the proper placement of antennas or measure radar cross section. Additionally, this type information might be valuable when studying the vulnerability of an existing or future weapon system to the effects of an Electromagnetic Pulse.

The more difficult problem is one which cannot be modeled because the materials the object is made from are relevant factors in the particular microwave interaction. An example is a missile or satellite constructed from conductive composites, iron alloys, aluminum, etc. Here the object itself must be irradiated and the resulting surface currents measured. To measure these currents, a different type coating arrangement is required. Two requirements exist; the coating must be thermally isolated from the surface to allow heating, plus it should be sufficiently distant from the surface so that the total (reflected plus incident) electric field is reasonably large. That is, the electric field must be large enough so that the heating in the coating will result in a temperature increase greater than one degree Centigrade. Neoprene rubber fills several of the requirements for the

insulating layer. It is a good thermal insulator; it is non-ferrous; it will easily conform to complex shapes with the aid of contact cement; and it has a high relative permittivity (measured to be 31 at 10 GHz). The high permittivity allows us to place the coating an electrically long distance from the surface even though the rubber may be physically thin. The advantage of this may be seen if one considers the infinite, perfectly conducting plane. At the surface we have a surface current magnitude given by  $2H_0$ , but the electric field is zero there; however, at a distance of one quarter wavelength from the plane the electric field magnitude is given by  $2E_0$ . Thus, if we placed a thin conductive layer at this distance from our infinite conducting plane, we would see maximum heating. A large permittivity material allows us to minimize the actual insulator thickness thus making it easier to apply. There is a disadvantage, however, in that the high permittivity insulator has a much higher reflection coefficient which has the effect of shielding the surface from the incident microwaves.

To optimize the above situation, that of placing our conductive coating on an insulating layer, we may use the following procedure. A computer program, Uthick, described in Appendix G, generates a square matrix in which the coating thickness and insulator thickness have been allowed to vary for the corresponding matrix

elements. The coating thickness changes linearly along the rows and the insulator thickness changes linearly along the columns. After this matrix is generated for a particular conductivity and insulator configuration, the results are plotted on a contour plot. The contour program, Contor, is located in the appendix also. Each coating configuration is examined with and without a conductor behind the insulating layer, thus simulating the situation of having currents present and not present. Finally, for comparison purposes a different contour is presented which indicates the thermal differences between a coating scheme with and without the conductor behind the insulator. Therefore, we can determine at a glance what the optimum coating configuration would be for a given situation. For electrical conductivities ranging from 0.1 to 40 mhos/m the appendix on electrical conductivity describes in detail how a particular conductivity coating may be made using a carbon and paraffin mixture. Figures 75 to 95 illustrate the various contour plots for conductivities of 1, 5, and 10 mhos/m with insulators of styrofoam (permittivity = 1.1) and neoprene (permittivity = 31). Additionally, a plot of aquadaq (conductivity = 315 mhos/m) on 1/16 inch plexiglas is given. The incident microwave field was set at  $10 \text{ mW/cm}^2$  and 2.45 GHz.

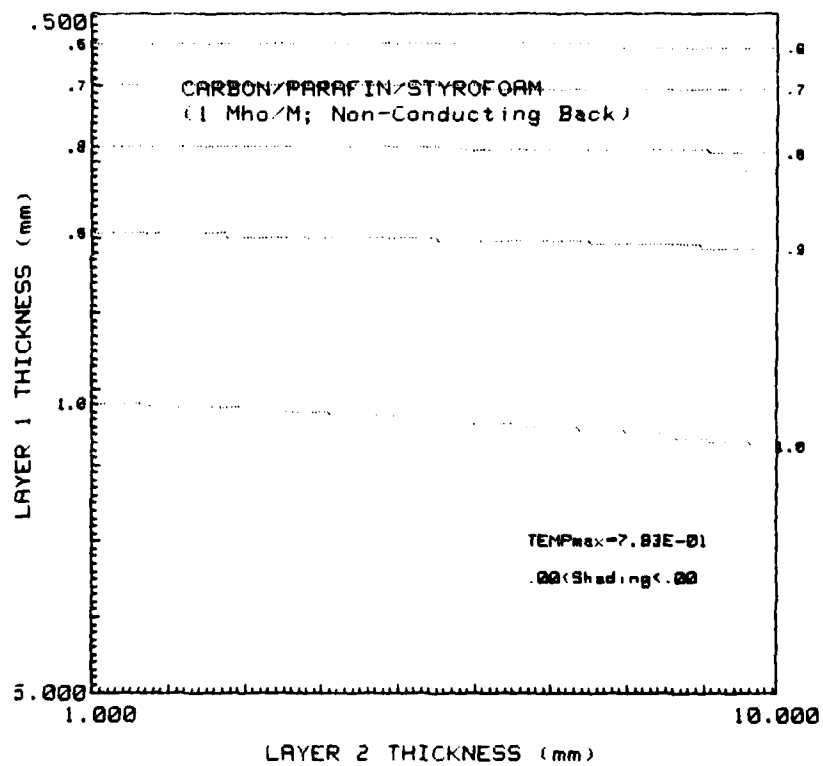


Figure 75: Carbon/Paraffin/Styrofoam Thermal Contours

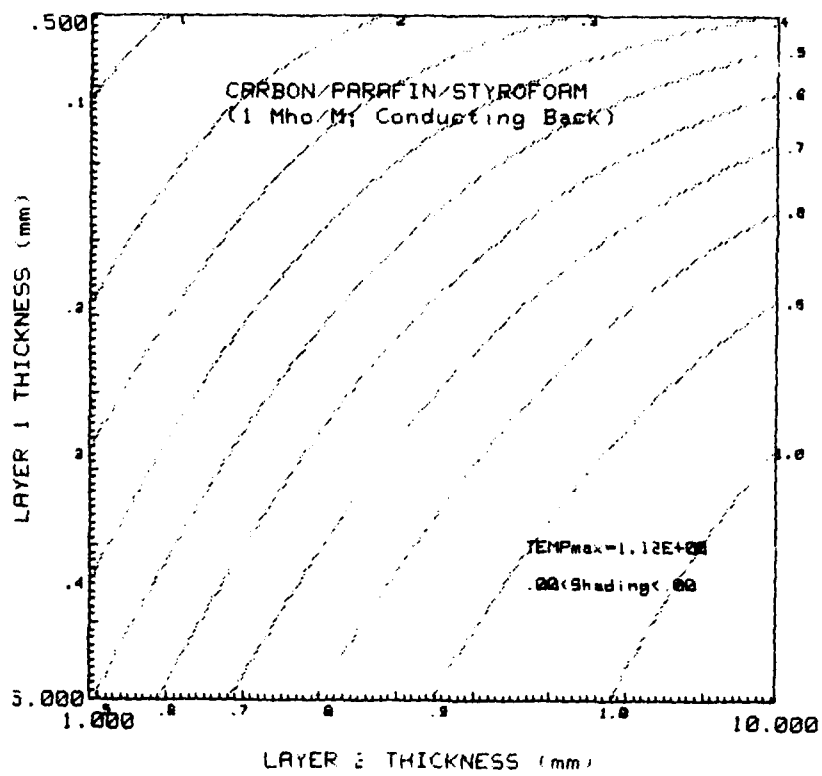


Figure 76: Carbon/Paraffin/Styrofoam/Copper Thermal  
Contours

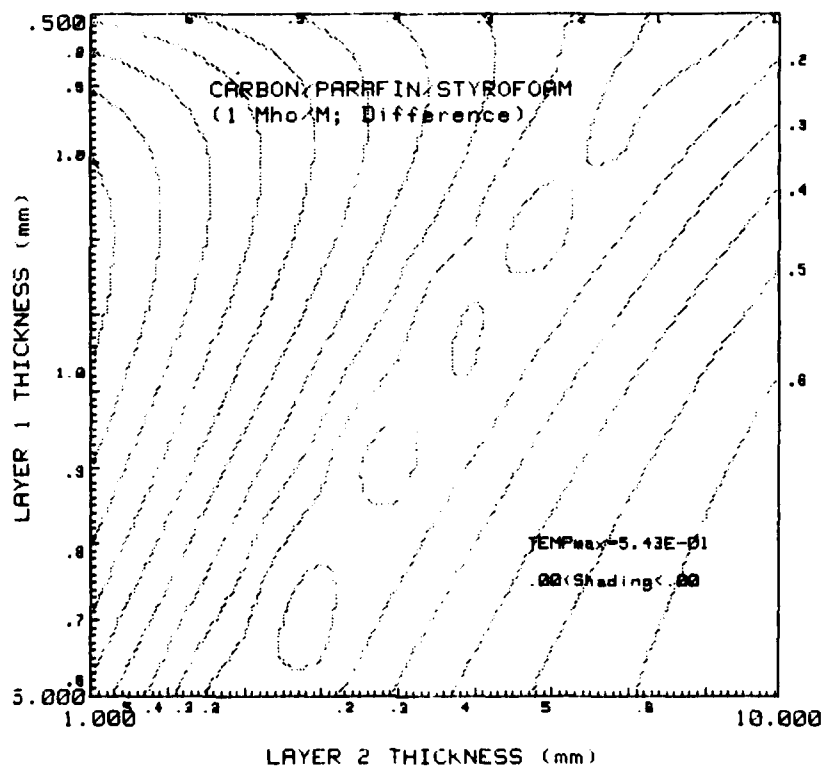


Figure 77: Carbon/Paraffin/Styrofoam/Copper Difference  
Contours

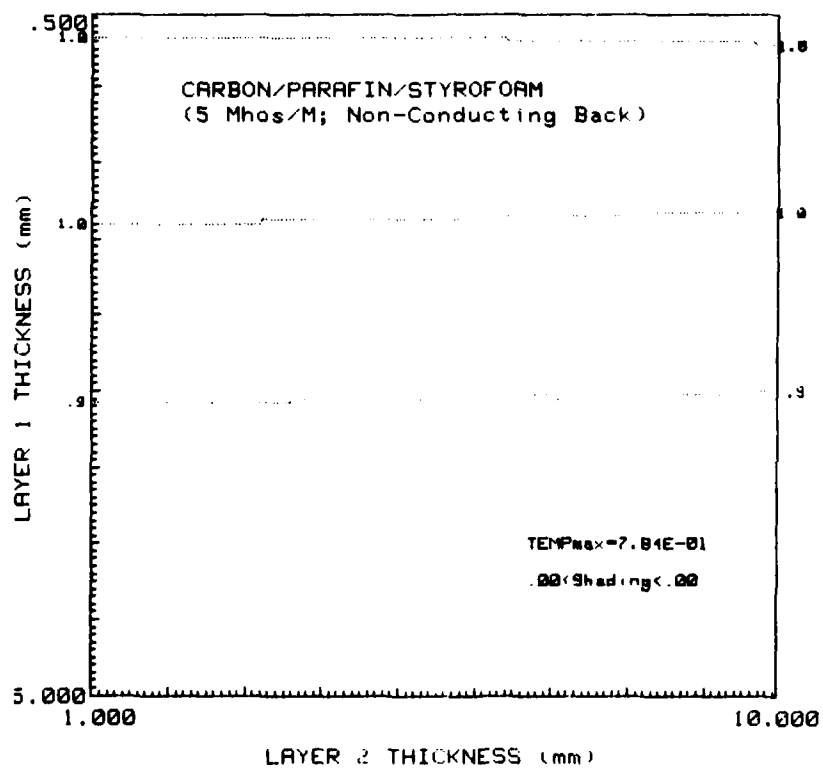


Figure 78: Carbon/Paraffin/Styrofoam/Thermal Contours

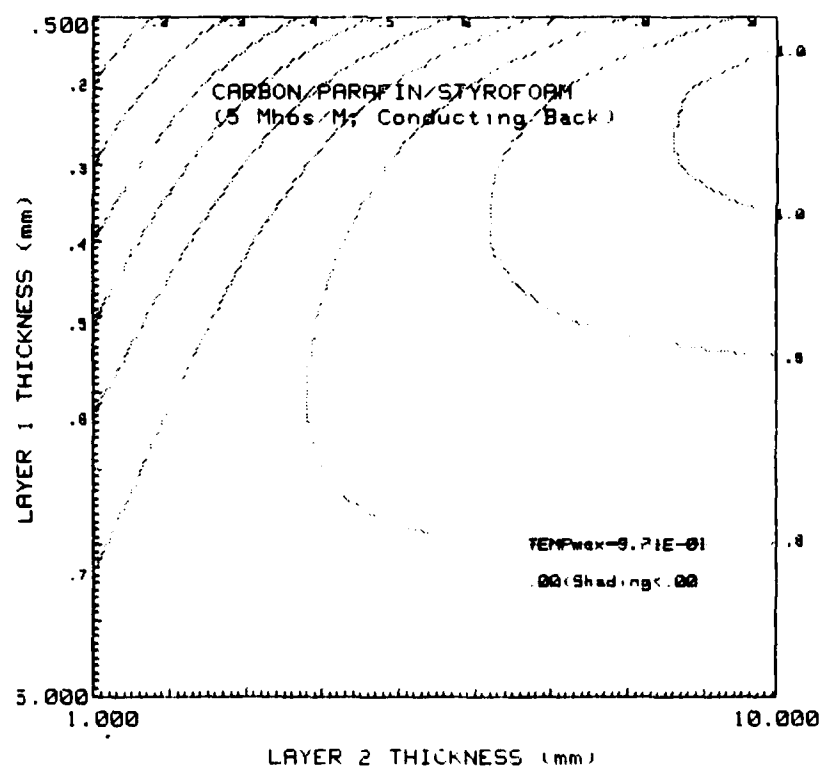


Figure 79: Carbon/Paraffin/Styrofoam/Copper Thermal Contours

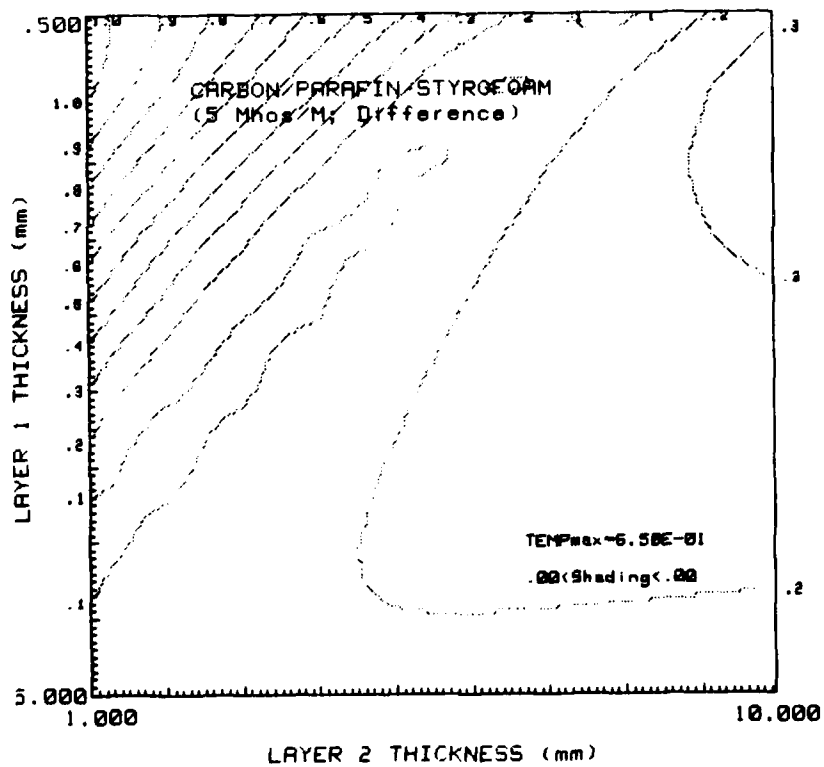


Figure 80: Carbon/Paraffin/Styrofoam/Copper Difference  
Contours

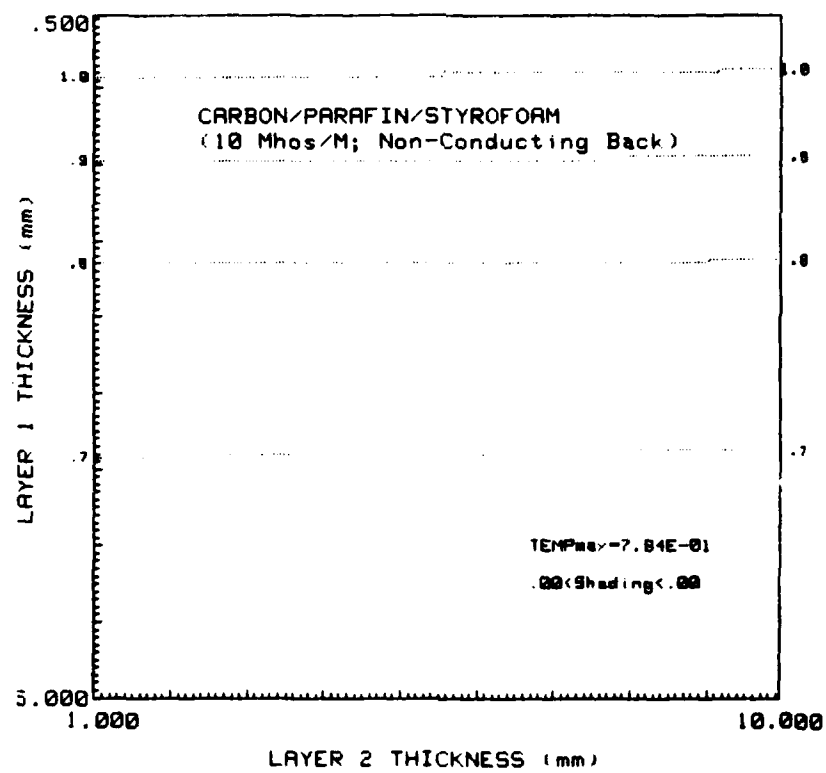


Figure 81: Carbon/Paraffin/Styrofoam/Thermal Contours

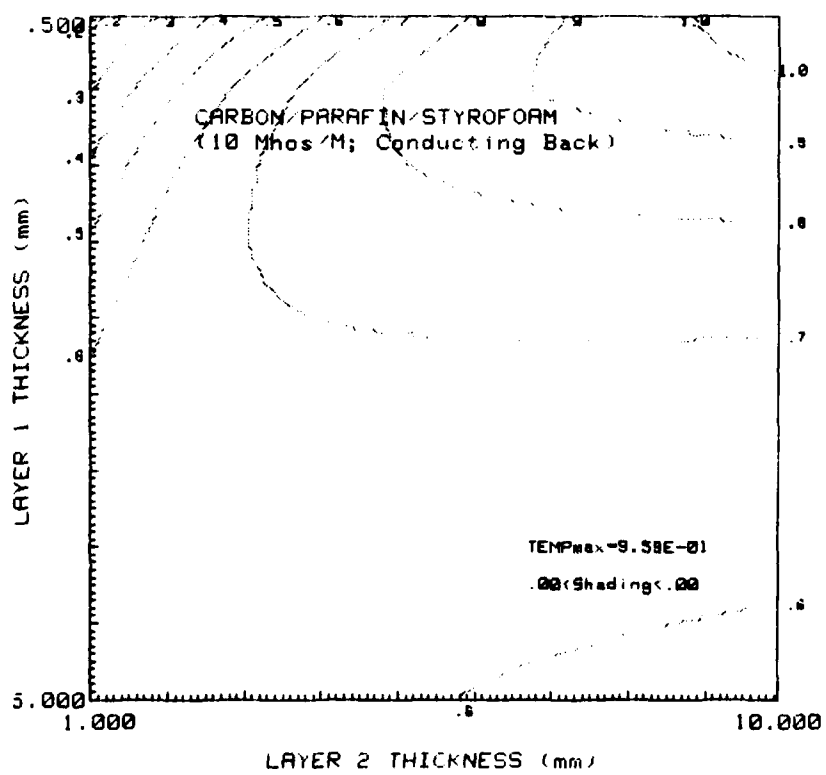


Figure 82: Carbon/Paraffin/Styrofoam/Copper Thermal  
Contours

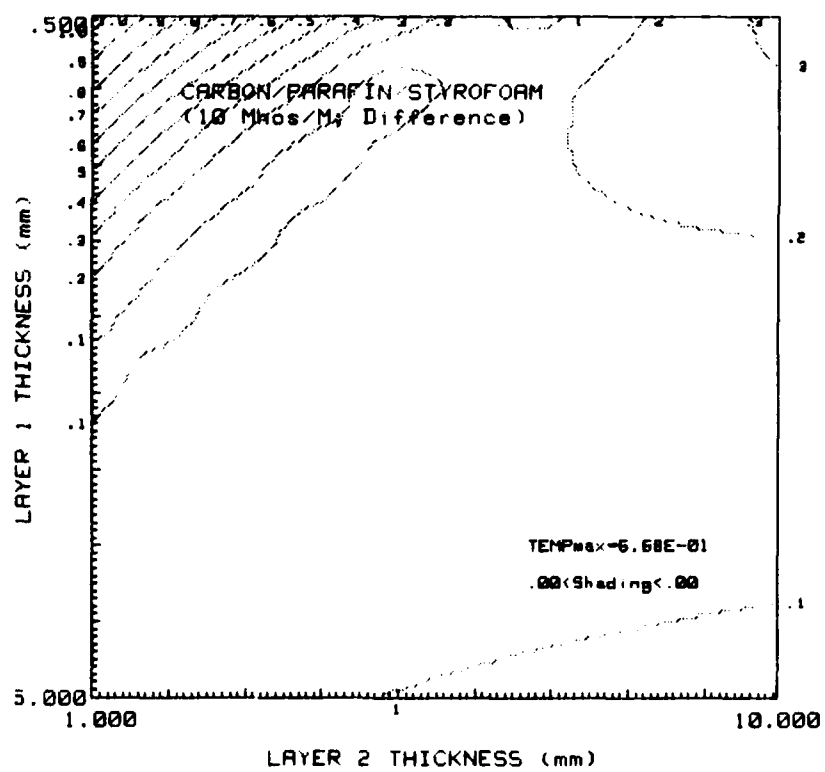


Figure 83: Carbon/Paraffin/Styrofoam/Copper Difference  
Contours

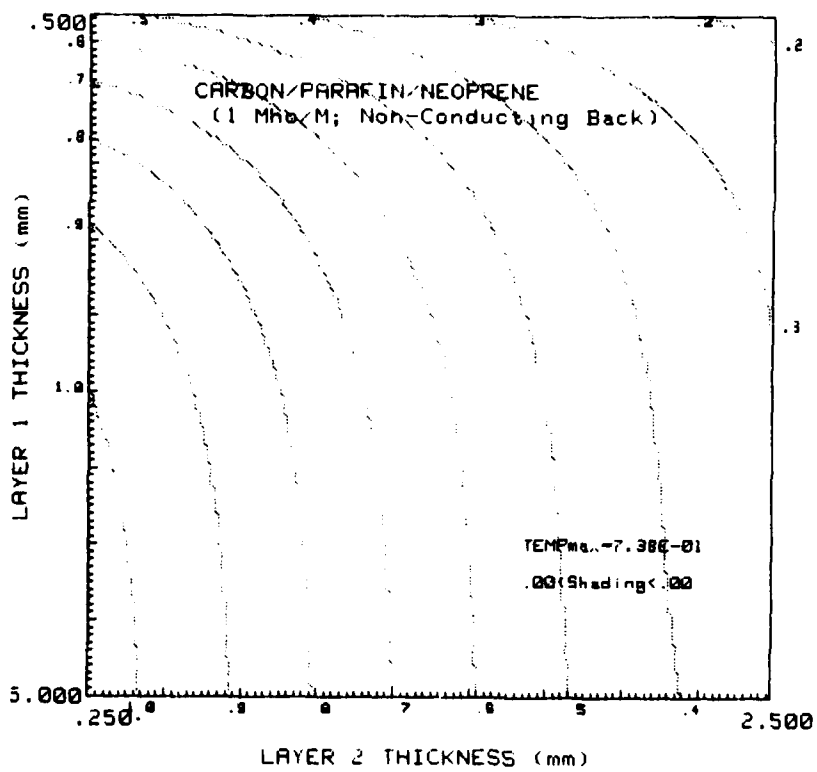


Figure 84: Carbon/Paraffin/Neoprene Thermal Profiles

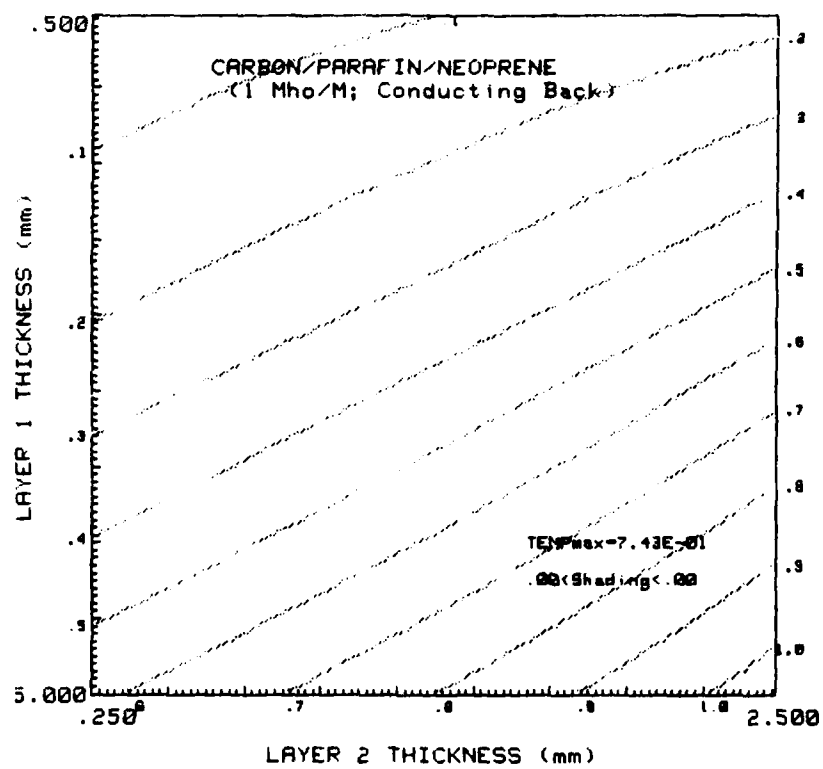


Figure 85: Carbon/Paraffin/Neoprene/Copper Thermal Profiles

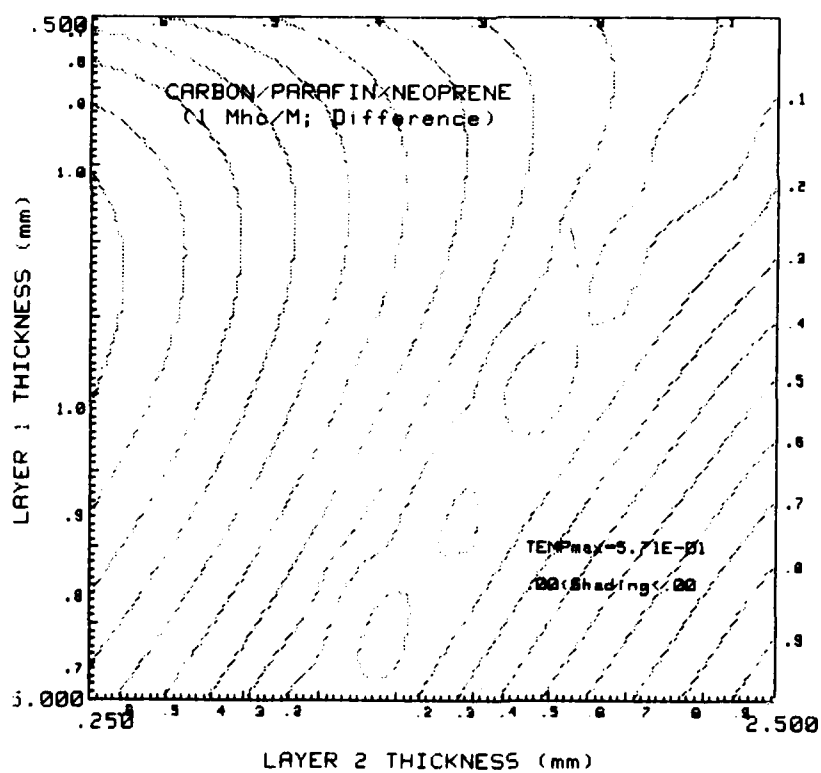


Figure 86: Carbon/Paraffin/Neoprene/Copper Difference  
Contours

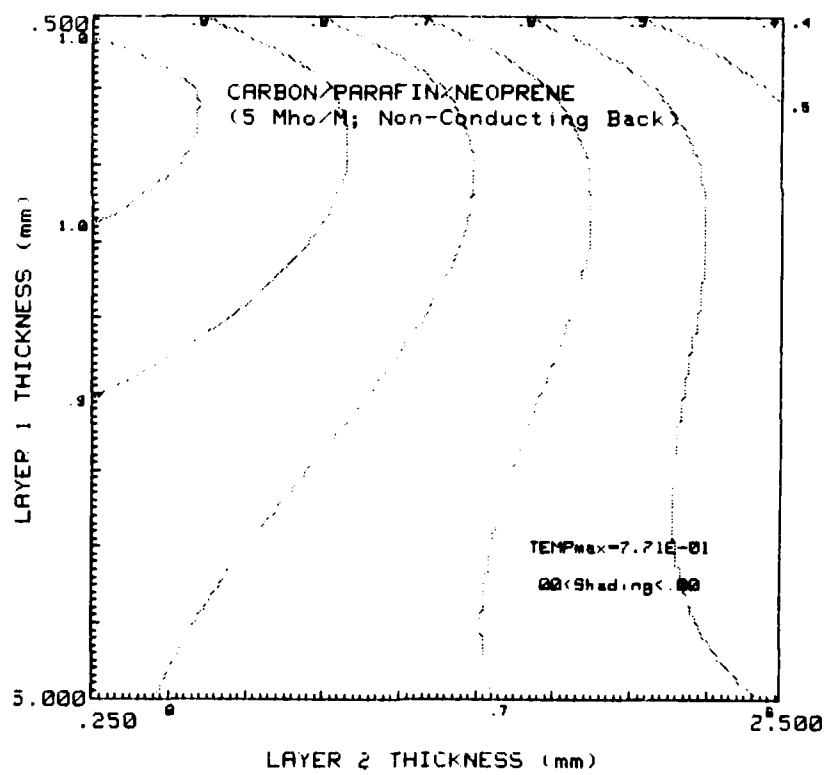


Figure 87: Carbon/Paraffin/Neoprene Thermal Contours

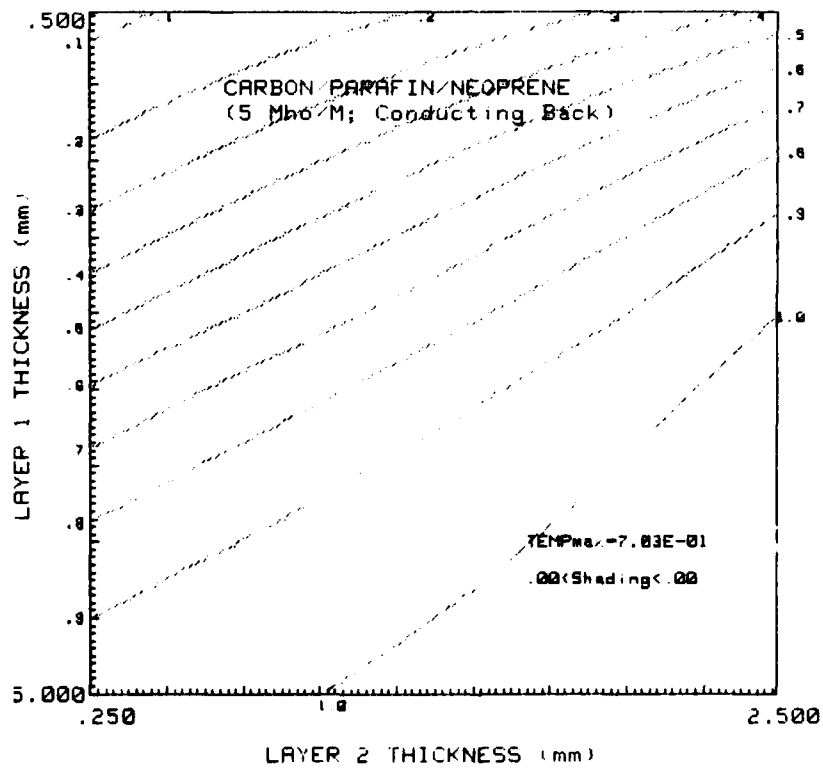


Figure 88 : Carbon/Paraffin/Neoprene/Copper Thermal  
Contours

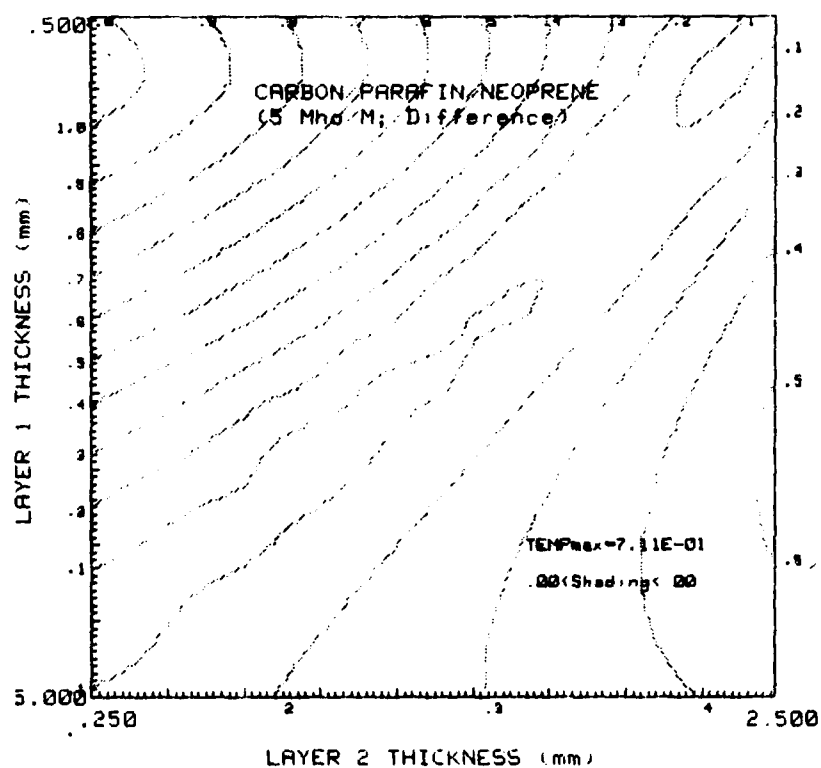


Figure 89: Carbon/Paraffin/Neoprene/Copper Difference  
Contours

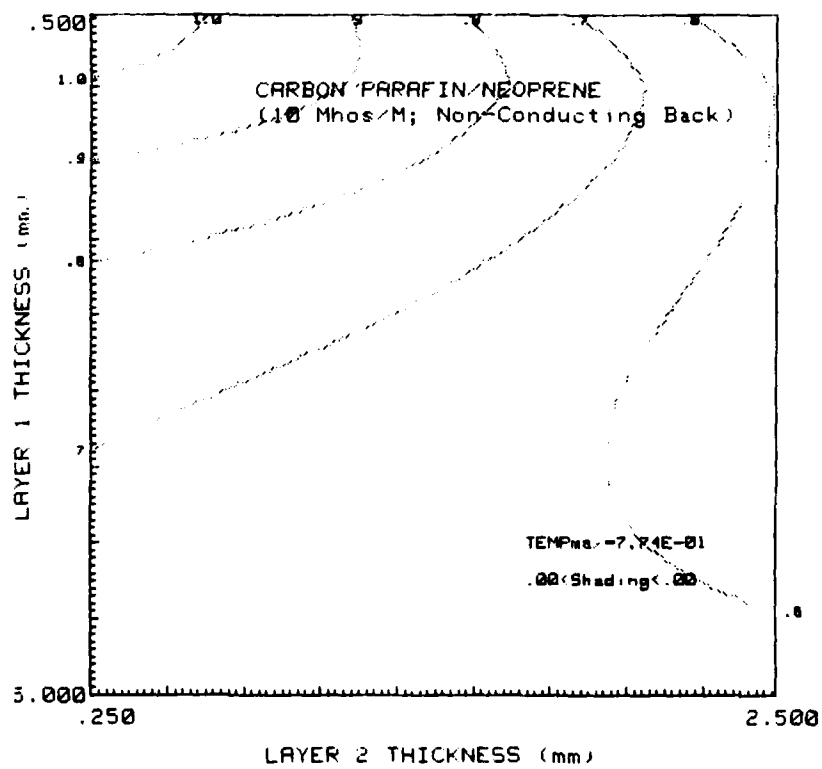


Figure 90: Carbon/Paraffin/Neoprene/Thermal Contours

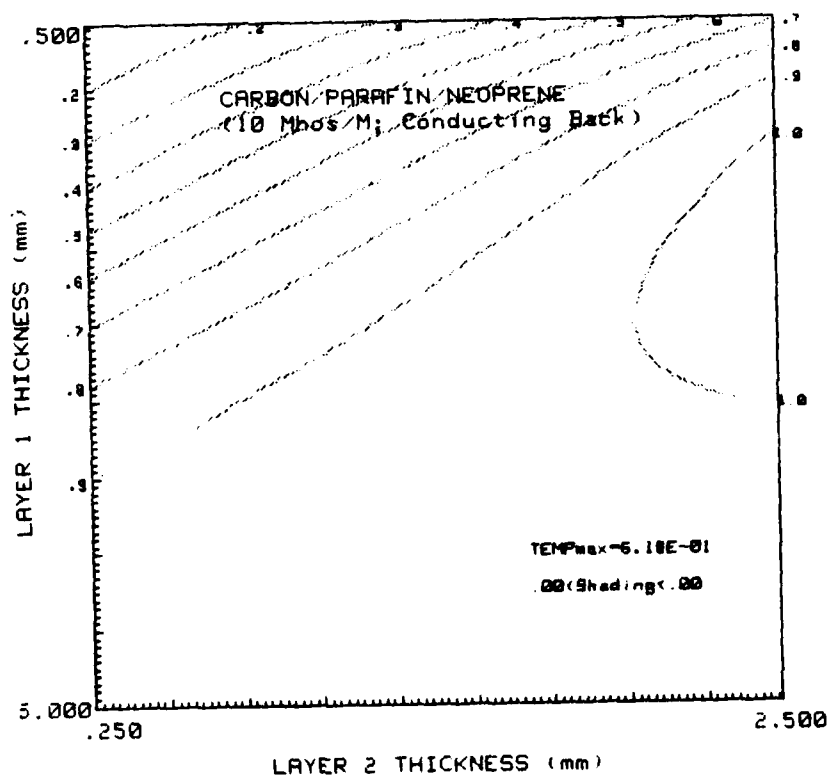


Figure 91: Carbon/Paraffin/Neoprene/Copper Thermal  
Contours

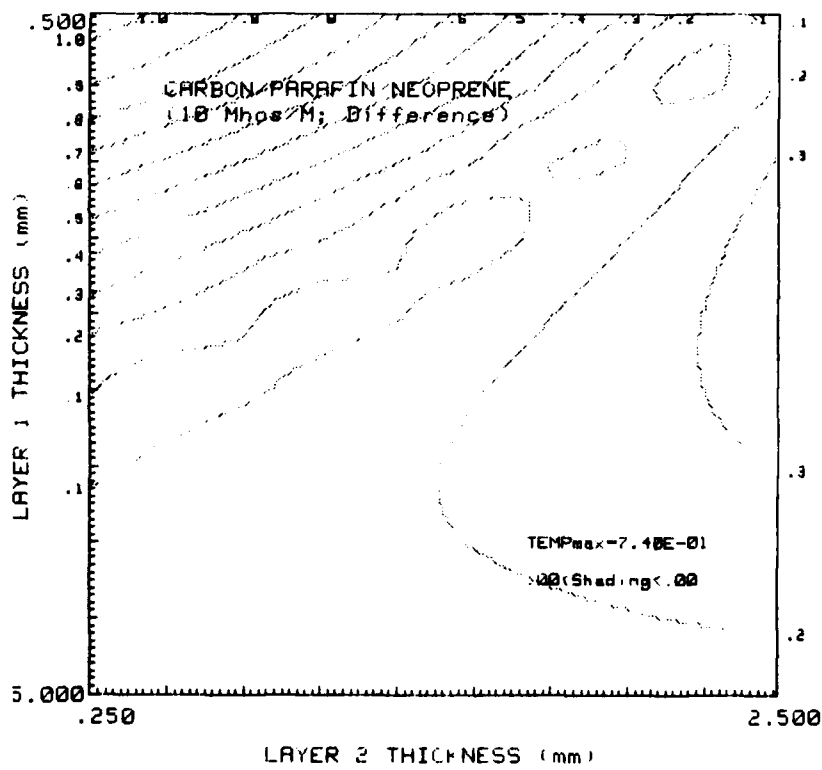


Figure 92: Carbon/Paraffin/Neoprene/Copper Difference  
Contours

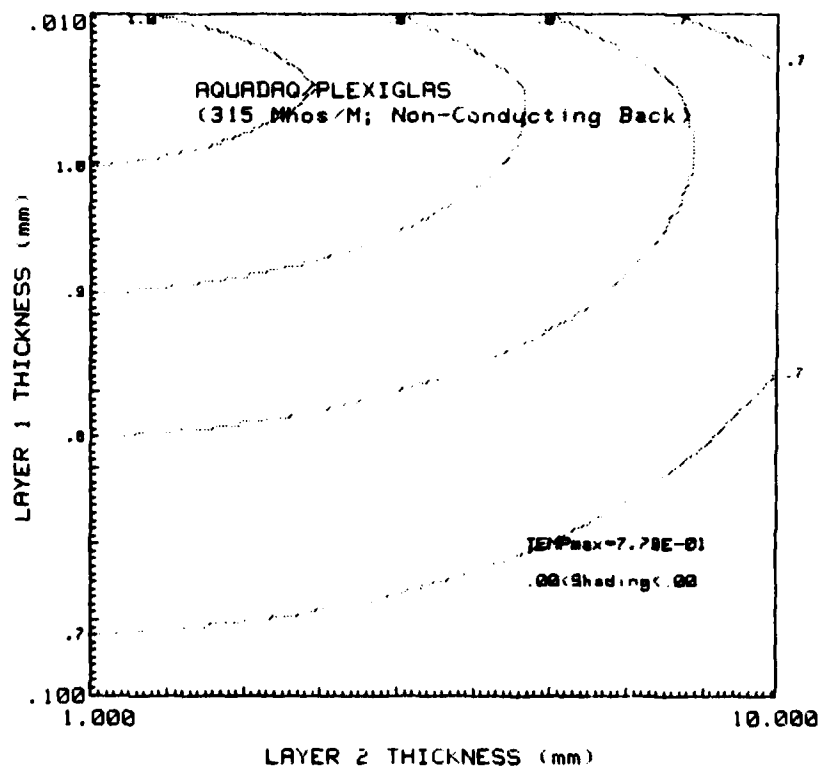


Figure 93: Aquadaq/Plexiglas Thermal Contours

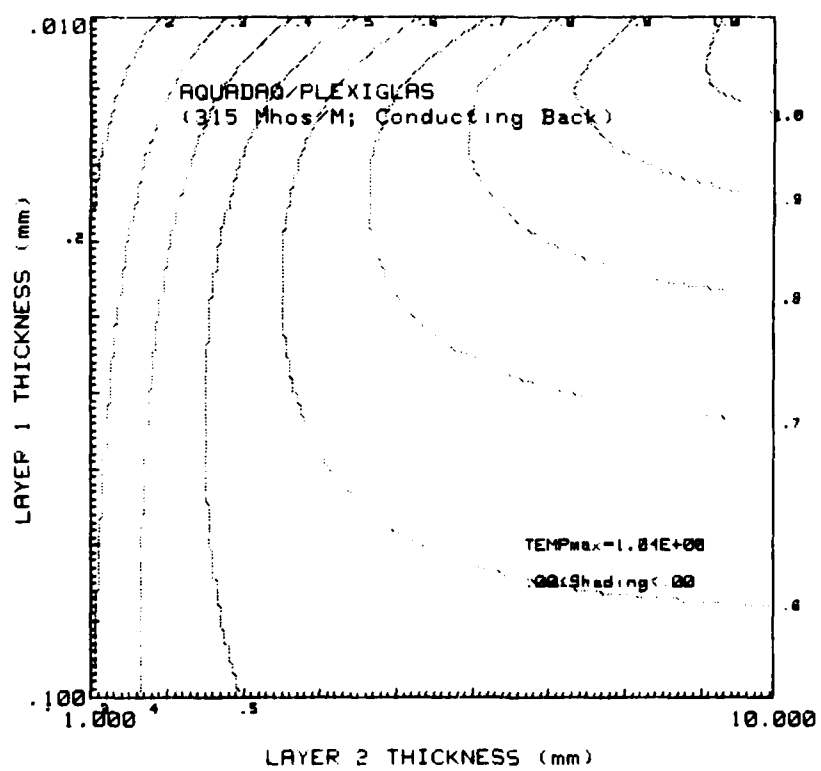


Figure 94: Aquadag/Plexiglas/Copper Thermal Contours

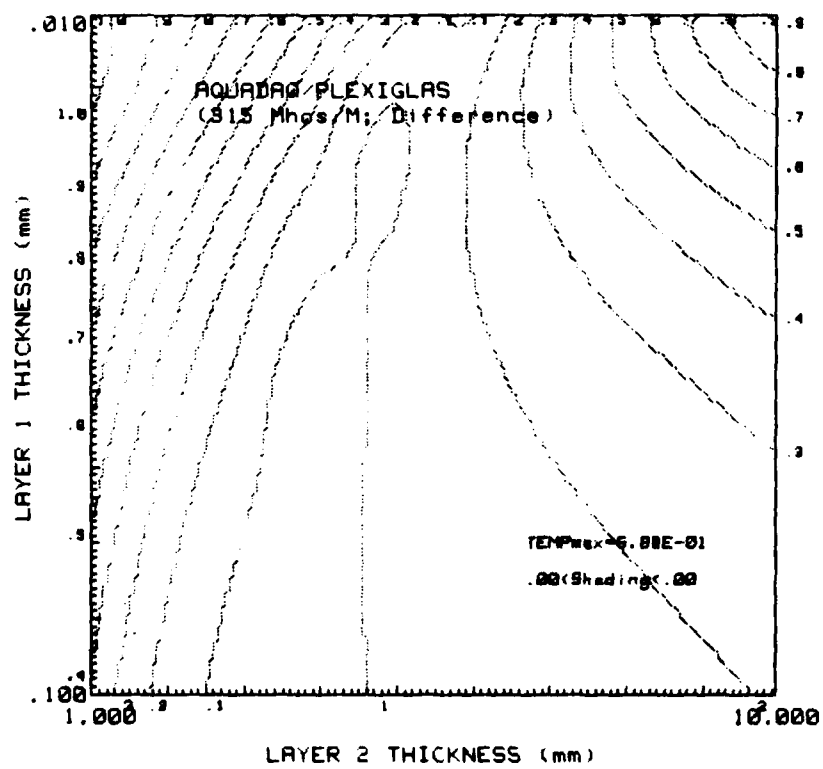


Figure 95: Aquadaq/Plexiglas/Copper Difference Contours

The preceding figures were included to primarily illustrate the effects of different coating/insulating layer combinations. Also, they are representative of the order in which one would use the algorithms included in the appendix in order to analyze a particular coating configuration. That is, assuming a certain material is available and has a measured electrical conductivity, how does one spatially arrange it for optimum effectiveness?

First of all, in addition to selecting a coating material, we must select a suitable thermal insulator. The four primary areas of concern in selecting an insulator are its electrical characteristics which include permittivity and electrical conductivity (or loss factor), its thermal conductivity, and its mechanical applicability. Extensive experimentation was conducted using Plexiglas, styrene plastic, styrofoam, urethane foam, neoprene rubber, glass, phenolic, paraffin wax, paper, etc.. It was found that the foams (styrofoam and urethane foam) exhibited superior electrical characteristics over the other materials. Their loss factors are very low and both have a relative permittivity very near 1; thus, the microwaves hardly know the insulators exist. In addition they are excellent thermal insulators. Therefore, where mechanical application is relatively straight forward,

either of the foams will perform excellently. Urethane foam is impervious to nearly all chemicals and, therefore, nearly any coating may be used without reacting with it. Styrofoam, on the other hand, is a styrene and exhibits disastrous results when used with nearly any petroleum based coating. This is especially true with toluene which is the carrier for the aquadaq coating. It was found that styrofoam performed very well with paraffin/carbon coatings or by chemically shielding it from a petroleum based product. The shield may be a very thin layer of paraffin wax, stick-on Mylar, or stick-on paper. For flat surfaces, there is a  $\frac{1}{4}$  inch foam sheet available at most art supply stores with a paper coating on each side. It is extremely easy to work with, inexpensive, and comes in sheets up to 3x4 feet square. When working on complex surfaces, the neoprene rubber exhibited the most flexibility from an applications point of view; however, it has a very large relative permittivity. The permittivity problem may be partially overcome by using neoprene foam which is commercially available in thicknesses from 1/16 to 1/2 inch. Even though the permittivity for neoprene foam was not measured it should be significantly less than the value of 31 measured for solid neoprene. This is the same foam used in diver's wet suits and should also be relatively inexpensive. It is easily applied to almost

any grease free surface using a typical rubber contact cement. It is also impervious to nearly all chemicals.

Having chosen a coating type and insulator, the final question that must be answered is related to the thickness of each. Using the algorithm included in the Appendix, we may generate a set of three contour plots similar to the ones presented earlier in this chapter. The first would be only with the coating and insulator and no substrate present. This will give us an idea of the differential temperatures that might be observed on the coating if there were zero surface currents located on the substrate. Next, we consider the coating/insulator/substrate combination. The temperatures illustrated would represent the  $\Delta T_{\infty}$  that might be expected. This is the same  $\Delta T_{\infty}$  discussed in the latter part of Chapter VII. In this case the surface currents on the substrate are not zero but something between zero and  $|\vec{H}_i|$ . The third step is to numerically subtract the above two results and display the difference as a contour. This is probably the most important step since it provides the insight required to choose the optimum thickness for both the coating and insulator. It allows us to choose thicknesses that will provide the greatest temperature difference between the case of no substrate ( $\vec{J}=0$ ) and infinite substrate ( $\vec{J}>0$ ).

Illustrative of the above process are two coating examples that have provided excellent results. The first is three layers of aquadaq (315 mhos/m), yielding a total thickness of approximately 15  $\mu$ m, placed on a 5.1 mm thick sheet of paper covered foam. This was the scheme used in the resolution experiments in Chapter VII. The second was a paraffin/carbon conductive coating used by Sega<sup>39</sup> approximately 1.5 mm thick ( $\approx$ 2.0 mhos/m) and placed on a layer of styrofoam 12.5 mm in thickness. There were some difficulties with this scheme in that the coating thickness tended to vary greatly even after machining. This resulted primarily from foam/paraffin expansion problems; therefore, if the paraffin/carbon coating is to be used, it should be kept thin (preferably less than 1 mm).

In summary then, for the case of a coating/insulator/substrate experiment, attempt to use a foam as the insulator: preferably styrofoam, urethane, or last choice, neoprene foam. Use a coating that is easily applied to a uniform thickness. In this case differential surface temperature is almost directly proportional to coating thickness so uniformity is paramount. Typically, the electrical conductivity will be a fixed value; however, for a spray any value from 10 to 500 mhos/m will probably work well (A conductivity between 20 to 100 mhos/m would be optimum.). Execute the above

mentioned computer program and determine the optimum thicknesses for the coating and insulator. Apply the coating/insulator to the substrate and after suitable curing the experiment should be ready for thermographic observation in the microwave field.

Most of the preceding discussion has centered predominantly on the coating/insulator/substrate problem; however, it should be pointed out again that this is not the only coating technique. If we are interested only in the geometrical shape of a particular object, the coating problem is much simplified. The idea, as was mentioned earlier, is to construct a model of foam and then coat it with 2 to 3 skin depths of conductive coating. In this case it can be shown that the surface temperature is independent of coating thickness and only a function of the surface currents present; thus, the coating application need not be critical. Clearly, if the coating has no conductivity (a dielectric) or infinite conductivity (perfect conductor), there will be no energy absorption and, thus, no surface temperature increase. The primary problem then is to determine the optimum conductivity. Chapter V provided the answer for us by referring to Figure 19. There it can be seen for an input power of  $10 \text{ mW/cm}^2$  and at a frequency of 2.45 GHz that the maximum conductivity we may have, and still have a suitable temperature increase ( $1^\circ \text{ K}$ ),

is 750 mhos/m. If we need to consider different microwave parameters, another three dimensional plot may be generated with the computer program included in the Appendix. In this coating scheme we must keep in mind that we want the electrical conductivity as large as possible so that it will more closely approximate a perfect conductor. If we absolutely need a conductivity greater than 750 mhos/m, we must increase our input power correspondingly in order to observe acceptable heating.

In conclusion we may reiterate some of the important aspects of this paper. Initially, a theoretical, one dimensional model is presented which couples the N-Layer electromagnetic problem with the thermodynamic problem; hence, we have a model which predicts equilibrium surface temperatures resulting from electromagnetic absorption in a system of N layers. This is provided as an analysis tool for the engineer interested in investigating different coating schemes. The computer program which solves this problem is included in the Appendix. This model is subsequently verified experimentally on particular multi-layered models. The applicability of the small sample verification process was discussed next. It was shown that a small sample may be a valid approximation for the one dimensional model. It was also shown that nearest neighbor considerations are minimized for coatings that are

placed near the substrate surface. As a rough rule of thumb, it was shown that the coating resolution may be approximated by the value  $a/\pi$ , where "a" is the insulator thickness. It was also shown that the differential temperature observed on the coating of an electrically large object may be thought of as a steady state term resulting from the one dimensional solution plus a higher order term resulting from the finite boundary conditions present. As a result of this analysis, the experimental engineer may be allowed to scale his infrared results by an additive constant in order to "calibrate" the thermographic system. In addition to the above, two particular coating schemes are illustrated that provided reasonable results; these were the carbon/paraffin/styrofoam and aquadaq/styrofoam coatings. Lastly, the Appendix includes information concerning techniques for measuring electrical permittivity and electrical conductivity as well as most of the major computer routines used.

Finally, it is important to reiterate that this entire development was classical in nature and thus only allowed for joule heating in the coating. Other absorption mechanisms, such as rotational coupling, may prove equally or more effective in coating design in the future. The thermographic detection of induced surface currents is only beginning to demonstrate its full

capability. The benefits of such a scheme should prove invaluable to the systems design engineer working in the ever increasing electronic warfare environment.

## BIBLIOGRAPHY

1. LaVarre, C.A. and Burton, R.W.; "Thermographic Imaging of Electromagnetic Fields," Thesis Report NPS-52ZN 75121; 1975; Monterey, CA; Naval Post-graduate School.
2. Martin, V.M., Sega, R.M., Stewart, C.V., and Burton, R.W.; "Applications of Infrared Thermography in the Analysis of Induced Surface Currents Due to Incident Electromagnetic (EM) Radiation on Complex Shapes," Proceedings of the Society of Photo-Optical Instrumentation Engineers/Infrared Systems; September 30-October 1, 1980, Volume 256; 16-26; Huntsville, AL.
3. Burton, R.W., Sega, R.M., and Martin, V.M.; "Experimental Determination of Electromagnetic Pulse (EMP) Absorption on Complex Shapes," NEM 1980 Record; August 5-7, 1980; 144; Anaheim, CA.
4. Burton, R.W. and Martin, V.M.; "Quantified Surface Current Detection Through the Use of Computer Enhanced Thermography," Proceedings of the National Radio Science (URSI) Meeting; 12-16 January, 1981; 2; Boulder, CO.
5. Sega, R.M., Martin, V.M., and Burton, R.W.; "Experimental Determination of Electromagnetic Energy Absorption on Complex Shapes; A Progress Report," Proceedings of the National Radio Science (URSI) Meeting; June 16-19, 1981; 31; Los Angeles, CA.
6. Sega, R.M., Martin, V.M., Warmuth, D.B., and Burton R.W.; "Infrared Application to the Detection of Induced Surface Currents," Proceedings of the Society of Photo-Optical Instrumentation Engineers/Modern Utilization of Infrared Technology VII; August 27-28, 1981, Volume 304; 84-91; San Diego, CA.
7. Martin, V.M. and Burton, R.W.; "Thermal Response of Thin Conductive Coatings to Microwave Absorption," Proceedings of the National Radio Science (URSI) Meeting; 13-15 January, 1982; 43; Boulder, CO.

8. Martin, V.M., Stewart, C.V., and Burton, R.W.; "An Optimized Conductive Coating for Thermographic Measurement of Microwave Induced Surface Currents," Proceedings of Institute of Electrical and Electronic Engineers (IEEE) Region 5 Conference and Exposition; May 3-9, 1982; 182-185; Colorado Springs.
9. Sega, R.M., Martin, V.M., and Burton, R.W.; "Microwave Induced Surface Current Measurement via Infrared Detection," Antennas and Propagation Society (APS) Digest: May 24-28, 1982, Volume 1; 231; Albuquerque.
10. Jackson, J.D.; Classical Electrodynamics; 1975; New York; John Wiley and Sons, Inc.
11. Jordan, E.C., and Balmain, K.G.; Electromagnetic Waves and Radiating Systems; 1968; Englewood Cliffs, N.J.; Prentice-Hall, Inc.
12. Marion, Jerry B.; Classical Electromagnetic Radiation; 1972; New York; Academic Press Inc.
13. Churchill, Ruel V., Brown, James W., and Verhey, Roger F.; Complex Variables and Applications; 1974; New York; McGraw-Hill Book Company.
14. Nobel, Ben and Daniel, James W.; Applied Linear Algebra; 1977; Englewood Cliffs, New Jersey; Prentice-Hall, Inc.
15. Hohn, Franz E.; Elementary Matrix Algebra; 1965; New York; The Macmillan Company.
16. Hansen, Wilford N.; "Electric Fields Produced by the Propagation of Plane Coherent Electromagnetic Radiation in a Stratified Medium;" Journal of the Optical Society of America; March, 1968, Vol 58, No. 3; 380-390; Washington.
17. Wait, James R.; Electromagnetic Waves in Stratified Media; 1970; New York; Pergamon Press.
18. Holman, J.P.; Heat Transfer; 1968; New York; McGraw-Hill Book Company.
19. Kreith, Frank; Principles of Heat Transfer; 1973; New York; Intext Educational Publishers.
20. Siegel, Robert and Howell, John R; Thermal Radiation Heat Transfer; 1981; New York; McGraw-Hill Book Company.
21. McAdams, W.H.; Heat Transmission; 1954; New York; McGraw-Hill Book Company.

22. Giblm, P.J.; Graphs, Surfaces and Homology; 1977; New York; John Wiley and Sons.
23. Sega, R.M., Martin, V.M., Warmuth, D.B., and Burton R.S.; "Infrared Application to the Detection of Induced Surface Currents," Proceedings of the Society of Photo-Optical Instrumentation Engineers/Modern Utilization of Infrared Technology VII; August 27-28, 1981, Volume 304; 84-91; San Diego, CA.
24. Kreith, Frank; Principles of Heat Transfer; 1973; New York; Intext Educational Publishers.
25. Jordan, E.C., and Balmain, K.G.; Electromagnetic Waves and Radiating Systems; 1968; Englewood Cliffs, N.J.; Prentice-Hall, Inc.
26. Strait, Bradley J.; Application of the Method of Moments to Electromagnetic Fields; 1980; St Cloud, Florida; The South-eastern Center for Electrical Engineering Education (SCEEE).
27. Andrejewski, W., "Die Beugung Elektromagnetischer Wellen an der Leitenden Kreisscheibe und an der Kreisförmigen Öffnung im Leitenden Ebenen Schirm;" Z. Angew. Physics 5, 178-186.
28. Bowman, J.J., Senior, T.B.A., and Uslenghi, P.L.E.; Electromagnetic and Acoustic Scattering by Simple Shapes; 1969; Amsterdam; North-Holland Publishing Company.
29. Mentzer, J.R.; Scattering and Diffraction of Radio Waves; 1955; New York; Pergamon Press.
30. Foch, V.A.; Electromagnetic Diffraction and Propagation Problems; 1965; New York; Pergamon Press Inc.
31. Skitch, G.G. and Marshall, S.V.; Electromagnetic Concepts and Application; 1982; Englewood Cliffs, N.J.; Prentice-Hall, Inc.
32. Naor, M. and Senior, T.B.A.; "Scattering by Resistive Plates," Technical Report, Contract F30602-78-C-0148; September 1981; Ann Arbor, MI; Southeastern Center for Electrical Engineering Education.
33. Sega, R.M., Martin, V.M., and Burton, R.W.; "Microwave Induced Surface Current Measurement via Infrared Detection," Antennas and Propagation Society (APS) Digest; May 24-28, 1982, Volume I; 231; Albuquerque.
34. Edwards, J.D.; Aluminum Paint and Powder; 1955; New York; Reinhold Publishing Co.

35. Donnet, Jean-Baptiste; Carbon Black; 1976; New York; Moral Dekker Inc.
36. Erf, Robert K.; Holographic Nondestructive Testing; 1974; New York; The Academic Press.
37. Rogers, G.L.; "Gabor Diffraction Microscopy: The Hologram as a Generalized Zone Plate;" Nature (London); 1950, Vol 166; 237; London.
38. Iizuka, Keigo and Yen, Jui L.; Personal Conversation at the University of Toronto; June 25, 1982.
39. Sega, Ronald M.; "Infrared Detection of Microwave Induced Surface Currents on Flat Plates;" 1982; University of Colorado Dissertation for the Department of Electrical Engineering; Boulder, CO.

## APPENDIX A

## ELECTRICAL CONDUCTIVITY MEASUREMENTS

The purpose of the electrical conductivity measurements was to determine the value of the electrical conductivity of the various coatings used in the infrared current measurement schemes.

The most likely source of inconsistency in the measurement process resulted from the method used to attach or input the current to the test specimen. The two point measurement technique used in this testing is recognized by the American Society of Testing and Materials (ASTM) as the most precise method for determining conductivity. However, care must be exercised to assure that the electrical current passed through the specimen is uniformly distributed over the entire cross sectional area of the test specimen.

Tests were conducted using two possible specimen configurations. The first consisted of a 10cm x 10cm square of the material placed on a plexiglas substrate (Fig 96 ).

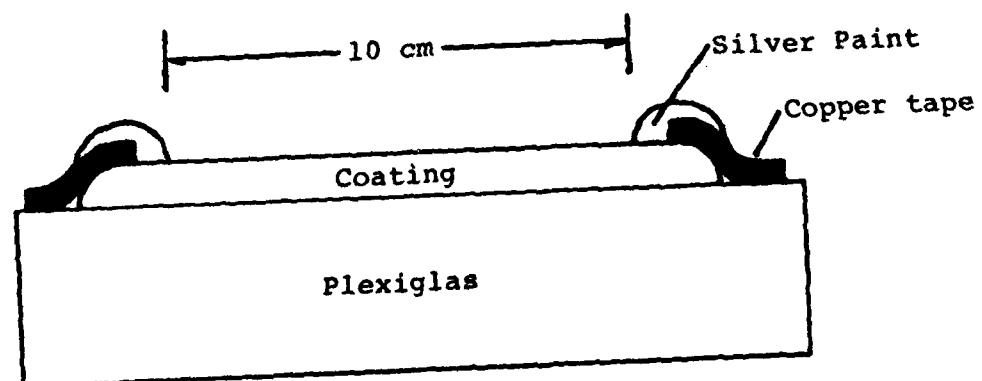


Figure 96: Coating Sample Cross Section

This arrangement was used predominately for thin coatings that were sprayed on the substrate from aerosol cans; thicknesses varied from 10-100 microns. The other configuration which was used with "moldable" materials such as carbon impregnated paraffin consisted of solid disks 2.54 cm in diameter and approximately 7mm thick (Fig 97).

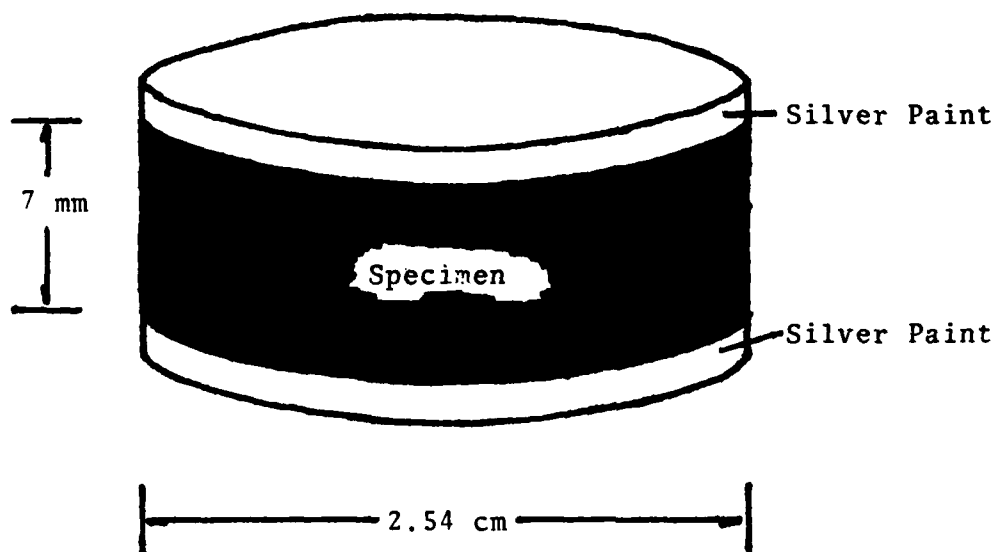


Figure 97 : Drawing of a Typical Disc Sample

In both cases a silver metal based lacquer was used to make final contact with the specimen thus helping insure a uniform electrical contact.

The current connections for the 10cm square were attached to each end of the specimen by means of a copper foil strip embedded in the silver lacquer. Connections for the disk were made by sandwiching it between copper plates which were subsequently clamped in three places with wave guide clamps. See Figures 98 and 99.

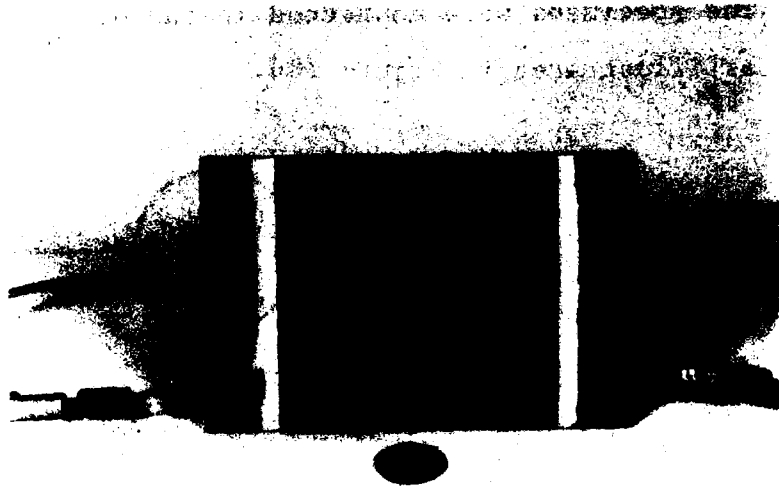


Figure 98: Square Sample Electrical Connections



Figure 99: Disc Sample with Clamps Attached

The specimens were connected in the electrical circuit as illustrated in Figure 100.

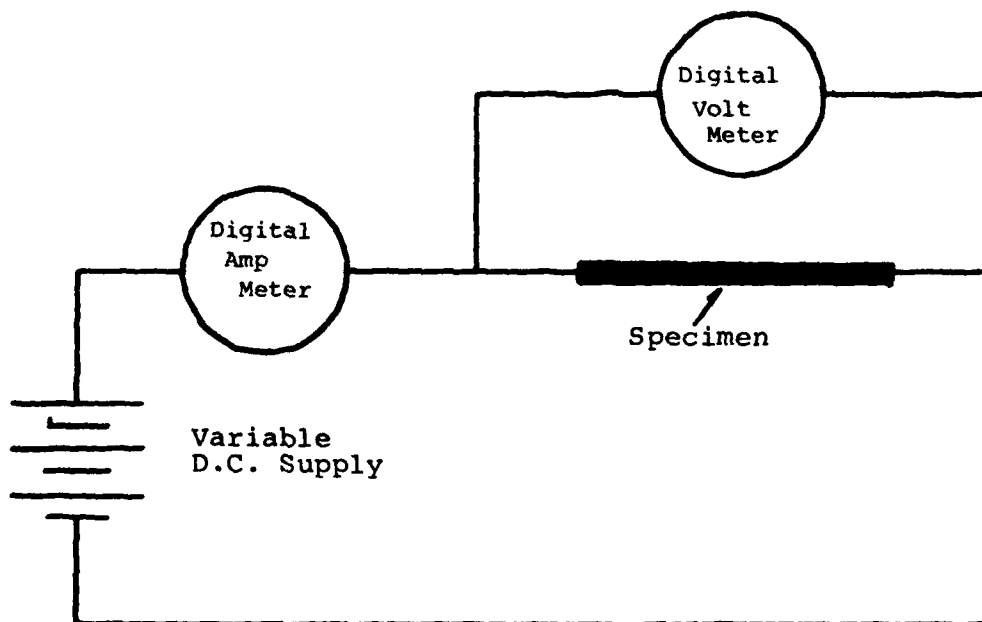


Figure 100: Schematic of Conductivity Measurements

This test arrangement is the ASTM two-point method.  
The following test equipment was used in the test arrangement:

<u>Nomenclature</u>	<u>Identification</u>
Power Supply	Regulated D.C. Power Supply 0-50 VDC, 0-1.5A Kepco Mfg Co, Flushing, NY
Ammeter	Digital Multimeter Hewlett-Packard Model 3466A
Voltmeter	Digital Multimeter Hewlett-Packard Model 3466A
Micrometer	Metric Micrometer Central Scientific Co, Chicago, IL

The conductivity ( $\sigma$ ) for each of the samples was calculated from the following equation:

$$\sigma = \frac{il}{VA}$$

where  $i$  = total current through specimens

$l$  = length of current travel

$V$  = voltage across sample

$A$  = area through which current travels

Conductivity versus temperature was also investigated for the 10cm x 10cm samples with an aquadaq coating. An AGA Thermovision<sub>(C)</sub> 680 infrared camera was used to measure the steady state surface temperature of the sample for various current inputs. See Figure 101 for a plot of  $\sigma$  versus temperatures ( $u$ ).

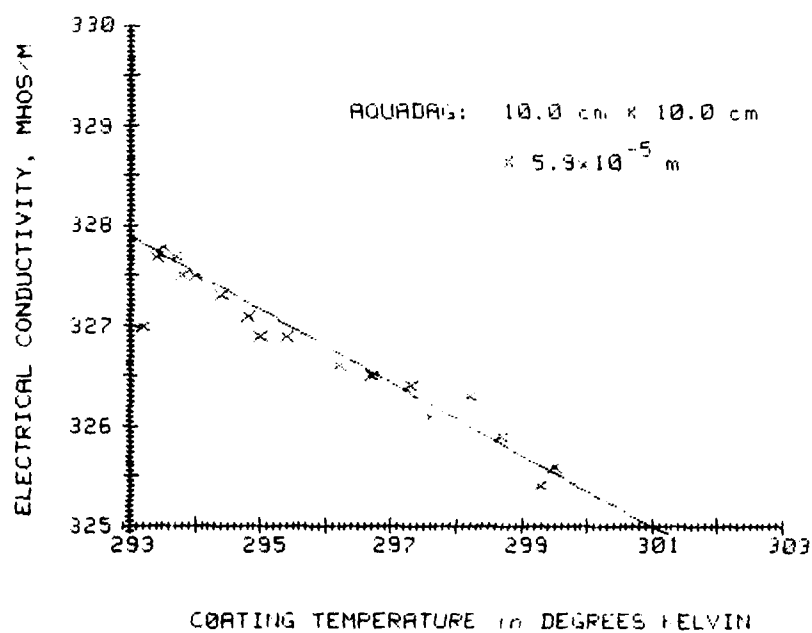


Figure 101: Electrical Conductivity Versus Absolute Temperature (Aquadaq Coating)

Using the technique outlined, the measured conductivity for a composite mixture of paraffin/carbon was measured for various mixing ratios. These plots simplify the process of designing a particular conductivity material since the particular mixing ratios are illustrated. See Figures 102 and 103 for a linear and log plot of sigma. The solid line is a plot of an empirical model of sigma as given in Figure 103.

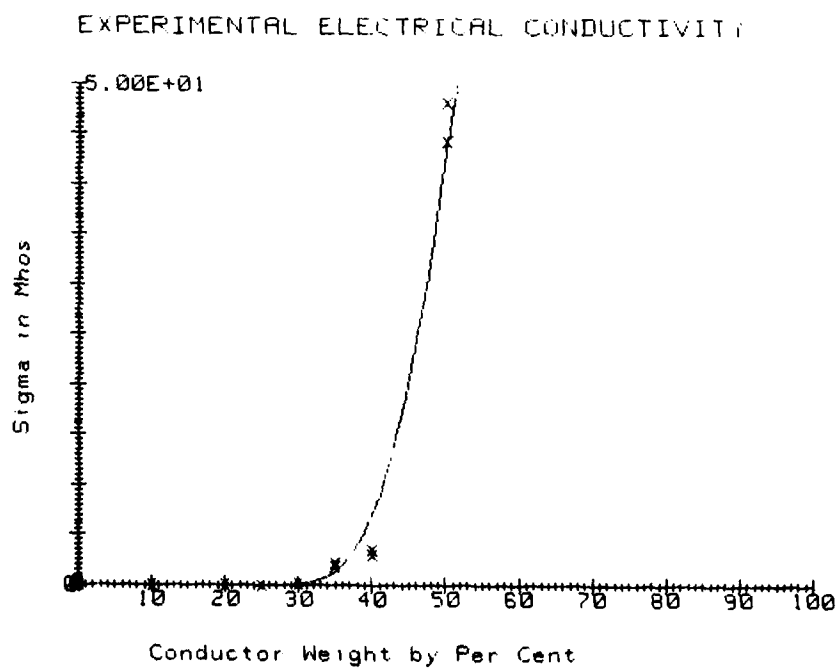


Figure 102: Electrical Conductivity Versus Carbon/Paraffin  
Mixing Ratios

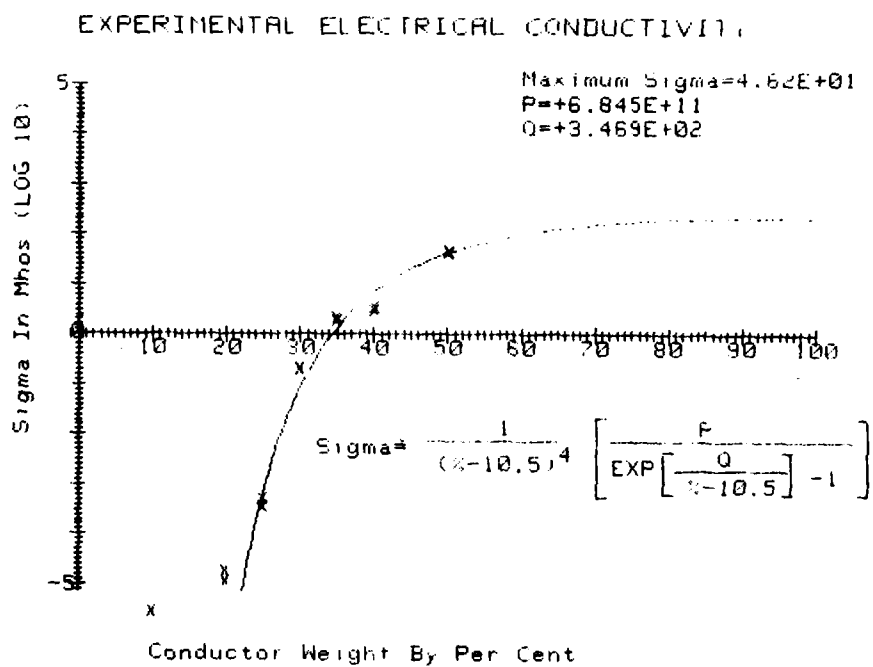


Figure 103: Electrical Conductivity Versus Carbon/Paraffin  
Mixing Ratios with Empirical Model

## APPENDIX B

## ELECTRICAL PERMITTIVITY

Electrical permittivity,  $\epsilon$ , is an exceedingly important variable in the analysis of effects of microwave absorption in a multi-layered system. It is typically frequency dependent and therefore the value used must be measured for each different operating condition. Fortunately, it does not vary greatly; the table below lists values taken from the Chemical Rubber Company's Handbook of Chemistry and Physics, 60th Edition, for some common materials.

Table 1: Relative Permittivity for Various Dielectrics

	<u>Sodium Light</u>	<u>1MHz</u>	<u>100 Mhz</u>	<u>Specific Heat</u>
Paraffin	2.0	2-2.5	*	*
Glass	2.3-3.6	4.0	*	*
Rock Salt	2.3	*	*	*
Gelatin	2.3	*	*	*
Quartz	2.3	*	*	*
Nylon (66)	2.3	3.3	3.2	.4
Polyethylene	2.3	2.3	2.3	.55
Methylmethacrylate (Plexiglas)	2.2	2.8	*	.35
Polystyrene	2.6	2.5-2.7	2.6	.32
Silicon Rubber	*	3.1-3.2	*	*
Porcelain	*	6-8	*	*

\*Value not available

Our permittivities were measured in the laboratory at a frequency of 10 GHz for styrofoam, window glass, paraffin, styrene, phenolic, plexiglas, and neoprene.

Figure 104 illustrates the experimental arrangement.

Test equipment used in this measurement scheme included the following:

<u>Nomenclature</u>	<u>Identification</u>
10 GHz Source	ED-SET MARK 2 Sargeant-Welch Scientific Co. Skokie, IL
10 GHz Detector	"
Microwave Bench	"

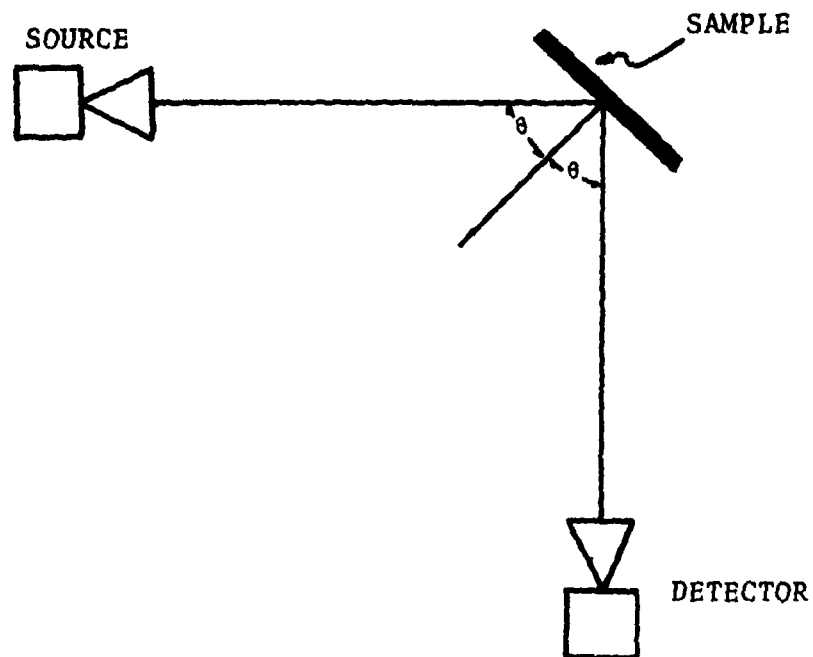


Figure 104: Schematic Arrangement of Permittivity Measurements

The procedure was to measure the reflectance for a given sample at various angles of incidence. E was polarized perpendicular to the plane of incidence. Because of limited sample sizes, incident angles were limited to between 20 and 60 degrees with measurements taken in 5 degree increments. The measured value versus angle was then plotted on a graph on which theoretical curves of reflectivity versus permittivity had been drawn for a particular sample thickness and incident angle. The permittivity is where the measured reflectance value intersects the particular curve. Figures 105 to 111 illustrate the plots for styrofoam, glass, paraffin, styrene, phenolic, Plexiglas, and neoprene respectively. (Only 10 degree increments are plotted for illustration purposes.)

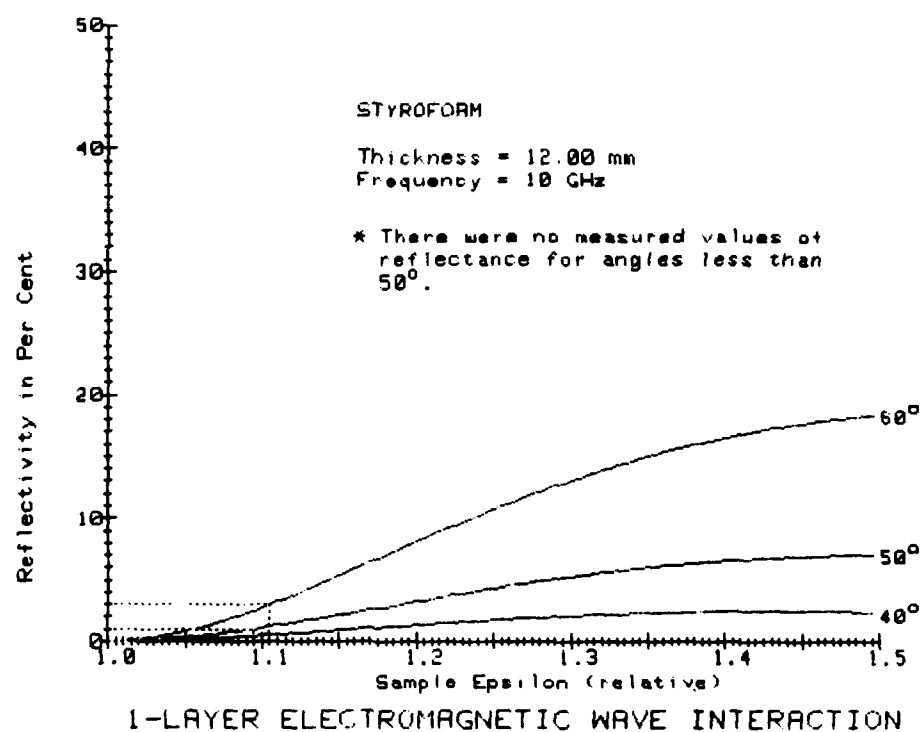


Figure 105: Permittivity Plot for Styrofoam at 10 GHz

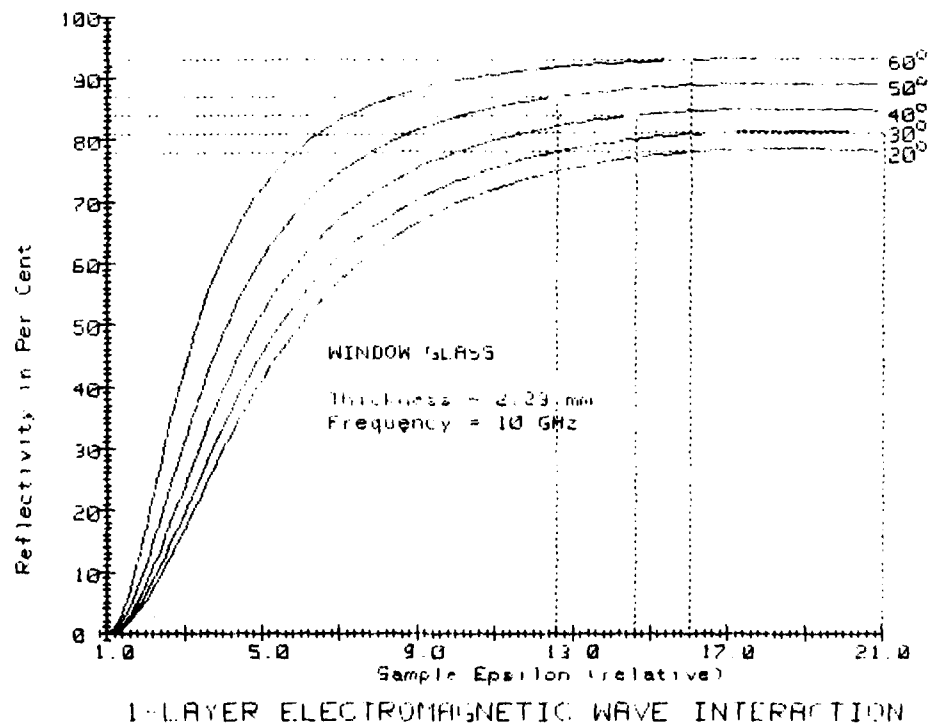


Figure 106: Permittivity Plot for Window Glass at 10 GHz

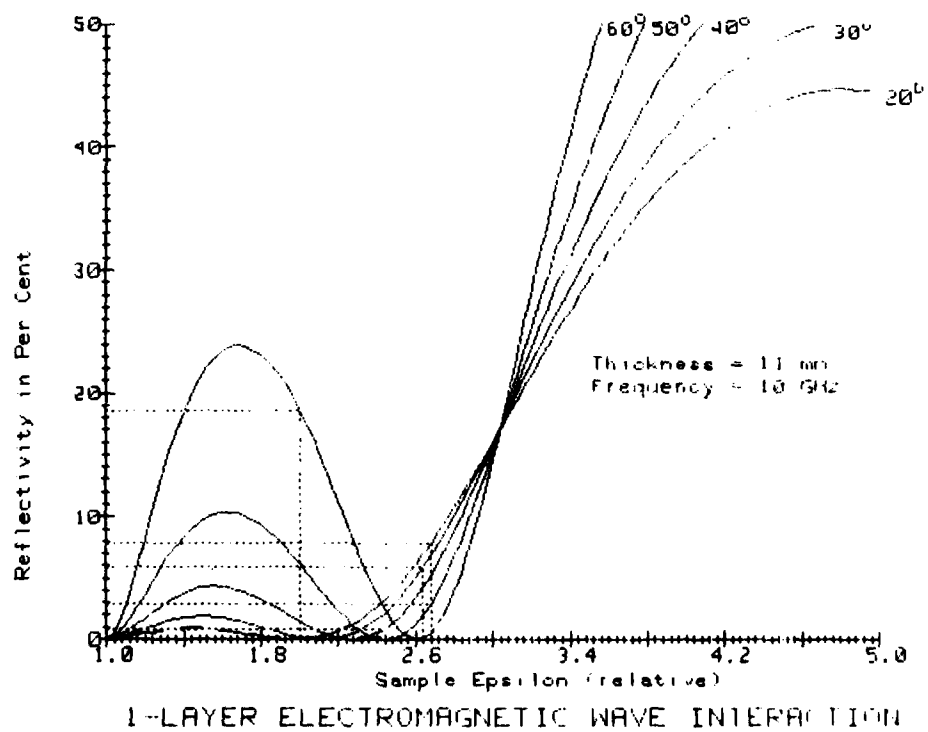


Figure 107: Permittivity Plot for Paraffin at 10 GHz

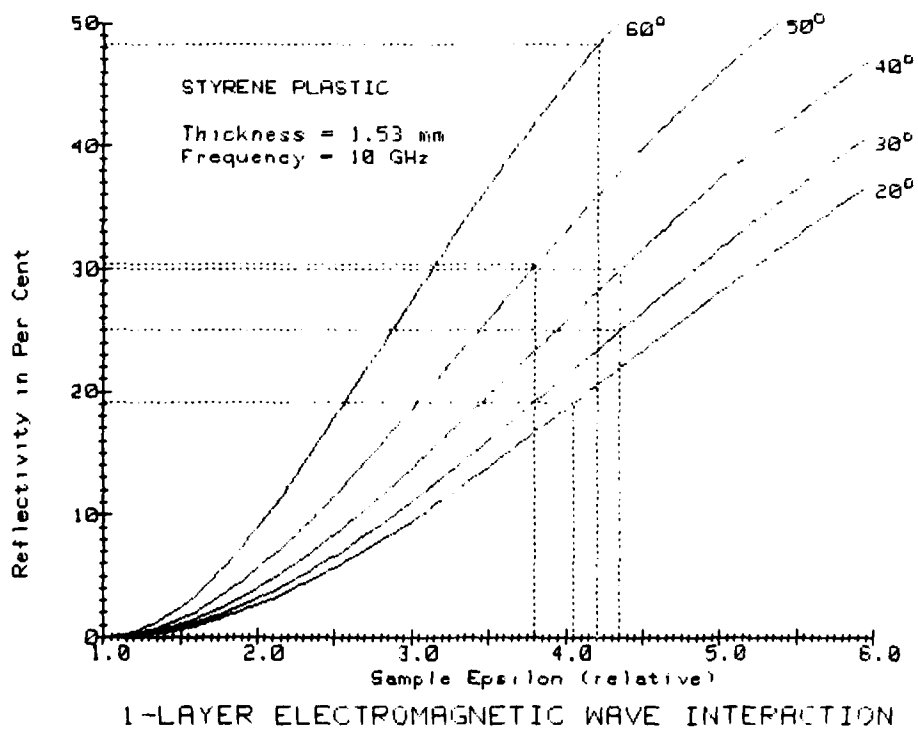


Figure 108: Permittivity Plot for Styrene at 10 GHz

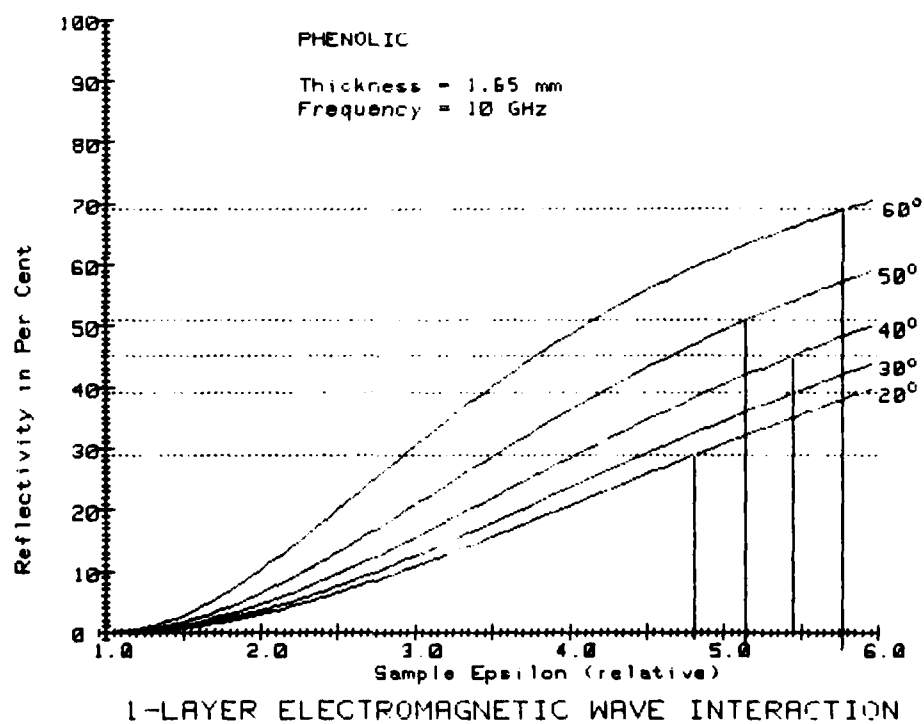


Figure 109 : Permittivity Plot for Phenolic at 10 GHz

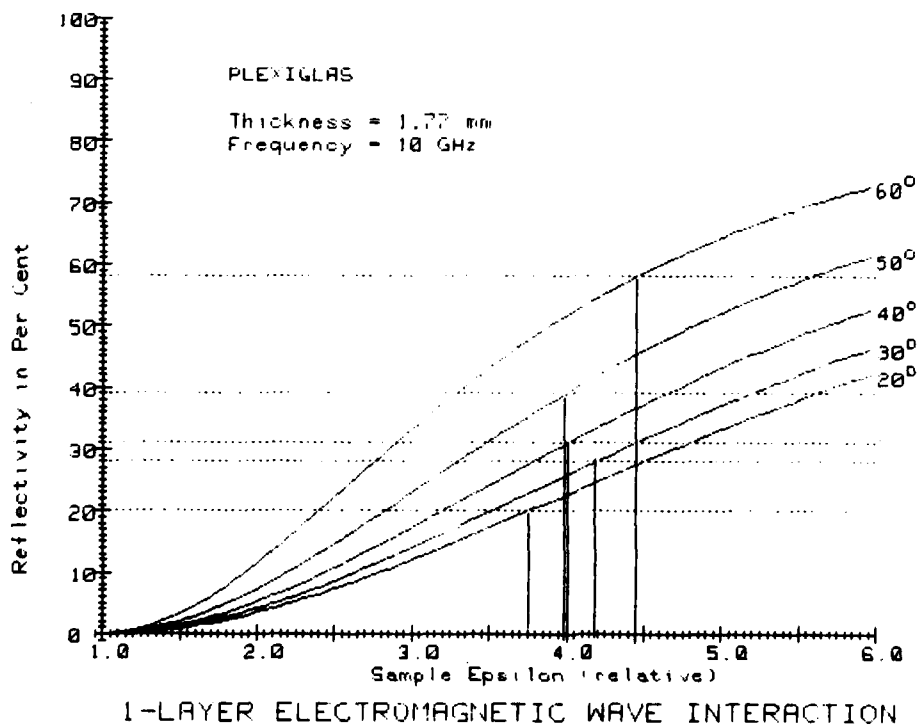


Figure 110 : Permittivity Plot for Plexiglas at 10 GHz

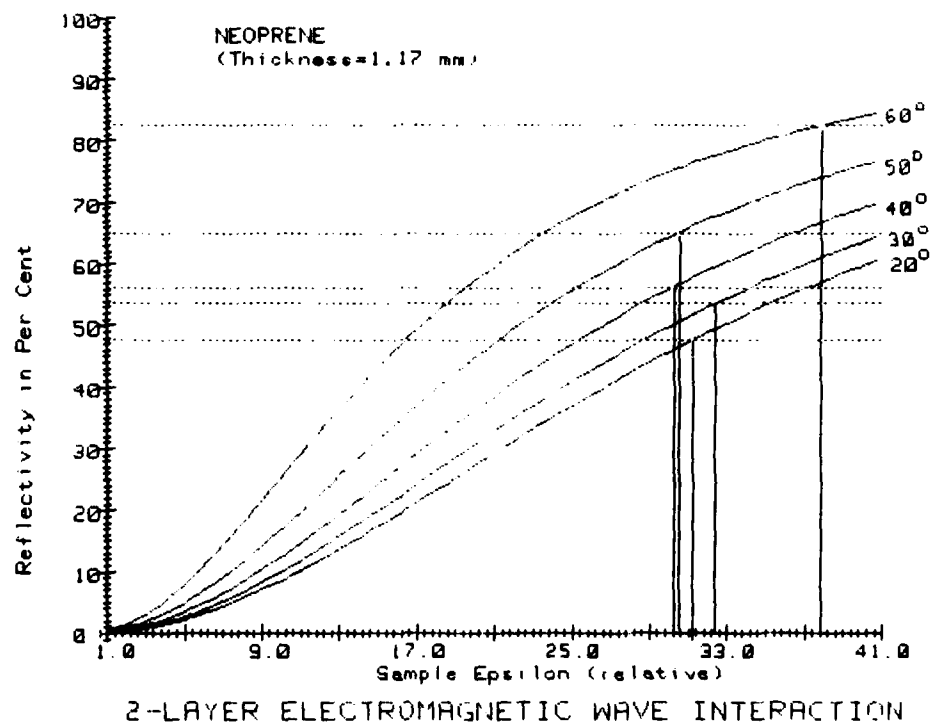


Figure 111 : Permittivity Plot for Neoprene at 10 GHz

No attempt was made to measure permittivities for any materials other than good dielectrics. Since Ohm's law was included explicitly in the solution of Maxwell's equations, it is not necessary to assume a complex permittivity for conductive materials; thus, the free space value is acceptable.

Table 2 lists the measured values of relative permittivity for the materials considered. The averaging procedure consisted of calculating an average value and a standard deviation for the nine incident angles. Then any measured permittivity outside the range  $\pm$  one standard deviation from the average was rejected and a new average and standard deviation calculated. These are the values that appear in Table 2 below.

Table 2: Measured Relative Permittivity at 10 GHz

<u>Material</u>	<u>Average Relative Permittivity (10 GHz)</u>	
Styrofoam	1.11	(One data point)
Window Glass	14.2	(St. Dev. = 1.3)
Paraffin	2.55	(St. Dev. = .14)
Styrene	4.28	(St. Dev. = .08)
Phenolic	5.32	(St. Dev. = .33)
Plexiglas	4.07	(St. Dev. = .24)
Neoprene	31.1	(St. Dev. = .83)

## APPENDIX C

## COMPUTER PROGRAM

The name of this program is "One-B". It is written for use on a Hewlett-Packard 9845B minicomputer. It calculates reflectivity, transmissivity, and absorptivity for a single interface. It will also calculate infrared emissivity for 5.3 microns wavelength. Input variables are medium two electrical conductivity, index of refraction, and magnetic permeability (relative) as well as the incident frequency in gigahertz.

```

10  ! THE NAME OF THIS PROGRAM IS ONE-B!
20  INTEGER I,J,O,N,K,L,M
30  DIM Para(4,5),Perp(4,5),Theda(90),Refpar(90),Refper(90),Jeffpa(90)
40  DIM Jeffpe(90)
50  GCLEAR
60  EXIT GRAPHICS
70  INPUT "Enter Sigma of medium two.",Sigma
80  INPUT "Enter the relative permeability of medium two.",Mu2r
90  INPUT "Enter the index of refraction of medium two.",N2r
100 INPUT "Enter the incident frequency in Gigahertz.",F
110 INPUT "Enter the input power in MW/Square Centimeter.",P
120 INPUT "For IR emissivity enter a 1; otherwise 0.",Emiss
130 Mu=4*PI*1E-7
140 Eps=8.8542E-12
150 Eps2=N2r^2*Eps
160 Mu2=Mu2r*Mu
170 E1=(Mu/Eps)^.25*SQR(20*P)      ! INCIDENT E IS CALCULATED FROM POWER!
180 IF Emiss=1 THEN F=1E5
190 Omega=2*PI*F*1E9
200 Lambda=2.998E8/(F*1E9)
210 Root=SQR(1+(Sigma/(Omega*Eps2))^2)
220 Coef=Omega*SQR(Mu2*Eps2/2)
230 Alpha=Coef*SQR(1+Root)
240 Gamma=Coef*SQR(-1+Root)
250 Mag=Alpha^2+Gamma^2
260 Mag2=Mag^2
270 Inc=PI/180
280 Bet0=2*PI/Lambda
290 K2=Bet0^2
300 IF Sigma=0 THEN Sigma=1E-12
310 Delta=SQR(2/(Omega*Mu2*Sigma))  ! SKIN DEPTH IS CALC.!
320 Diff=Alpha^2-Gamma^2
330 FOR M=1 TO 90
340 IF M/10-M DIV 10=0 THEN PRINT USING 350;M
350 IMAGE "M=",DD

```

```

360 Cothed=cos(Theda)
370 IF Cothed=0 THEN Cothed=1E-8
380 Sin2=sin(Theda)^2
390 P=.5*(1-K2*Sin2*Diff/Mag2)
400 Q=K2*Sin2*Alpha*Gamma/Mag2
410 Cophir=sqr(P+sqr(P^2+Q^2))
420 Cophii=sqr(ABS(-P+sqr(P^2+Q^2)))
430 FOR I=1 TO 4
440   FOR J=1 TO 5
450     Para(I,J)=0
460     Perp(I,J)=0
470   NEXT J
480 NEXT I
490 Para(1,1)=Cophir/Cothed
500 Para(2,1)=Cophii/Cothed
510 Para(3,1)=Alpha*Mu/(Bet0*MU2)
520 Para(4,1)=Gamma*MU/(Bet0*MU2)
530 Para(1,2)=-Cophii/Cothed
540 Para(2,2)=Cophir/Cothed
550 Para(3,2)=-Gamma*MU/(Bet0*MU2)
560 Para(4,2)=Alpha*MU/(Bet0*MU2)
570 Para(1,3)=-1
580 Para(3,3)=1
590 Para(2,4)=-1
600 Para(4,4)=1
610 Perp(1,1)=1
620 Perp(3,1)=Mu*(Alpha*Cophir-Gamma*Cophii)/(Mu2*Bet0*Cothed)
630 Perp(4,1)=Mu*(Alpha*Cophii+Gamma*Cophir)/(Mu2*Bet0*Cothed)
640 Perp(2,2)=1
650 Perp(3,2)=-Mu*(Alpha*Cophii+Gamma*Cophir)/(Mu2*Bet0*Cothed)
660 Perp(4,2)=Mu*(Alpha*Cophir-Gamma*Cophii)/(Mu2*Bet0*Cothed)
670 Perp(1,3)=-1
680 Perp(3,3)=1
690 Perp(2,4)=-1

```

!CALC. THE VALUE OF COS(THEDA)!

!THE REAL AND IMAG. PARTS OF COS(PHI) CALC.!

!COEF. MATRICES ARE ZEROED!

!DATA IS LOADED INTO THE COEF. MATRICES!

```

700 Perp(4,4)=1
710 Para(1,5)=E1
720 Para(3,5)=E1
730 Perp(1,5)=E1
740 Perp(3,5)=E1
750 FOR I=1 TO 4
760 IF Para(I,1)=0 THEN 780
770 GOTO 870
780 FOR N=I+1 TO 4
790 IF Para(N,1)=0 THEN 810
800 GOTO 810
810 NEXT N
820 FOR J=1 TO 5
830 V19=Para(I,J)
840 Para(I,J)=Para(N,J)
850 Para(N,J)=V19
860 NEXT J
870 FOR J=1 TO 5
880 IF I=J THEN 900
890 Para(I,J)=Para(I,J)/Para(I,I)
900 NEXT J
910 Para(I,I)=1
920 FOR O=I+1 TO 4
930 V20=Para(O,I)
940 FOR J=1 TO 5
950 Para(O,J)=Para(O,J)-V20*Para(I,J)
960 NEXT J
970 NEXT O
980 NEXT I
990 FOR I=0 TO 3
1000 FOR O=I+1 TO 3
1010 V20=Para(4-O,4-I)
1020 FOR J=4-I TO 5
1030 Para(4-O,J)=Para(4-O,J)-V20*Para(4-I,J)
1040 NEXT J

```

!Para MATRIX IS ROW REDUCED FOR SOLN!

```

1050 NEXT 0
1060 NEXT I
1070 FOR I=1 TO 4
1080 IF Perp(I,I)=0 THEN 1100
1090 GOTO 1190
1100 FOR N=I+1 TO 4
1110 IF Perp(N,I)=0 THEN 1130
1120 GOTO 1140
1130 NEXT N
1140 FOR J=1 TO 5
1150 V19=Perp(I,J)
1160 Perp(I,J)=Perp(N,J)
1170 Perp(N,J)=V19
1180 NEXT J
1190 FOR J=1 TO 5
1200 IF I=J THEN 1220
1210 Perp(I,J)=Perp(I,J)/Perp(I,I)
1220 NEXT J
1230 Perp(I,I)=1
1240 FOR O=I+1 TO 4
1250 V20=Perp(O,I)
1260 FOR J=1 TO 5
1270 Perp(O,J)=Perp(O,J)-V20*Perp(I,J)
1280 NEXT J
1290 NEXT O
1300 NEXT I
1310 FOR I=0 TO 3
1320 FOR O=I+1 TO 3
1330 V20=Perp(4-O,4-I)
1340 FOR J=4-I TO 5
1350 Perp(4-O,J)=Perp(4-O,J)-V20*Perp(4-I,J)
1360 NEXT J
1370 NEXT O
1380 NEXT I
1390 Theda(M)=Theda

```

!Perp MATRIX IS ROW REDUCED FOR SOLN.!

!EFF. SURFACE CURRENTS ARE CALCULATED!

```

1400 Denom=Alpha*Cophii+Gamma*Cophir
1410 IF Denom=0 THEN Denom=1E-5
1420 Jeffpa(M)=Sigma*SQR(Para(1,5)^2+Para(2,5)^2)/(Delta*Derom)
1430 Jeffpe(M)=Sigma*SQR(Perp(1,5)^2+Perp(2,5)^2)/(Delta*Denom)
1440 Refpar(M)=(Para(3,5)^2+Para(4,5)^2)/E1^2
1450 Refper(M)=(Perp(3,5)^2+Perp(4,5)^2)/E1^2
1460 Theda=Theda+Inc
1470 NEXT M
1480 GCLEAR
1490 GRAPHICS
1500 DEG
1510 CSIZE 3,9/15,15
1520 LINE TYPE 1
1530 LOCATE 20,115,15,80
1540 SCALE 0,PI/2,0,1
1550 LOCATE 19,115,14,80
1560 AXES PI/180,.01,0,0,10,10
1570 MOVE Theda(1),ABS(Emiss-Refpar(1))
1580 FOR M=2 TO 90
1590 DRAW Theda(M),ABS(Emiss-Refpar(M))
1600 NEXT M
1610 LINE TYPE 3
1620 MOVE Theda(1),ABS(Emiss-Refper(1))
1630 FOR M=2 TO 90
1640 DRAW Theda(M),ABS(Emiss-Refper(M))
1650 NEXT M
1660 IF Emiss=0 THEN GOTO 1720
1670 MOVE Theda(1),ABS(Emiss-Refper(1))
1680 LINE TYPE 4
1690 FOR M=2 TO 90
1700 DRAW Theda(M),1-(Refpar(M)+Refper(M))/2
1710 NEXT M
1720 IF Emiss=1 THEN 1830
1730 LINE TYPE 4

```

! REFLECTIVITY AND J ARE PLOTTED!

```

1740 MOVE Theda(1),LGT(Jeffpa(1))/10
1750 FOR M=2 TO 90
1760 DRAW Theda(M),LGT(Jeffpa(M))/10
1770 NEXT M
1780 LINE TYPE 5
1790 MOVE Theda(1),LGT(Jeffpe(1))/10
1800 FOR M=2 TO 90
1810 DRAW Theda(M),LGT(Jeffpe(M))/10
1820 NEXT M
1830 LINE TYPE 1
1840 Devx=PI/18
1850 Devy=.1
1860 MOVE -.3*Devx,-.5*Devy
1870 LABEL 0
1880 MOVE -.7*Devx,.8*Devy
1890 LABEL 10
1900 MOVE -.7*Devx,1.8*Devy
1910 LABEL 20
1920 MOVE -.7*Devx,2.8*Devy
1930 LABEL 30
1940 MOVE -.7*Devx,3.8*Devy
1950 LABEL 40
1960 MOVE -.7*Devx,4.8*Devy
1970 LABEL 50
1980 MOVE -.7*Devx,5.8*Devy
1990 LABEL 60
2000 MOVE -.7*Devx,6.8*Devy
2010 LABEL 70
2020 MOVE -.7*Devx,7.8*Devy
2030 LABEL 80
2040 MOVE -.7*Devx,8.8*Devy
2050 LABEL 90
2060 MOVE PI/2-.35*Devx,-.4*Devy
2070 LABEL 90
2080 MOVE -.7*Devx,-.2*Devy

```

```

2090 LABEL 0
2100 MOVE -.9*Devx,1-.2*Devy
2110 LABEL 100
2120 MOVE .65*Devx,-.4*Devy
2130 LABEL 10
2140 MOVE 1.65*Devx,-.4*Devy
2150 LABEL 20
2160 MOVE 2.65*Devx,-.4*Devy
2170 LABEL 30
2180 MOVE 3.65*Devx,-.4*Devy
2190 LABEL 40
2200 MOVE 2.5*Devx,-Devy
2210 LABEL "Incident Angle in Degrees"
2220 MOVE 4.65*Devx,-.4*Devy
2230 LABEL 50
2240 MOVE 5.65*Devx,-.4*Devy
2250 LABEL 60
2260 MOVE 6.65*Devx,-.4*Devy
2270 LABEL 70
2280 MOVE 7.65*Devx,-.4*Devy
2290 LABEL 80
2300 LDIR 90
2310 MOVE -1.2*Devx,Devy
2320 IF Emiss=1 THEN GOTO 2370
2330 LABEL "Reflectivity as a Per Cent"
2340 MOVE -.8*Devx,0
2350 LABEL "Effective Surface Current (LOG)x.1"
2360 GOTO 2390
2370 MOVE -Devx,Devy
2380 LABEL "Emissivity as a Per Cent"
2390 LDIR 0
2400 LOCATE 10,115,15,115
2410 MOVE -1.5*Devx,1.2
2420 DRAW 0,1.2
2430 MOVE .25*Devx,1.2

```

```

2440 IF Emiss=1 THEN GOTO 2470
2450 LABEL "Parallel Reflectivity"
2460 GOTO 2480
2470 LABEL "Parallel Emissivity"
2480 MOVE 4*Devx,1.2
2490 LINE TYPE 3
2500 DRAW 4.7*Devx,1.2
2510 MOVE 4.95*Devx,1.2
2520 LINE TYPE 1
2530 IF Emiss=1 THEN GOTO 2560
2540 LABEL "Perpendicular Reflectivity"
2550 GOTO 2570
2560 LABEL "Perpendicular Emissivity"
2570 IF Emiss=1 THEN GOTO 2690
2580 LINE TYPE 4
2590 MOVE -1.5*Devx,1.12
2600 DRAW 0,1.12
2610 LINE TYPE 5
2620 MOVE 4*Devx,1.12
2630 DRAW 5.5*Devx,1.12
2640 LINE TYPE 1
2650 MOVE .25*Devx,1.12
2660 LABEL "J Effective Parallel"
2670 MOVE 5.75*Devx,1.12
2680 LABEL "J Effective Perp."
2690 LOCATE 20,115,15,80
2700 LINE TYPE 1
2710 MOVE -Devx,-2*Devx
2720 CSIZE 4.2,9/15,0
2730 IF Emiss=1 THEN GOTO 2770
2740 LABEL "REFLECTIVITY FROM A SINGLE PLANE INTERFACE"
2750 CSIZE 3,9/15,15
2760 GOTO 2890
2770 LABEL "DIRECTIONAL SPECTRAL EMISSIVITY AT 3 MICRONS"
2780 CSIZE 3,9/15,15

```

```

2790 IF Emiss=0 THEN GOTO 2890
2800 LOCATE 10,115,15,115
2810 MOVE -1.5*Devx,1.15
2820 LINE TYPE 4
2830 DRAW 0,1.15
2840 MOVE .25*Devx,1.15
2850 LINE TYPE 1
2860 LABEL "Total Emissivity (Parallel and Perpendicular Avg.)"
2870 LINE TYPE 1
2880 IF Emiss=1 THEN GOTO 2920
2890 MOVE 0,1.05
2900 LABEL USING 2910;F
2910 IMAGE "Freq. in GHz=",D.DD
2920 MOVE 3.3*Devx,1.05
2930 LABEL USING 2940;N2r
2940 IMAGE "N2=",D.DD
2950 MOVE 5*Devx,1.05
2960 LABEL USING 2970;Sigma
2970 IMAGE "Sigma=",D.DDE
2980 MOVE 8*Devx,1.05
2990 LABEL USING 3000;Mu2r
3000 IMAGE "Mu=",DDD
3010 MOVE 5*Devx,1
3020 LABEL USING 3030;Delta
3030 IMAGE "Skin Depth=",D.DDE
3040 RAD
3050 STOP

```

## APPENDIX D

## COMPUTER PROGRAM

The name of this program is "Basic". It calculates the reflectivity, transmissivity, and absorptivity for an N-layer electromagnetic interaction problem. The input parameters are the number of layers (not to exceed 10), the incident frequency in gigahertz, the incident power in  $\text{mW/cm}^2$ , and the individual layer conductivities, permittivities, permeability, and thickness.

```

10  ! THE NAME OF THIS PROGRAM IS 'Basic' !
20  ! IT CALCULATES THE REFLECTANCE, TRANSMITTANCE, AND ABSORBANCE FOR A N-LAY
ER SYSTEM!
30  INTEGER I,J,K,L,M,N,O,P,Q,R,Lp,Np
40  DIM Beta(11,2),Z(11),Cothd(12,2),Sigma(10),Mu(12),Epsilon(12),Theda(91),Pa
ra(22,22,2),Perp(22,22,2),Paraex(44,45),Perpex(44,45)
50  DIM Reperp(91),Repara(91),Trperp(91),Trpara(91),Abpara(91),Abperp(91)
60  GCLEAR
70  EXIT GRAPHICS
80  INPUT "Enter the Number of Layers not to Exceed 10.",N
90  INPUT "Enter the Incident Power in MW/Cm^2",Power
100 INPUT "Enter the Incident Frequency in Gigahertz.",F
110 INPUT "Enter the 'STEP' increment for Theda.",Step
120 Np=N+1
130 L=4*Np
140 Lp=L+1
150 Omega=2*PI*F*1E9
160 Beta0=Omega/2.998E8
170 Beta02=Beta0^2
180 Power=10*Power
190 FOR I=1 TO N
200 DISP "Sigma(;;):";
210 INPUT Sigma(I)
220 DISP "Mu(;;):";
230 INPUT Mu
240 Mu(I)=Mu+4*PI*1E-7
250 DISP "Epsilon(;;):";
260 INPUT Epsilon
270 Epsilon(I)=Epsilon+8.8542E-12
280 DISP "Thickness(;;):";
290 INPUT Thick
300 Z(I)=Z(I-1)+Thick
310 Coef=0*Omega*SQR(Mu(I)*Epsilon(I)/2)
320 Sroot=SQR(1+(Sigma(I)/(Omega*Epsilon(I)))^2)

```

! DIMENSION OF EXPANDED MATRICES!

! ANGULAR FREQUENCY IS CALCULATED!

! FREE SPACE WAVE VECTOR IS CALCULATED!

! THE WAVE VECTOR IS SQUARED!

! CONVERTS TO WATT/METER^2!

! ELEC. PROPERTIES OF LAYERS IS INSERTED!

! ELECTRICAL CONDUCTIVITY IN MHOS!

! RELATIVE MAGNETIC PERMEABILITY!

! RELATIVE ELECTRIC PERMITTIVITY!

! EACH LAYER THICKNESS IN METERS!

! Z(n) IS CALCULATED FROM THICKNESSES!

Sroot=SQR(1+(Sigma(I)/(Omega\*Epsilon(I)))^2)

```

330 Beta(I,1)=Coef*SQR(1+Sqrroot)      !REAL WAVE VECTOR (Alpha) IS CALC.!
340 Beta(I,2)=Coef*SQR(Sqrroot-1)      !IMAG WAVE VECTOR (Gamma) IS CALC.!
350 NEXT I
360 Mu(0)=4*PI*1E-7
370 Epsilon(0)=8.8542E-12
380 Mu(Np)=4*PI*1E-7
390 Epsilon(Np)=8.8512E-12
400 Z(0)=0
410 Beta(0,1)=Beta0
420 Beta(0,2)=0
430 Beta(Np,1)=Beta0
440 Beta(Np,2)=0
450 E1=(Mu(0)/Epsilon(0))^.25*SQR(2*Power)
460 E12=E1^2
470 Deg=PI/180
480 ! !
490 ! WE BEGIN ITERATING FROM 0 TO 90 DEGREES ANGLE OF INCIDENCE!
500 ! !
510 FOR Theda=0 TO 90 STEP Step
520 IF Theda/10-Theda DIV 10=0 THEN PRINT USING 530;Theda
530 IMAGE "Theda=",DD
540 X=COS(Theda*Deg)
550 IF X=0 THEN X=1E-8
560 Cothed(Np,1)=X
570 Cothed(Np,2)=0
580 Cothed(0,1)=X
590 Cothed(0,2)=0
600 ! !
610 ! WE CALCULATE REAL AND IMAGINARY COS(Theda).!
620 ! !
630 FOR I=1 TO N
640 Sin2=SIN(Theda*Deg)^2
650 Denom=(Beta(I,1)^2+Beta(I,2)^2)^2
660 Pee=.5*(1-Beta02*Sin2*(Beta(I,1)^2-Beta(I,2)^2)/Denom)
670 Que=Beta02*Sin2*Beta(I,1)*Beta(I,2)/Denom

```

```

680 X=SQR(Pee^2+Que^2)
690 Cothed(I,1)=SQR(Pee+X)          !REAL COS(Theda N) IS CALCULATED!
700 Cothed(I,2)=SQR(ABS(X-Pee))     !IMAG COS(Theda N) IS CALCULATED!
710 A(I)=Beta(I,1)*Cothed(I,1)-Beta(I,2)*Cothed(I,2)
720 B(I)=Beta(I,1)*Cothed(I,2)+Beta(I,1)*Cothed(I,1)
730 NEXT I
740 ! !
750 ! WE BEGIN TO CALCULATE THE COMPLEX MATRIX!
760 ! !
770 FOR I=1 TO 2*N+1 STEP 2
780 K=(I-1)/2
790 M=I-1
800 R=I+1
810 O=I+2
820 X=-Z(K)*(Beta(K,1)*Cothed(K,2)+Beta(K,2)*Cothed(K,1))
830 Y=Z(K)*(Beta(K,1)*Cothed(K,1)-Beta(K,2)*Cothed(K,2))
840 P=K+1
850 Xx=-Z(K)*(Beta(P,1)*Cothed(P,2)+Beta(P,2)*Cothed(P,1))
860 Yy=Z(K)*(Beta(P,1)*Cothed(P,1)-Beta(P,2)*Cothed(P,2))
870 IF X>200 THEN X=200             !X>200 IMPLIES A LAYER THICKNESS >200 SKIN DEPTHS!
880 IF Xx>200 THEN Xx=200          !Xx>200 IMPLIES A LAYER THICKNESS >200 SKIN DEPTHS!
890 ExpX=EXP(X)
900 ExpMx=EXP(-X)
910 ExpXx=EXP(Xx)
920 ExpMxx=EXP(-Xx)
930 CosY=COS(Y)
940 SinY=SIN(Y)
950 CosYy=COS(Yy)
960 SinYy=SIN(Yy)
970 Expr=ExpX*CosY
980 Expi=ExpX*SinY
990 Bcr=Beta(K,1)*Cothed(K,1)-Beta(K,2)*Cothed(K,2)
1000 Bci=Beta(K,1)*Cothed(K,2)+Beta(K,2)*Cothed(K,1)
1010 ! !
1020 ! WE CALCULATE THE (I,I-1) AND (I+1,I-1) COMPLEX MATRIX ELEMENTS!

```

```

1030 ! !
1040 IF I=1 THEN 1140
1050 Para(I,M,1)=Cothed(K,1)*Expr-Cothed(K,2)*Expi
1060 Para(I,M,2)=Cothed(K,1)*Expi+Cothed(K,2)*Expr
1070 Perp(I,M,1)=Expr
1080 Perp(I,M,2)=Expi
1090 Para(R,M,1)=(Beta(K,1)*Expr-Beta(K,2)*Expi)/Mu(K)
1100 Para(R,M,2)=(Beta(K,1)*Expi+Beta(K,2)*Expr)/Mu(K)
1110 Perp(R,M,1)=(Bcr*Expr-Bci*Expi)/Mu(K)
1120 Perp(R,M,2)=(Bcr*Expi+Bci*Expr)/Mu(K)
1130 ! !
1140 ! WE CALCULATE THE <I,I> AND <I+1,I> COMPLEX MATRIX ELEMENTS!
1150 ! !
1160 Expr=ExpixxCosy
1170 Expi=-ExpixxSiny
1180 Para(I,I,1)=Cothed(K,1)*Expr-Cothed(K,2)*Expi
1190 Para(I,I,2)=Cothed(K,1)*Expi+Cothed(K,2)*Expr
1200 Perp(I,I,1)=Expr
1210 Perp(I,I,2)=Expi
1220 Para(R,I,1)=(Beta(K,1)*Expr-Beta(K,2)*Expi)/Mu(K)
1230 Para(R,I,2)=(Beta(K,1)*Expi+Beta(K,2)*Expr)/Mu(K)
1240 Perp(R,I,1)=(Bcr*Expr-Bci*Expi)/Mu(K)
1250 Perp(R,I,2)=(Bcr*Expi+Bci*Expr)/Mu(K)
1260 ! !
1270 ! WE CALCULATE THE <I,I+1> AND <I+1,I+1> COMPLEX MATRIX ELEMENTS!
1280 ! !
1290 Expr=ExpixxCosy
1300 Expi=ExpixxSiny
1310 Bcr=Beta(P,1)*Cothed(P,1)-Beta(P,2)*Cothed(P,2)
1320 Bci=Beta(P,1)*Cothed(P,2)+Beta(P,2)*Cothed(P,1)
1330 Para(I,R,1)=(Cothed(P,1)*Expr-Cothed(P,2)*Expi)
1340 Para(I,R,2)=(Cothed(P,1)*Expi+Cothed(P,2)*Expr)
1350 Perp(I,R,1)=Expr
1360 Perp(I,R,2)=-Expi

```

```

1370 Para(R,R,1)=- (Beta(P,1)*Expr-Beta(P,2)*Expi)/Mu(P)
1380 Para(R,R,2)=- (Beta(P,1)*Expi+Beta(P,2)*Expr)/Mu(P)
1390 Perp(R,R,1)=- (Bcr*Expr-Bci*Expi)/Mu(P)
1400 Perp(R,R,2)=- (Bcr*Expi+Bci*Expr)/Mu(P)
1410 ! !
1420 ! WE CALCULATE THE (I,I+2) AND (I+1,I+2) COMPLEX MATRIX ELEMENTS!
1430 ! !
1440 Expr=ExpmaxxCosyy
1450 Expi=-ExpmaxxSinyy
1460 IF I=2*N+1 THEN 1550
1470 Para(I,0,1)=- (Cothd(P,1)*Expr-Cothd(P,2)*Expi)
1480 Para(I,0,2)=- (Cothd(P,1)*Expi+Cothd(P,2)*Expr)
1490 Perp(I,0,1)=- Expr
1500 Perp(I,0,2)=- Expi
1510 Para(R,0,1)=- (Beta(P,1)*Expr-Beta(P,2)*Expi)/Mu(P)
1520 Para(R,0,2)=- (Beta(P,1)*Expi+Beta(P,2)*Expr)/Mu(P)
1530 Perp(R,0,1)=- (Bcr*Expr-Bci*Expi)/Mu(P)
1540 Perp(R,0,2)=- (Bcr*Expi+Bci*Expr)/Mu(P)
1550 NEXT I
1560 ! !
1570 ! COMPLEX MATRICES ARE EXPANDED INTO REAL MATRICES!
1580 ! !
1590 MAT Paraex=ZER
1600 MAT Perpex=ZER
1610 FOR I=1 TO L/2
1620 FOR J=I-2 TO I+2
1630 IF J<1 THEN 1770
1640 IF J>L/2 THEN 1770
1650 M=2*I
1660 R=2*J
1670 O=M-1
1680 P=R-1
1690 Paraex(O,P)=Para(I,J,1)
1700 Paraex(M,R)=Para(I,J,1)
1710 Paraex(M,P)=Para(I,J,2)

```

!ZERGES PREVIOUS ROW REDUCTION DATA!

!AVOIDS CYCLING THRU THE WHOLE MATRIX!

AD-A131 091

MICROWAVE INTERACTION WITH THIN MULTIPLE CONDUCTIVE  
COATINGS(U) ROME AIR DEVELOPMENT CENTER GRIFFISS AFB NY  
V M MARTIN MAR 83 RADC-TR-83-62

313

UNCLASSIFIED

F/G 11/3

NL

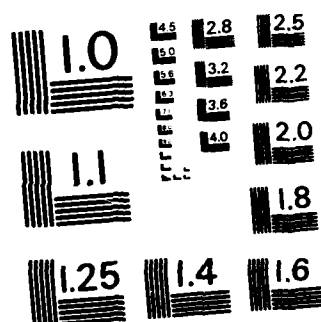
END

DATE \_\_\_\_\_

FILMED

5. 8.

0114



MICROCOPY RESOLUTION TEST CHART  
NATIONAL BUREAU OF STANDARDS-1963-A

```

1720 Paraex(0,R)=-Para(I,J,2)
1730 Perpex(0,P)=Perp(I,J,1)
1740 Perpex(M,R)=Perp(I,J,1)
1750 Perpex(M,P)=Perp(I,J,2)
1760 Perpex(0,R)=-Perp(I,J,2)
1770 NEXT J
1780 NEXT I
1790 Paraex(1,Lp)=-E1*Cothed(Np,1)
1800 Paraex(3,Lp)=-E1*(Beta0/Mu(0))
1810 Perpex(1,Lp)=-E1
1820 Perpex(3,Lp)=-E1*Cothed(Np,1)*(Beta0/Mu(0))
1830 ! !
1840 ! AT THIS POINT WE ARE READY FOR THE MATRIX SOLUTION!
1850 ! !
1860 FOR I=1 TO L
1870   FOR J=1-5 TO I+5
1880     IF J>L THEN 1930
1890     IF J<1 THEN 1930
1900     IF I=J THEN 1930
1910     Paraex(I,J)=Paraex(I,J)/Paraex(I,I)
1920     Perpex(I,J)=Perpex(I,J)/Perpex(I,I)
1930   NEXT J
1940   Paraex(I,Lp)=Paraex(I,Lp)/Paraex(I,I)
1950   Perpex(I,Lp)=Perpex(I,Lp)/Perpex(I,I)
1960   Paraex(I,I)=1
1970   Perpex(I,I)=1
1980   FOR K=I+1 TO I+5
1990     IF K>L THEN 2090
2000     X=Paraex(K,I)
2010     Y=Perpex(K,I)
2020     FOR J=1 TO I+5
2030       IF J>L THEN 2060
2040       Paraex(K,J)=Paraex(K,J)-X*Paraex(I,J)
2050       Perpex(K,J)=Perpex(K,J)-Y*Perpex(I,J)
2060     NEXT J

```

!WE ZERO THE COLUMN BELOW THE Ith DIAGONAL!

```

2070 Paraex(K,Lp)=Paraex(K,Lp)-X*Paraex(I,Lp)
2080 Perpex(K,Lp)=Perpex(K,Lp)-Y*Perpex(I,Lp)
2090 NEXT K
2100 NEXT I
2110 ! !
2120 ! Paraex AND Perpex ARE NOW IN UPPER TRIANGULAR FORM!
2130 ! !
2140 FOR I=0 TO L-1
2150 FOR K=I+1 TO I+5
2160 IF K>L-1 THEN 2280
2170 O=L-K
2180 P=L-I
2190 X=Paraex(O,P)
2200 Y=Perpex(O,P)
2210 FOR J=P TO P+4
2220 IF J>L THEN 2250
2230 Paraex(O,J)=Paraex(O,J)-X*Paraex(P,J)
2240 Perpex(O,J)=Perpex(O,J)-Y*Perpex(P,J)
2250 NEXT J
2260 Paraex(O,Lp)=Paraex(O,Lp)-X*Paraex(P,Lp)
2270 Perpex(O,Lp)=Perpex(O,Lp)-Y*Perpex(P,Lp)
2280 NEXT K
2290 NEXT I
2300 ! !
2310 ! THE MAG. OF THE ELECTRIC FIELDS ARE NOW CALCULATED IN THE L+1 COLUMN!
2320 ! !
2330 Repara(Theda)=(Paraex(1,Lp)^2+Paraex(2,Lp)^2)/E12
2340 Reperp(Theda)=(Perpex(1,Lp)^2+Perpex(2,Lp)^2)/E12
2350 Trpara(Theda)=(Paraex(L-1,Lp)^2+Paraex(L,Lp)^2)/E12
2360 Trperp(Theda)=(Perpex(L-1,Lp)^2+Perpex(L,Lp)^2)/E12
2370 Abpara(Theda)=1-Repara(Theda)-Trpara(Theda)
2380 Abperp(Theda)=1-Reperp(Theda)-Trperp(Theda)
2390 Theda(Theda)=Theda
2400 NEXT Theda
2410 ! !

```

```

2420 ! WE BEGIN THE GRAPHICS PORTION HERE !
2430 ! !
2440 GCLEAR
2450 GRAPHICS
2460 CSIZE 3.3,9/15,0
2470 LINE TYPE 1
2480 LOCATE 20,80,20,80
2490 SCALE 0,90,0,1
2500 LOCATE 19,80,19,80
2510 AXES 1,.01,0,0,10,10
2520 MOVE Theda(0),Repara(0)
2530 FOR J=Step TO 90 STEP Step
2540 DRAW Theda(J),Repara(J)
2550 NEXT J
2560 LETTER
2570 MOVE Theda(0),Reperp(0)
2580 FOR J=Step TO 90 STEP Step
2590 DRAW Theda(J),Reperp(J)
2600 NEXT J
2610 LETTER
2620 MOVE Theda(0),Trpara(0)
2630 FOR J=Step TO 90 STEP Step
2640 DRAW Theda(J),Trpara(J)
2650 NEXT J
2660 LETTER
2670 MOVE Theda(0),Trperp(0)
2680 FOR J=Step TO 90 STEP Step
2690 DRAW Theda(J),Trperp(J)
2700 NEXT J
2710 LETTER
2720 MOVE Theda(0),Abpara(0)
2730 FOR J=Step TO 90 STEP Step
2740 DRAW Theda(J),Abpara(J)
2750 NEXT J
2760 LETTER

```

```

2770 MOVE Theda(0),Abperp(0)
2780 FOR J=Step TO 90 STEP Step
2790 DRAW Theda(J),Abperp(J)
2800 NEXT J
2810 LETTER
2820 ! !
2830 ! PLOTS ARE DRAWN NOW LABELING IS INSERTED !
2840 ! !
2850 PAUSE
2860 PEN 1
2870 GOTO 2810
2880 INPUT "For Data Printout Enter 1; 0 otherwise.",Data
2890 GOTO 2810
2900 IF Data=1 THEN PRINTER IS 0
2910 CSIZE 3.3,9/15,0
2920 PRINT
2930 PRINT
2940 PRINT
2950 PRINT
2960 PRINT
2970 PRINT
2980 PRINT
2990 PRINT USING 3000;N;Power/10;F
3000 IMAGE "Number of Layers=",DD,"      Power in W/Cm^2=",DD,"      Freq. in
      GHz=",D.DD
3010 PRINT USING 3020;Uair-273.16;Del;Fe;H
3020 IMAGE "Air Temp (C)=",DD.D,"      Convective Exp=",D.DD,"      Emissivity=",D.DD,"
      Plate Height (M)=",D.DDD
3030 PRINT
3040 PRINT
3050 FOR I=1 TO N
3060 X=4*PI*1E-7
3070 Y=0.8542E-12
3080 PRINT USING 3090;I,Sigma(I),I,Mu(I)/X,I,Epslon(I)/Y,I,Z(I)-Z(I-1)

```

```
3090 IMAGE "Sigma(",D,")="",D.DDE," Mu(",D,")="",DD.D," Epsilon(",D,")="",D.DD,"  
      Thickness(",D,")="",D.DDE  
3100 NEXT I  
3110 PRINTER IS 16  
3120 STOP
```

## APPENDIX E

## COMPUTER PROGRAM

The name of this program is "SIGNIF". It calculates the ratio of heat lost through infrared radiation to that lost by way of heat convection on a vertical flat surface. The input variables are air temperature (C), the convection exponent, and plate height (m).

```

10      ! THEN NAME OF THIS PROGRAM IS 'SIGNIF'. IT CALCULATES THE MAX. SURFACE
      TEMP SUCH THAT IR LOSSES ARE INSIGNIFICANT REL. TO CONVECTION!
20      ! !
30      INPUT "ENTER Uair.",Uair
40      INPUT "ENTER Delta, THE CONVECTION EXP.",Del
50      INPUT "ENTER THE PLATE HEIGHT.",H
60      DIM U(200),Ratio(200,10)
70      INTEGER I,J
80      Uair=Uair+273.16
90      Uo=Uair
100     Gamma=5.67E-8
110     Inc=.05
120     FOR I=1 TO 200
130       Uo=Uo+Inc
140       FOR J=2 TO 10 STEP 2
150         Fe=.1*I
160         Qir=Gamma*Fe*(Uo^4-Uair^4)
170         Qcon=1.42/H*Del*(Uo-Uair)^(Del+1)
180         Ratio(I,J)=Qir/Qcon
190         U(I)=Uo-Uair
200       NEXT J
210     NEXT I
220     BEEP
230     PAUSE
240     GRAPHICS
250     GCLEAR
260     CSIZE 3.3,9/15,0
270     LINE TYPE 1
280     LOCATE 15,85,15,85
290     SCALE 0,10,0,5
300     LOCATE 14,85,14,85
310     AXES .1,.1,0,0,10,10
320     FOR J=2 TO 10 STEP 2
330       Fe=.1*I

```

```

340 LINE TYPE J/2+2
350 MOVE 0,4*Gamma*Fe*Uair^3/(1.42*(1+De1)/H^De1)
360 FOR I=1 TO 200
370 DRAW U(I),Ratio(I,J)
380 NEXT I
390 MOVE 4,4.25-.1*J
400 DRAW 5,4.25-.1*J
410 NEXT J
420 LINE TYPE 1
430 MOVE 1,-.75
440 LABEL "(Uo-Uair) IN DEGREES CENTIGRADE"
450 MOVE -.8,.25
460 LDIR PI/2
470 LABEL "RATIO OF INFRARED TO CONVECTION LOSSES"
480 LDIR 0
490 MOVE 9.6,-.25
500 LABEL 10
510 CSIZE 2.5,9/15,0
520 MOVE 4,5
530 LABEL USING 540;H

```

```
540 IMAGE "PLATE HEIGHT=",D.DD," METERS"  
550 MOVE 4,4.75  
560 LABEL USING 570;De1  
570 IMAGE "CONVECTION EXPONENT=",.DDD  
580 MOVE 4,4.5  
590 LABEL USING 600;Uair-273.16  
600 IMAGE "AIR TEMPERATURE (C)=",DD.DD  
610 MOVE -.6,5  
620 LABEL 5  
630 MOVE -.6,-.25  
640 LABEL 0  
650 LETTER  
660 CSIZE 3.3,9/15,0  
670 GOTO 230  
680 GCLEAR  
690 EXIT GRAPHICS  
700 STOP
```

## APPENDIX F

## COMPUTER PROGRAM

The name of this program is "Uo-3D". It calculates the equilibrium surface temperature for a system of N layers in the presence of electromagnetic radiation. It plots the temperature as a function of the first layer thickness and conductivity on a three dimensional plot. The input variables are the number of layers, the incident power, the incident frequency, the ambient air temperature, the convection exponent, the surface emissivity, the vertical flat plate height, the incident angle, and the smallest electrical conductivity for the first layer. Additionally, the inputs for the various other layers are the permittivity, conductivity, permeability, and thickness.

```

10  ! THE NAME OF THIS PROGRAM IS 'Uo-3D' !
20  ! IT CALCULATES THE SURFACE TEMPERATURE (Uo) ON THE Z=0 INTERFACE IF THERE
   ARE NO HEAT LOSSES FROM THE Z=Zn INTERFACE !
30  ! IT CALCULATES Uo AS A FUNCTION OF SIGMA AND THICKNESS IN SKIN DEPTHS AND
   THEN PLOTS THE RESULTS ON A THREE DIMENSIONAL DISPLAY!
40  ASSIGN #1 TO "UoYBL:T14"
50  ASSIGN #2 TO "UoSML:T14"
60  ASSIGN #3 TO "UoBIG:T14"
70  INTEGER I,J,K,L,M,N,O,P,Q,R,Lp,Np,Aye,Jay,Thed
80  SHORT Beta<11,2>,Z<11>,Cothed<12,2>,Sigma<10>,Mu<12>,Epsilon<12>,Para<22,22
   ,2>,Perp<22,22>,Paraex<44,45>,Perpex<44,45>,A<10>,B<10>
90  SHORT Uoperp<20,22,10>,Uopara<20,22,10>,Thick<10>,Max<60,10>,Last<60,10>,P
   amax<10>,Pemax<10>,Delta<20>
100 INPUT "For data calculation enter I; 'for replot a 2.',Plot
110 GCLEAR
120 EXIT GRAPHICS
130 IF Plot=2 THEN 3020
140 INPUT "Enter the Number of Layers not to Exceed 10.",N
150 INPUT "Enter the Incident Power in MW/Cm^2",Power
160 INPUT "Enter the Incident Frequency in Gigahertz.",F
170 INPUT "Enter the ambient air temperature in Centigrade.",Uair
180 INPUT "Enter the convection exponent, Delta.",Del
190 INPUT "Enter the surface emissivity.",Fe
200 INPUT "Enter the plate height in meters.",H
210 INPUT "Enter the Theda Step>=10 degrees.",Step
220 INPUT "Enter the Sigma Step>=1.",Stepp
230 Np=N+1
240 L=4+Np
250 Lp=L+1
260 Gamma=5.67E-8
270 Uair=Uair+273.16
280 Omega=2*PI*F*1E9
290 Beta0=Omega/2.998E8

! DIMENSION OF EXPANDED MATRICES!

! CONVERTS Uair TO KELVIN!
! ANGULAR FREQUENCY IS CALCULATED!
! FREE SPACE WAVE VECTOR IS CALCULATED!

```

```

300 Beta02=Beta0^2
310 Power=10*Power
320 FOR I=1 TO N
330 IF I=1 THEN 360
340 DISP "Sigma(";I;")";
350 INPUT Sigma(I)
360 DISP "Mu(";I;")";
370 INPUT Mu
380 Mu(I)=Mu*4*PI*IE-7
390 DISP "Epsilon(";I;")";
400 INPUT Epsilon
410 Epsilon(I)=Epsilon*8.8542E-12
420 IF I=1 THEN 450
430 DISP "Thickness(";I;")";
440 INPUT Thick(I)
450 Coef=Omega*SQR(Mu(I)*Epsilon(I)/2)
460 Sqrroot=SQR(1+(Sigma(I)/(Omega*Epsilon(I)))^2)
470 Beta(I,1)=Coef*SQR(1+Sqrroot)
480 Beta(I,2)=Coef*SQR(Sqrroot-1)
490 NEXT I
500 Mu(0)=4*PI*IE-7
510 Epsilon(0)=8.8542E-12
520 Mu(Np)=4*PI*IE-7
530 Epsilon(Np)=8.8542E-12
540 Z(0)=0
550 Beta(0,1)=Beta0
560 Beta(0,2)=0
570 Beta(Np,1)=Beta0
580 Beta(Np,2)=0
590 E1=(Mu(0)/Epsilon(0))^.25*SQR(2*Power)
600 E12=E1^2
610 Deg=PI/180
620 ! !
630 ! WE BEGIN ITERATING FROM 0 TO 90 DEGREES ANGLE OF INCIDENCE!
640 ! !

```

!THE WAVE VECTOR IS SQUARED!  
!CONVERTS TO WATT/METER^2!  
!ELEC. PROPERTIES OF LAYERS IS INSERTED!  
!ELECTRICAL CONDUCTIVITY IN MHOS!  
!RELATIVE MAGNETIC PERMEABILITY!  
!RELATIVE ELECTRIC PERMITTIVITY!  
!EACH LAYER THICKNESS IN METERS!

```

650 FOR Theda=0 TO 90 STEP Step
660 IF Theda/10-Theda DIV 10=0 THEN PRINT USING 670;Theda
670 IMAGE "Theda=",DD
680 FOR Aye=1 TO 20 STEP Stepp
690 Sigma(1)=10^(8-.5*(Aye-1))
700 PRINT USING 710;Aye
710 IMAGE "WE ARE ON SIGMA ROW NUMBER ",DD
720 Delta(Aye)=SQR(2/(Omega*Mu(1)*Sigma(1)))
730 Thick(1)=0
740 MAT Z=ZER
750 Coef=Omega*SQR(Mu(1)*Epsilon(1)/2)
760 Sqrroot=SQR(1+(Sigma(1)/(Omega*Epsilon(1)))^2)
770 Beta(1,1)=Coef*SQR(1+Sqrroot)
780 Beta(1,2)=Coef*SQR(Sqrroot-1)
790 FOR Jay=2 TO 21
800 Thick(1)=Thick(1)+Delta(Aye)/5
810 FOR I=1 TO N
820 Z(I)=Z(I-1)+Thick(I)
830 NEXT I
840 X=COS(Theda*Deg)
850 IF X=0 THEN X=.01
860 Cothed(Np,1)=X
870 Cothed(Np,2)=0
880 Cothed(0,1)=X
890 Cothed(0,2)=0
900 ! !
910 ! WE CALCULATE REAL AND IMAGINARY COS(Theda).!
920 ! !
930 FOR I=1 TO N
940 Sin2=SIN(Theda*Deg)^2
950 IF Sin2=1 THEN Sin2=.99
960 Denom=(Beta(1,1)^2+Beta(1,2)^2)^2
970 Pee=.5*(1-Beta02*Sin2*(Beta(1,1)^2-Beta(1,2)^2)/Denom)
980 Que=Beta02*Sin2*Beta(1,1)*Beta(1,2)/Denom
990 X=SQR(Pee^2+Que^2)

```

!WE BEGIN ITERATING OVER SIGMA!  
!SIGMA IS INCREMENTED BY 10^.5!

!WE ITERATE OVER THICKNESS HERE!

!WE CALC. SIN(Theda) SQUARED!

```

1000 Cothed(I,1)=SQR(Pee+X)      !REAL COS(Theda N) IS CALCULATED!
1010 Cothed(I,2)=SQR(ABS(X-Pee)) !IMAG COS(Theda N) IS CALCULATED!
1020 A(I)=Beta(I,1)*Cothed(I,1)-Beta(I,2)*Cothed(I,2)
1030 B(I)=Beta(I,1)*Cothed(I,2)+Beta(I,1)*Cothed(I,1)
1040 NEXT I
1050 ! !
1060 ! WE BEGIN TO CALCULATE THE COMPLEX MATRIX!
1070 ! !
1080 FOR I=1 TO 2*N+1 STEP 2
1090 K=(I-1)/2
1100 M=I-1
1110 R=I+1
1120 O=I+2
1130 X=-Z(K)*(Beta(K,1)*Cothed(K,2)+Beta(K,2)*Cothed(K,1))
1140 Y=Z(K)*(Beta(K,1)*Cothed(K,1)-Beta(K,2)*Cothed(K,2))
1150 P=K+1
1160 Xx=-Z(K)*(Beta(P,1)*Cothed(P,2)+Beta(P,2)*Cothed(P,1))
1170 Yy=Z(K)*(Beta(P,1)*Cothed(P,1)-Beta(P,2)*Cothed(P,2))
1180 IF X>75 THEN X=75      !X>75 IMPLIES A LAYER THICKNESS >75 SKIN DEPTHS!
1190 IF Xx>75 THEN Xx=75   !Xx>75 IMPLIES A LAYER THICKNESS >75 SKIN DEPTHS!
1200 ExpX=EXP(X)
1210 ExpXx=EXP(Xx)
1220 IF X<-75 THEN X=-75
1230 IF Xx<-75 THEN Xx=-75
1240 ExpMx=EXP(-X)
1250 ExpMxX=EXP(-Xx)
1260 CosY=COS(Y)
1270 SinY=SIN(Y)
1280 CosYy=COS(Yy)
1290 SinYy=SIN(Yy)
1300 Expr=ExpX*CosY
1310 Expi=ExpX*SinY
1320 Bcr=Beta(K,1)*Cothed(K,1)-Beta(K,2)*Cothed(K,2)
1330 Bci=Beta(K,1)*Cothed(K,2)+Beta(K,2)*Cothed(K,1)
1340 ! !

```

```

1350 ! WE CALCULATE THE <I,I-1> AND <I+1,I-1> COMPLEX MATRIX ELEMENTS!
1360 ! !
1370 IF I=1 THEN 1470
1380 Para(I,M,1)=Cothed(K,1)*Expr-Cothed(K,2)*Expi
1390 Para(I,M,2)=Cothed(K,1)*Expi+Cothed(K,2)*Expr
1400 Perp(I,M,1)=Expr
1410 Perp(I,M,2)=Expi
1420 Para(R,M,1)=(Beta(K,1)*Expr-Beta(K,2)*Expi)/Mu(K)
1430 Para(R,M,2)=(Beta(K,1)*Expi+Beta(K,2)*Expr)/Mu(K)
1440 Perp(R,M,1)=(Bcr*Expr-Bci*Expi)/Mu(K)
1450 Perp(R,M,2)=(Bcr*Expi+Bci*Expr)/Mu(K)
1460 ! !
1470 ! WE CALCULATE THE <I,I> AND <I+1,I> COMPLEX MATRIX ELEMENTS!
1480 ! !
1490 Expr=Expmax*Cosy
1500 Expi=-Expmax*Siny
1510 Para(I,1,1)=Cothed(K,1)*Expr-Cothed(K,2)*Expi
1520 Para(I,1,2)=Cothed(K,1)*Expi+Cothed(K,2)*Expr
1530 Perp(I,1,1)=Expr
1540 Perp(I,1,2)=Expi
1550 Para(R,1,1)=(Beta(K,1)*Expr-Beta(K,2)*Expi)/Mu(K)
1560 Para(R,1,2)=(Beta(K,1)*Expi+Beta(K,2)*Expr)/Mu(K)
1570 Perp(R,1,1)=(Bcr*Expr-Bci*Expi)/Mu(K)
1580 Perp(R,1,2)=(Bcr*Expi+Bci*Expr)/Mu(K)
1590 ! !
1600 ! WE CALCULATE THE <I,I+1> AND <I+1,I+1> COMPLEX MATRIX ELEMENTS!
1610 ! !
1620 Expr=Expmax*Cosyy
1630 Expi=Expmax*Sinyy
1640 Bcr=Beta(P,1)*Cothed(P,1)-Beta(P,2)*Cothed(P,2)
1650 Bci=Beta(P,1)*Cothed(P,2)+Beta(P,2)*Cothed(P,1)
1660 Para(I,R,1)=(Cothed(P,1)*Expr-Cothed(P,2)*Expi)
1670 Para(I,R,2)=(Cothed(P,1)*Expi+Cothed(P,2)*Expr)
1680 Perp(I,R,1)=-Expr
1690 Perp(I,R,2)=-Expi

```

```

1700 Para(R,R,1)=- (Beta(P,1)*Expr-Beta(P,2)*Expi)/Mu(P)
1710 Para(R,R,2)=- (Beta(P,1)*Expi+Beta(P,2)*Expr)/Mu(P)
1720 Perp(R,R,1)=- (Bcr*Expr-Bci*Expi)/Mu(P)
1730 Perp(R,R,2)=- (Bcr*Expi+Bci*Expr)/Mu(P)
1740 ! !
1750 ! WE CALCULATE THE (I,I+2) AND (I+1,I+2) COMPLEX MATRIX ELEMENTS!
1760 ! !
1770 Expr=ExpmaxxCosyy
1780 Expi=-ExpmaxxSinyy
1790 IF I=2*N+1 THEN 1880
1800 Para(I,0,1)=- (Cothed(P,1)*Expr-Cothed(P,2)*Expi)
1810 Para(I,0,2)=- (Cothed(P,1)*Expi+Cothed(P,2)*Expr)
1820 Perp(I,0,1)=- Expr
1830 Perp(I,0,2)=- Expi
1840 Para(R,0,1)=- (Beta(P,1)*Expr-Beta(P,2)*Expi)/Mu(P)
1850 Para(R,0,2)=- (Beta(P,1)*Expi+Beta(P,2)*Expr)/Mu(P)
1860 Perp(R,0,1)=- (Bcr*Expr-Bci*Expi)/Mu(P)
1870 Perp(R,0,2)=- (Bcr*Expi+Bci*Expr)/Mu(P)
1880 NEXT I
1890 ! !
1900 ! COMPLEX MATRICES ARE EXPANDED INTO REAL MATRICES!
1910 ! !
1920 MAT Paraex=ZER
1930 MAT Perpex=ZER
1940 FOR I=1 TO L/2
1950 FOR J=I-2 TO I+2
1960 IF J<1 THEN 2100
1970 IF J>L/2 THEN 2100
1980 M=2*I
1990 R=2*J
2000 O=M-1
2010 P=R-1
2020 Paraex(O,P)=Para(I,J,1)
2030 Paraex(M,R)=Para(I,J,1)
2040 Paraex(M,P)=Para(I,J,2)

```

!ZERGES PREVIOUS ROW REDUCTION DATA!

!AVOIDS CYCLING THRU THE WHOLE MATRIX!

```

2050 Paraex(0,R)=-Para(I,J,2)
2060 Perpex(0,P)=Perp(I,J,1)
2070 Perpex(M,R)=Perp(I,J,1)
2080 Perpex(M,P)=Perp(I,J,2)
2090 Perpex(0,R)=-Perp(I,J,2)
2100 NEXT J
2110 NEXT I
2120 Paraex(1,Lp)=-E1*Cothed(Np,1)
2130 Paraex(3,Lp)=-E1*(Beta0/Mu(0))
2140 Perpex(1,Lp)=-E1
2150 Perpex(3,Lp)=-E1*Cothed(Np,1)*(Beta0/Mu(0))
2160 ! !
2170 ! AT THIS POINT WE ARE READY FOR THE MATRIX SOLUTION!
2180 ! !
2190 FOR I=1 TO L
2200 FOR J=I-5 TO I+5
2210 IF J>L THEN 2280
2220 IF J<1 THEN 2280
2230 IF I=J THEN 2280
2240 IF Paraex(I,I)=0 THEN Paraex(I,I)=1E-12
2250 IF Perpex(I,I)=0 THEN Perpex(I,I)=1E-12
2260 Paraex(I,J)=Paraex(I,J)/Paraex(I,I)
2270 Perpex(I,J)=Perpex(I,J)/Perpex(I,I)
2280 NEXT J
2290 Paraex(I,Lp)=Paraex(I,Lp)/Paraex(I,I)
2300 Perpex(I,Lp)=Perpex(I,Lp)/Perpex(I,I)
2310 Paraex(I,I)=1
2320 Perpex(I,I)=1
2330 FOR K=I+1 TO I+5
2340 IF K>L THEN 2440
2350 X=Paraex(K,I)
2360 Y=Perpex(K,I)
2370 FOR J=I TO I+5
2380 IF J>L THEN 2410
2390 Paraex(K,J)=Paraex(K,J)-X*Paraex(I,J)

```

!L IS THE DIMENSION OF THE EXPANDED MATRICES!  
!1810-1870 DIVIDES THE Ith ROW BY DIAGONAL ELE.!

!WE ZERO THE COLUMN BELOW THE Ith DIAGONAL!

```

2400 Perpex(K,J)=Perpex(K,J)-Y*Perpex(I,J)
2410 NEXT J
2420 Paraex(K,Lp)=Paraex(K,Lp)-X*Paraex(I,Lp)
2430 Perpex(K,Lp)=Perpex(K,Lp)-Y*Perpex(I,Lp)
2440 NEXT K
2450 NEXT I
2460 ! !
2470 ! Paraex AND Perpex ARE NOW IN UPPER TRIANGULAR FORM!
2480 ! !
2490 FOR I=0 TO L-1
2500 FOR K=I+1 TO I+5
2510 IF K>L-1 THEN 2630
2520 O=L-K
2530 P=L-I
2540 X=Paraex(O,P)
2550 Y=Perpex(O,P)
2560 FOR J=P TO P+4
2570 IF J>L THEN 2600
2580 Paraex(O,J)=Paraex(O,J)-X*Paraex(P,J)
2590 Perpex(O,J)=Perpex(O,J)-Y*Perpex(P,J)
2600 NEXT J
2610 Paraex(O,Lp)=Paraex(O,Lp)-X*Paraex(P,Lp)
2620 Perpex(O,Lp)=Perpex(O,Lp)-Y*Perpex(P,Lp)
2630 NEXT K
2640 NEXT I
2650 ! !
2660 ! THE MAG. OF THE ELECTRIC FIELDS ARE NOW CALCULATED IN THE L+1 COLUMN!
2670 ! !
2680 ! WE NOW FIND THE SURF. TEMP. Uo FOR NO LOSSES ON Zn BOUNDARY!
2690 ! !
2700 Papara=Power-.5*SQR(Epslon(0)/Mu(0))*(Paraex(1,Lp)^2+Paraex
(L-1,Lp)^2+Paraex(L,Lp)^2)
2710 Paperp=Power-.5*SQR(Epslon(0)/Mu(0))*(Perpex(1,Lp)^2+Perpex
(L-1,Lp)^2+Perpex(L,Lp)^2)
2720 ! WE NOW DO A NEWTON ALGORITHM TO FIND THE SURFACE TEMP., Uo!

```

```

2730 Uopa=Uair
2740 Uope=Uair
2750 J=0
2760 Fupara=1.42/H*Del*ABS(Uopa-Uair)^(Del+1)+Fe*Gamma*(Uopa^4-Uair^4)-Papara
2770 Fuperp=1.42/H*Del*ABS(Uope-Uair)^(Del+1)+Fe*Gamma*(Uope^4-Uair^4)-Paparp
2780 Fupap=(Del+1)*(1.42/H*Del)*ABS(Uopa-Uair)^(Del+4)*Fe*Gamma*Uopa^3
2790 Fupep=(Del+1)*(1.42/H*Del)*ABS(Uope-Uair)^(Del+4)*Fe*Gamma*Uope^3
2800 Uopal=Uopa-Fupara/Fupap
2810 Uopel=Uope-Fuperp/Fupep
2820 IF (ABS(Uopa-Uopal)<1E-8) AND (ABS(Uope-Uopel)<1E-8) THEN 2880
2830 Uopa=Uopal
2840 Uope=Uopel
2850 J=J+1
2860 IF J=100 THEN 2880
2870 GOTO 2760
2880 IF J>=100 THEN BEEP
2890 Thed=(Theda+Step)/Step
2900 Uopara(Aye,Jay,Thed)=Uopa
2910 Uoperp(Aye,Jay,Thed)=Uope
2920 IF Uopa>Pamax(Thed) THEN Pamax(Thed)=Uopa
2930 IF Uope>Pemax(Thed) THEN Pemax(Thed)=Uope
2940 PRINT "Uopa=",Uopa-Uair," Papara=",Papara
2950 NEXT Jay
2960 NEXT Aye
2970 NEXT Theda
2980 PRINT #1;Step,Stepp,Uair,N,Power,F,Del,Fe,H
2990 MAT PRINT #2;Sigma,Mu,Epsilon,Z,Pamax,Pemax
3000 MAT PRINT #3;Uopara,Uoperp
3010 IF Plot=1 THEN 3050
3020 READ #1;Step,Stepp,Uair,N,Power,F,Del,Fe,H
3030 MAT READ #2;Sigma,Mu,Epsilon,Z,Pamax,Pemax
3040 MAT READ #3;Uopara,Uoperp
3050 ! WE BEGIN THE GRAPHICS PORTION HERE !
3060 ! !
3070 INPUT "ENTER: 1-Uopara; 2-Uoperp",Mat

```

!Thed IS THE MAT STORAGE ELE FOR Theda STEPS!

```

3080 IF Mat=0 THEN GOTO 4370
3090 PRINT "THE Theda STEP VALUE=",Step
3100 INPUT "ENTER: Incident Angle (multiple of step).",Theda
3110 Theda=<Theda+Step>/Step
3120 FOR I=1 TO 20
3130 Uopara<I,22,Theda>=Uopara<I,21,Theda>
3140 Uoperp<I,22,Theda>=Uoperp<I,21,Theda>
3150 NEXT I
3160 GRAPHICS
3170 GCLEAR
3180 MAT Max=ZER
3190 MAT Last=ZER
3200 CSIZE 2.3,9/15,0
3210 LINE TYPE 1
3220 LDIR 0
3230 LOCATE 15,90,15,90
3240 SCALE 0,40,0,40
3250 LOCATE 14,90,14,90
3260 AXES 1,2,0,0,5,10
3270 Tmax=0
3280 FOR I=1 TO 10
3290 IF <Pamax<I>>Tmax> AND <Mat=1> THEN Tmax=Pamax<I>
3300 IF <Pemax<I>>Tmax> AND <Mat=2> THEN Tmax=Pemax<I>
3310 NEXT I
3320 Tmax=Tmax-Uair
3330 FOR I=1 TO 20 STEP Stepp
3340 MOVE 19+I,I-1
3350 FOR J=21 TO 1 STEP -1
3360 JJ=J-2+I
3370 IF Mat<>1 THEN 3410
3380 Var=I-1+20*<Uopara<I,J,Theda>-Uair>/Tmax
3390 Varp=I-1+20*<Uopara<I,J+1,Theda>-Uair>/Tmax
3400 Var=I-1+20*<Uopara<I,J-1,Theda>-Uair>/Tmax
3410 IF Mat<>2 THEN 3450
3420 Var=I-1+20*<Uoperp<I,J,Theda>-Uair>/Tmax

```

!WE DRAW THE X CONTOURS!

```

3430 Varp=I-1+20*(Uoperp(I,J+1,Thed)-Uair)/Tmax
3440 Varm=I-1+20*(Uoperp(I,J-1,Thed)-Uair)/Tmax
3450 X1=Jj-1+1E-8
3460 X2=Jj+1E-9
3470 X3=Jj+1+1E-10
3480 Y1=Varm
3490 Y2=Var
3500 Y3=Varp
3510 Det=X1^2*X2+X1*X3^2+X3*X2^2-X2*X3^2-X3*X1^2-X1*X2^2
3520 A=(X2*Y1+X1*Y3+Y2*X3-X2*Y3-Y1*X3-X1*Y2)/Det
3530 B=(X1^2*Y2+Y1*X3^2+Y3*X2^2-Y2*X3^2-Y3*X1^2-Y1*X2^2)/Det
3540 C=(X2*Y3*X1^2+X1*Y2*X3^2+Y1*X3*X2^2-Y1*X2*X3^2-X3*Y2*X1^2-X1*Y3*X2^2)/Det
3550 FOR K=1 TO 10
3560 X=Jj-.1*K
3570 Y=A*X^2+B*X+C
3580 IF (J=21) AND (K=1) THEN DRAW X,Y
3590 IF I=1 THEN 3610
3600 Last(Jj+1-Stepp,K)=Max(Jj+1-Stepp,K)
3610 IF Y>Max(Jj,K) THEN 3640
3620 MOVE X,Y
3630 GOTO 3660
3640 Max(Jj,K)=Y
3650 DRAW X,Y
3660 NEXT K
3670 NEXT J
3680 I I
3690 I HERE IS THE PLACE TO DRAW Y CONTOURS!
3700 I I
3710 FOR J=21 TO 2 STEP -1
3720 Jj=J-2+I
3730 MOVE Jj-Stepp,Last(Jj+1-Stepp,10) (Jj+1,10) YIELDS THE Jj COORD. I
3740 IF I=1 THEN 3760
3750 IF Max(Jj+1,10)>Last(Jj+1,10) THEN DRAW Jj,Max(Jj+1,10)
3760 NEXT J

```

```

3770 NEXT I
3780 MOVE 9,-2
3790 LABEL "COATING THICKNESS IN SKIN DEPTHS"
3800 CSIZE 3.3,9/15,0
3810 MOVE -4,-6
3820 IF Mat=1 THEN LABEL USING 3830;Theda
3830 IMAGE "PARALLEL INCIDENCE: Theta=",DD," Degrees"
3840 IF Mat=2 THEN LABEL USING 3850;Theda
3850 IMAGE "PERPENDICULAR INCIDENCE: Theta=",DD," Degrees"
3860 CSIZE 2.5,9/15,0
3870 LDIR PI/2
3880 MOVE -2,1
3890 LABEL USING 3900;Tmax
3900 IMAGE "Delta Temperature Normalized To ",DD.DD," Degrees C."
3910 LDIR 0
3920 LINE TYPE 3
3930 MOVE 0,0
3940 DRAW 20,20
3950 LINE TYPE 1
3960 MOVE 20.25,0
3970 DRAW 40,19.75
3980 FOR I=1 TO 19
3990 MOVE I+20.25,I
4000 DRAW I+20.75,I-.5
4010 MOVE I+20.25,I-1.2
4020 J=I/2
4030 IF ABS(I/2-J)>0 THEN 4060
4040 LABEL USING 4050;7.5-.5*(I-1)
4050 IMAGE DD.D
4060 NEXT I
4070 LDIR PI/4
4080 MOVE 30,2
4090 LABEL "Sigma in Mhos/M (LOG 10)"
4100 LDIR 0
4110 PAUSE

```

```

4120 INPUT "For a paper copy enter a 1; otherwise 0.",Copy
4130 IF Copy=1 THEN DUMP GRAPHICS
4140 EXIT GRAPHICS
4150 IF Copy=1 THEN PRINTER IS 0
4160 PRINT
4170 PRINT
4180 PRINT
4190 PRINT
4200 PRINT
4210 PRINT
4220 PRINT
4230 PRINT USING 4240;N;Power/10;F
4240 IMAGE "Number of Layers=",DD,"      Power in W/Cm^2=",DD,"      Freq. in
      GHz=",D.DD
4250 PRINT USING 4260;Uair-273.16;Del;Fe;H
4260 IMAGE "Air Temp (C)=",DD.D,"      Convective Exp=",D.DD,"      Emissivity=",D.DD,"
      Plate Height (M)=",D.DDD
4270 PRINT
4280 PRINT
4290 FOR I=1 TO N
4300 X=4*PI*I-E-7
4310 Y=8.8542E-12
4320 PRINT USING 4330;I,Sigma(I),I,Mu(I)/X,I,Epsilon(I)/Y,I,Z(I)-Z(I-1)
4330 IMAGE "Sigma(",D,")=","D.DDE,"      Mu(",D,")=","D.DD.D,"      Epsilon(",D,")=","D.DD,"
      Thickness(",D,")=","D.DDE
4340 NEXT I
4350 PRINTER IS 16
4360 GOTO 3070
4370 STOP

```

## APPENDIX G

## COMPUTER PROGRAM

The name of this program is "Uthick". It calculates the surface temperature of a system of N layers as a function of the thickness of any two of the layers. The result is plotted on contour plot of constant temperatures. The input variables are the number of layers, which layers to vary the thickness of, the incident power, the incident frequency, the incident angle, the ambient air temperature, the plate height, surface emissivity, the convective exponent, and the layer characteristics of conductivity, permittivity, permeability, and thickness.

```

10  ! THE NAME OF THIS PROGRAM IS 'UTHICK' !
20  ! IT CALCULATES THE SURFACE TEMPERATURE OF A SYSTEM OF N LAYERS AS A FUNCT
30  ION OF COATING THICKNESS AND LAYER THICKNESS!
40  INTEGER I,J,K,L,M,N,O,P,Q,R,Lp,Np,Aye,Jay,L1,L2
50  SHORT Beta(11,2),Z(11),Cothd(12,2),Sigma(10),Mu(12),Epsilon(12),Para(22,22
60  ),Perp(22,22),Paraex(44,44),Perpex(44,44),Sithd(12,2),Betcos(10,2)
70  SHORT Parabx(44),Perpbx(44),Epara(44),Eperp(44),Dum(44,44),Thick(11),X(10,
80  10),Y(10,10)
90  SHORT Jpara(10,50),Jperp(10,50),Ppara(10,50),Pperp(10,50),Jparat(10),Jperp
100 t(10),Uopara(10,10),Uoperp(10,10),Jpapct(10,10),Jpepct(10,10)
110  PRINTER IS 16
120  PRINT PAGE
130  GCLEAR
140  EXIT GRAPHICS
150  PRINT "THE FIRST RUN SHOULD BE WITHOUT A PERFECT LAST CONDUCTOR."
160  Second=0
170  INPUT "For Second Run Enter 2.",Second
180  INPUT "Enter the Number of Layers not to Exceed 10.",N
190  INPUT "Enter Which Layer Thickness to Vary (Two).",L1,L2
200  INPUT "Enter the Step Increment for Each Layer (Two).",Incl,Inc2
210  INPUT "Enter the Incident Power in MW/Cm^2",Power
220  INPUT "Enter the Incident Frequency in Gigahertz.",F
230  INPUT "Enter the Ambient Air Temperature in Centigrade.",Uair
240  INPUT "Enter the Plate Height in Meters.",H
250  INPUT "Enter Theda.",Theda
260  INPUT "Enter the Surface Emissivity.",Fe
270  INPUT "Enter the Convective Heat Transfer Coefficient.",Del
280  ASSIGN #1 TO "UoBIG"
290  IF Second<>2 THEN 330
300  MAT READ #1;Uopara,Uoperp,Jpapct,Jpepct
310  MAT X=Uopara
320  MAT Y=Jpapct
330  PURGE "UoBIG"
340  CREATE "UoBIG",4,1E3

```

```

310 ASSIGN #1 TO "UoBIG"
320 GOTO 360
330 PURGE "UoBIG"
340 CREATE "UoBIG",4,1E3
350 ASSIGN #1 TO "UoBIG"
360 Gamma=5.67E-8
370 Uair=Uair+273.16
380 Omega=2*PI*F*1E9
390 Beta0=Omega/2.998E8
400 Beta02=Beta0^2
410 Power=10*Power
420 FOR I=1 TO N
430 DISP "Sigma(";I;");";
440 INPUT Sigma(I)
450 IF Sigma(I)=0 THEN Sigma(I)=1E-12
460 DISP "Mu(";I;");";
470 INPUT Mu
480 Mu(I)=Mu*4*PI*1E-7
490 DISP "Epsilon(";I;");";
500 INPUT Epsilon
510 Epsilon(I)=Epsilon*8.8542E-12
520 DISP "Initial Thickness(";I;");";
530 INPUT Thick(I)
540 Delta=SQR(2/(Omega*Mu(I)*Sigma(I)))
550 IF Thick(I)<23*Delta THEN 620
560 Thick(I)=23*Delta
570 N=N+1
580 Key=1
590 PRINT USING 600;I,I,Thick(I)
600 IMAGE "LAYER ",DD," WAS THICKER THAN 23 SKIN DEPTHS. THE PROBLEM IS TRUNCA
TED AT ",DD," LAYERS, WITH LAYER ",DD," ",D.DDE," METERS THICK."
610 PRINT
620 Coef=Omega*SQR(Mu(I)*Epsilon(I)/2)
630 Sqrroot=SQR(1+(Sigma(I)/(Omega*Epsilon(I)))^2)
640 Beta(I,1)=Coef*SQR(1+Sqrroot)      !REAL WAVE VECTOR (Alpha) IS CALC.!
```

```

!STEFAN-BOLTZMAN CONSTANT!
!AIR TEMPERATURE IN KELVIN!
!ANGULAR FREQUENCY IS CALCULATED!
!FREE SPACE WAVE VECTOR IS CALCULATED!
!THE WAVE VECTOR IS SQUARED!
!CONVERTS TO WATT/METER^2!
!ELEC. PROPERTIES OF LAYERS IS INSERTED!
!ELECTRICAL CONDUCTIVITY IN MHOS!
```

```
!RELATIVE MAGNETIC PERMEABILITY!
```

```
!RELATIVE ELECTRIC PERMITTIVITY!
```

```
!EACH LAYER THICKNESS IN METERS!
```

```

650 Beta(I,2)=Coef*SQR(Sqroot-1)      ! IMAG WAVE VECTOR (Gamma) IS CALC.!
660 NEXT I
670 Np=N+1
680 L=4*Np
690 Lp=L+1
700 Mu(0)=4*PI*1E-7
710 Epsilon(0)=8.8542E-12
720 Mu(Np)=4*PI*1E-7
730 Epsilon(Np)=8.8542E-12
740 Beta(0,1)=Beta0
750 Beta(0,2)=0
760 Beta(Np,1)=Beta0
770 Beta(Np,2)=0
780 E1=(Mu(0)/Epsilon(0))^.25*SQR(2*Power)
790 E12=E1^2
800 Deg=PI/180
810 Tck1=Thick(L1)
820 Tck2=Thick(L2)
830 Aye=1
840 I !
850 I !!! NOW WE START !!!!!
860 I !
870 FOR Thick1=Tck1 TO 9*Inc1+Tck1 STEP Inc1
880 Jay=1
890 Thick(L1)=Thick1
900 FOR Thick2=Tck2 TO 9*Inc2+Tck2 STEP Inc2
910 Thick(L2)=Thick2
920 FOR I=1 TO N
930 Z(I)=Z(I-1)+Thick(I)
940 NEXT I
950 IF Key<>1 THEN 1000
960 Shift=Z(N-1)
970 FOR I=0 TO N
980 Z(I)=Z(I)-Shift
990 NEXT I

```

!ELEC. CHARAC. EA. SIDE OF LAYERS!

!REAL Beta 0!  
!IMAGINARY Beta 0!

!CALCULATES Z's FOR THICKNESSES!

!SHIFTS AXIS IN CASE OF TRUNCATION!

```

1000 X=COS<Theda*Deg>
1010 Y=SIN<Theda*Deg>
1020 IF X=0 THEN X=1E-5
1030 IF Y=1 THEN Y=.999999999999999
1040 Sin2=Y^2
1050 Hlpara=2*E1*SQR(Epsilon(0))/Mu(0)>
1060 Hlpara=Hlpara*X
1070 Cothed(Np,1)=X
1080 Cothed(Np,2)=0
1090 Cothed(0,1)=X
1100 Cothed(0,2)=0
1110 Sithed(Np,1)=Y
1120 Sithed(Np,2)=0
1130 Sithed(0,1)=Y
1140 Sithed(0,2)=0
1150 ! !
1160 ! WE CALCULATE REAL AND IMAGINARY COS<Theda> AND SIN<Theda> !
1170 ! !
1180 FOR I=1 TO N
1190 Denom=(Beta(I,1)^2+Beta(I,2)^2)^2
1200 Pee=.5*(1-Beta(0,2)*Sin2*(Beta(I,1)^2-Beta(I,2)^2)/Denom)
1210 Que=Beta(0,2)*Sin2*(Beta(I,1)*Beta(I,2))/Denom
1220 X=SQR(Pee^2+Que^2)
1230 Cothed(I,1)=SQR(Pee*X)
1240 Cothed(I,2)=SQR(ABS(X-Pee))
1250 Sithed(I,1)=Beta(0,1)*Y*Beta(I,1)/(Beta(I,1)^2+Beta(I,2)^2)
1260 Sithed(I,2)=-Beta(0,1)*Y*Beta(I,2)/(Beta(I,1)^2+Beta(I,2)^2)
1270 Betcos(I,1)=Beta(I,1)*Cothed(I,1)-Beta(I,2)*Cothed(I,2) !REAL Beta x Cos<
Theda> !
1280 Betcos(I,2)=Beta(I,1)*Cothed(I,2)+Beta(I,1)*Cothed(I,1) !IMAG Beta x Cos<
Theda> !
1290 IF Betcos(I,1)*2(I)>75 THEN Betcos(I,1)=75/Z(I)
1300 IF Betcos(I,2)*2(I)>75 THEN Betcos(I,2)=75/Z(I)
1310 NEXT I

```

```

1320 ! !
1330 ! WE BEGIN TO CALCULATE THE COMPLEX MATRIX!
1340 ! !
1350 FOR I=1 TO 2*(N-Key)+1 STEP 2 ! WE ENTER ROWS BY BOUNDARY, 2 PER BOU
NDRY !
1360 K=(I-1)/2
1370 M=I-1
1380 R=I+1
1390 O=I+2
1400 X=-Z(K)*(Beta(K,1)*Cothed(K,2)+Beta(K,2)*Cothed(K,1))
1410 Y=Z(K)*(Beta(K,1)*Cothed(K,1)-Beta(K,2)*Cothed(K,2))
1420 P=K+1
1430 Xx=-Z(K)*(Beta(P,1)*Cothed(P,2)+Beta(P,2)*Cothed(P,1))
1440 Yy=Z(K)*(Beta(P,1)*Cothed(P,1)-Beta(P,2)*Cothed(P,2))
1450 IF X>170 THEN X=170 !X>170 IMPLIES A LAYER THICKNESS >170 SKIN DEPTHS!
1460 IF Xx>170 THEN Xx=170 !Xx>170 IMPLIES A LAYER THICKNESS >170 SKIN DEPTHS!
1470 ExpX=EXP(X)
1480 ExpXx=EXP(Xx)
1490 IF X<-170 THEN X=-170
1500 IF Xx<-170 THEN Xx=-170
1510 ExpMx=EXP(-X)
1520 ExpMxX=EXP(-Xx)
1530 CosY=COS(Y)
1540 SinY=SIN(Y)
1550 CosYy=COS(Yy)
1560 SinYy=SIN(Yy)
1570 Expr=ExpX*CosY
1580 Expi=ExpX*SinY
1590 Bcr=Beta(K,1)*Cothed(K,1)-Beta(K,2)*Cothed(K,2)
1600 Bci=Beta(K,1)*Cothed(K,2)+Beta(K,2)*Cothed(K,1)
1610 ! !
1620 ! WE CALCULATE THE (I,I-1) AND (I+1,I-1) COMPLEX MATRIX ELEMENTS!
1630 ! !
1640 IF I=1 THEN 1740

```

```

1650 Para(I,M,1)=Cothed(K,1)*Expr-Cothed(K,2)*Expi
1660 Para(I,M,2)=Cothed(K,1)*Expi+Cothed(K,2)*Expr
1670 Perp(I,M,1)=Expr
1680 Perp(I,M,2)=Expi
1690 Para(R,M,1)=(Beta(K,1)*Expr-Beta(K,2)*Expi)/Mu(K)
1700 Para(R,M,2)=(Beta(K,1)*Expi+Beta(K,2)*Expr)/Mu(K)
1710 Perp(R,M,1)=(Bcr*Expr-Bci*Expi)/Mu(K)
1720 Perp(R,M,2)=(Bcr*Expi+Bci*Expr)/Mu(K)
1730 ! !
1740 ! WE CALCULATE THE (I,I) AND (I+1,I) COMPLEX MATRIX ELEMENTS!
1750 ! !
1760 Expr=Expmx*Cosy
1770 Expi=-Expmx*Siny
1780 Para(I,1,1)=Cothed(K,1)*Expr-Cothed(K,2)*Expi
1790 Para(I,1,2)=Cothed(K,1)*Expi+Cothed(K,2)*Expr
1800 Perp(I,1,1)=Expr
1810 Perp(I,1,2)=Expi
1820 Para(R,1,1)=(Beta(K,1)*Expr-Beta(K,2)*Expi)/Mu(K)
1830 Para(R,1,2)=(Beta(K,1)*Expi+Beta(K,2)*Expr)/Mu(K)
1840 Perp(R,1,1)=(Bcr*Expr-Bci*Expi)/Mu(K)
1850 Perp(R,1,2)=(Bcr*Expi+Bci*Expr)/Mu(K)
1860 ! !
1870 ! WE CALCULATE THE (I,I+1) AND (I+1,I+1) COMPLEX MATRIX ELEMENTS!
1880 ! !
1890 Expr=Expxx*Cosyy
1900 Expi=Expxx*Sinyy
1910 Bcr=Beta(P,1)*Cothed(P,1)-Beta(P,2)*Cothed(P,2)
1920 Bci=Beta(P,1)*Cothed(P,2)+Beta(P,2)*Cothed(P,1)
1930 Para(I,R,1)=(Cothed(P,1)*Expr-Cothed(P,2)*Expi)
1940 Para(I,R,2)=(Cothed(P,1)*Expi+Cothed(P,2)*Expr)
1950 Perp(I,R,1)=Expr
1960 Perp(I,R,2)=Expi
1970 Para(R,R,1)=(Beta(P,1)*Expr-Beta(P,2)*Expi)/Mu(P)
1980 Para(R,R,2)=(Beta(P,1)*Expi+Beta(P,2)*Expr)/Mu(P)
1990 Perp(R,R,1)=(Bcr*Expr-Bci*Expi)/Mu(P)

```

```

2000 Perp(R,R,2)=- (Bcr*Expi+Bci*Expr)/Mu(P)
2010 ! !
2020 ! WE CALCULATE THE (I,I+2) AND (I+1,I+2) COMPLEX MATRIX ELEMENTS!
2030 ! !
2040 Expr=ExpmaxxCosyy
2050 Expi=-ExpmaxxSinyy
2060 IF I=2*N+1 THEN 2150
2070 Para(I,0,1)=- (Cothed(P,1)*Expr-Cothed(P,2)*Expi)
2080 Para(I,0,2)=- (Cothed(P,1)*Expi+Cothed(P,2)*Expr)
2090 Perp(I,0,1)=-Expr
2100 Perp(I,0,2)=-Expi
2110 Para(R,0,1)=- (Beta(P,1)*Expr-Beta(P,2)*Expi)/Mu(P)
2120 Para(R,0,2)=- (Beta(P,1)*Expi+Beta(P,2)*Expr)/Mu(P)
2130 Perp(R,0,1)=- (Bcr*Expr-Bci*Expi)/Mu(P)
2140 Perp(R,0,2)=- (Bcr*Expi+Bci*Expr)/Mu(P)
2150 NEXT I
2160 ! !
2170 ! COMPLEX MATRICES ARE EXPANDED INTO REAL MATRICES!
2180 ! !
2190 MAT Paraex=IDN(L,L)
2200 MAT Perpex=IDN(L,L)
2210 MAT Dum=IDN(L,L)
2220 FOR I=1 TO L/2-2*Key
2230 FOR J=I-2 TO I+2
2240 IF J<1 THEN 2300
2250 IF J>L/2-2*Key THEN 2300
2260 M=2*I
2270 R=2*J
2280 O=M-1
2290 P=R-1
2300 Paraex(O,P)=Para(I,J,1)
2310 Paraex(M,R)=Para(I,J,1)
2320 Paraex(M,P)=Para(I,J,2)
2330 Paraex(O,R)=-Para(I,J,2)
2340 Perpex(O,P)=Perp(I,J,1)

```

! FORMS AN IDENTITY MATRIX !

! LOADS 4 ELEMENTS FOR EACH COMPLEX ONE !  
! AVOIDS CYCLING THRU THE WHOLE MATRIX !

```

2350 Perpex(M,R)=Perp(I,J,1)
2360 Perpex(M,P)=Perp(I,J,2)
2370 Perpex(O,R)=-Perp(I,J,2)
2380 NEXT J
2390 NEXT I
2400 Parabx(1)=-E1*Cothd(0,1)
2410 Parabx(3)=-E1*(Beta0/Mu(0))
2420 Perpbx(1)=-E1
2430 Perpbx(3)=-E1*Cothd(0,1)*(Beta0/Mu(0))
2440 ! !
2450 ! AT THIS POINT WE ARE READY FOR THE MATRIX SOLUTION!
2460 ! !
2470 MAT Dum=INV(Parabx)
2480 FOR I=1 TO L
2490 Epara(I)=Dum(I,1)*Parabx(1)+Dum(I,3)*Parabx(3)
2500 NEXT I
2510 MAT Dum=INV(Perpex)
2520 FOR I=1 TO L
2530 Eperp(I)=Dum(I,1)*Perpbx(1)+Dum(I,3)*Perpbx(3)
2540 NEXT I
2550 ! !
2560 ! THE MAG. OF THE ELECTRIC FIELDS ARE NOW CALCULATED IN Epara AND Eperp !
2570 ! !
2580 ! WE NOW CALCULATE THE VALUE OF J THROUGHOUT THE N LAYERS!
2590 ! !
2600 J=3
2610 FOR I=1 TO N
2620 Z=Z(I-1)
2630 FOR K=1 TO 50
2640 Zinc=(Z(I)-Z(I-1))/49
2650 U=EXP(-Betcos(I,2)*Z)
2660 Rv=COS(Betcos(I,1)*Z)
2670 Iv=SIN(Betcos(I,1)*Z)
2680 X=EXP(Betcos(I,2)*Z)
2690 Ry=Rv

```

```

2700 Iy=-Iv
2710 Rt=U*(Epara(J)*Rv-Epara(J+1)*Iv)
2720 It=U*(Epara(J)*Iv+Epara(J+1)*Rv)
2730 Ru=X*(Epara(J+2)*Ry-Epara(J+3)*Iy)
2740 Iv=X*(Epara(J+2)*Iy+Epara(J+3)*Ry)
2750 Rf=Rt+Rv
2760 If=It+Iv
2770 Rg=Rt-Rv
2780 Ig=It-Iv
2790 Ppara(I,K)=Sigma(I)*((Rf^2+If^2)*(Cothed(I,1)^2+Cothed(I,2)^2)+(Rg^2+Ig^2)
*(Sithed(I,1)^2+Sithed(I,2)^2))
2800 Jpara(I,K)=Sigma(I)*SQR((Rf^2+If^2)*(Cothed(I,1)^2+Cothed(I,2)^2)+(Rg^2+Ig
^2)*(Sithed(I,1)^2+Sithed(I,2)^2))
2810 IF K=1 THEN 2860
2820 Alpha=-LOG(Jpara(I,K)/Jpara(I,K-1))/Zinc
2830 IF Alpha=0 THEN Alpha=1E-10
2840 Coef=Jpara(I,K-1)*EXP(Alpha*(Z-Zinc))
2850 Jparat(I)=Jparat(I)-Coef/Alpha*EXP(-Alpha*Z)*(EXP(-Alpha*Zinc)-1)
2860 Rt=U*(Eperp(J)*Rv-Eperp(J+1)*Iv)
2870 It=U*(Eperp(J)*Iv+Eperp(J+1)*Rv)
2880 Ru=X*(Eperp(J+2)*Ry-Eperp(J+3)*Iy)
2890 Iv=X*(Eperp(J+2)*Iy+Eperp(J+3)*Ry)
2900 Pperp(I,K)=Sigma(I)*((Rt+Rv)^2+(It+Iv)^2)
2910 Jperp(I,K)=Sigma(I)*SQR((Rt+Rv)^2+(It+Iv)^2)
2920 IF K=1 THEN 2970
2930 Alpha=-LOG(Jperp(I,K)/Jperp(I,K-1))/Zinc
2940 IF Alpha=0 THEN Alpha=1E-10
2950 Coef=Jperp(I,K-1)*EXP(Alpha*(Z-Zinc))
2960 Jperpt(I)=Jperpt(I)-Coef/Alpha*EXP(-Alpha*Z)*(EXP(-Alpha*Zinc)-1)
2970 Z=Z+Zinc
2980 NEXT K
2990 J=J+4
3000 NEXT I
3010 FOR I=1 TO N

```

```

3020 Jao=Jao+Jparat(I)
3030 Jeo=Jeo+Jperpt(I)
3040 NEXT I
3050 !
3060 ! THE PARALLEL AND PERPENDICULAR CURRENT DENSITIES ARE NOW CALCULATED!
3070 !
3080 Jpapt(Aye,Jay)=(Jao-Jparat(N))/Jao*100
3090 Jperpt(Aye,Jay)=(Jeo-Jperpt(N))/Jeo*100
3100 !
3110 ! WE NOW FIND THE SURF. TEMP. Uo FOR NO LOSSES ON Zn BOUNDARY!
3120 !
3130 Papara=Power-.5*SQR(Epslon(0)/Mu(0))*(Epara(1)^2+Epara(2)^2+Epara(L-1)^2+E
para(L)^2)
3140 Paperp=Power-.5*SQR(Epslon(0)/Mu(0))*(Eperp(1)^2+Eperp(2)^2+Eperp(L-1)^2+E
perp(L)^2)
3150 ! WE NOW DO A NEWTON ALGORITHM TO FIND THE SURFACE TEMP., Uo!
3160 Uopa=Uair
3170 Uope=Uair
3180 J=0
3190 Fupara=15/H^Del*ABS(Uopa-Uair)^(Del+1)+Fe*Gamma*(Uopa^4-Uair^4)-Papara
3200 Fuperp=15/H^Del*ABS(Uope-Uair)^(Del+1)+Fe*Gamma*(Uope^4-Uair^4)-Paperp
3210 Fupap=(Del+1)*(15/H^Del)*ABS(Uopa-Uair)^(Del+4)*Fe*Gamma*Uopa^3
3220 Fuperp=(Del+1)*(15/H^Del)*ABS(Uope-Uair)^(Del+4)*Fe*Gamma*Uope^3
3230 Uopal=Uopa-Fupara/Fupap
3240 Uopel=Uope-Fuperp/Fuperp
3250 IF (ABS(Uopa-Uopal)<1E-8) AND (ABS(Uope-Uopel)<1E-8) THEN 3310
3260 Uopa=Uopal
3270 Uope=Uopel
3280 J=J+1
3290 IF J=100 THEN 3310
3300 GOTO 3190
3310 IF J>100 THEN PRINT "SURFACE TEMP. WOULD NOT CONVERGE."
3320 Uopara(Aye,Jay)=Uopa-Uair
3330 Uoperp(Aye,Jay)=Uope-Uair

```

```
3340 PRINT "Aye=",Aye," Jay=",Jay>
3350 PRINT "Uopa=",Uopa-Uair," Papct=",Jpapct(Aye,Jay>
3360 Jay=Jay+1
3370 NEXT Thick2
3380 Aye=Aye+1
3390 NEXT Thick1
3400 IF Second<>2 THEN 3430
3410 MAT Uoperp=X
3420 MAT Jpepct=Y
3430 MAT PRINT #1;Uopara,Uoperp,Jpapct,Jpepct
3440 ! CONDUCTING LAST LAYER IS IN Uopara AND Jpapct !
3450 STOP
```

## APPENDIX H

## COMPUTER PROGRAM

The name of this program is "CONTOR". It will plot and smooth contour lines for an arbitrary matrix of values. It will do linear smoothing, circular or parabolic smoothing. The matrix data is read from a data file named "X-Data". Plot labeling is accomplished manually when the flashing cursor appears on the 9845 CRT. The only inputs are the number of rows and columns of the input matrix.

```

10 ! THE NAME OF THIS PROGRAM IS CONTOUR !
20 ! IT WILL PLOT AND SMOOTH CONTOURS FOR AN ARBITRARY MATRIX !
30 ! IT DOES A SECOND ORDER CURVE FIT BETWEEN POINTS !
40 ! THE DATA MATRIX MUST BE INPUTED INTO THE X MATRIX !
50 ! THE DATA IS TO BE READ FROM THE 'X-Data' FILE IN LOCATION T14!
60 GCLEAR
70 EXIT GRAPHICS
80 OPTION BASE 1
90 INPUT "ENTER THE HEIGHT/WIDTH RATIO OF PRINTOUT.",Ratio
100 INTEGER I,J,K,L,L1,L2,M,N,Center,Up,Down,Left,Right
110 SHORT X(64,64),Fit(180,180),Coef(3,3),Inv(3,3),B(3),Abc(3),Ctest(180)
120 ASSIGN #1 TO "X-Data:T14"
130 INPUT "ENTER NUMBER OF ROWS OF INPUT MATRIX.",M
140 INPUT "ENTER NUMBER OF COLUMNS OF INPUT MATRIX.",N
150 REDIM X(M,N)
160 MAT READ #1;X
170 Devx=18
180 Devy=18
190 INPUT "ENTER 1 FOR PARABOLIC FIT, 2 CIRCLE FIT, 3 LINEAR.",Type
200 FOR I=1 TO M
210   X=1
220   K=1
230   L=(I-1)*179/(M-1)+1
240   PRINT USING 250;I
250   IMAGE "I=",DD
260   FOR J=1 TO N-2
270     X1=(J-1)*179/(N-1)+1
280     X2=J*179/(N-1)+1
290     X3=(J+1)*179/(N-1)+1
300     Y1=X(I,J)
310     Y2=X(I,J+1)
320     Y3=X(I,J+2)
330     IF Type<>1 THEN 540
340     Coef(1,1)=X1^2

```

! PARABOLIC SMOOTHING!

```

350 Coef(1,2)=X1
360 Coef(1,3)=1
370 Coef(2,1)=X2^2
380 Coef(2,2)=X2
390 Coef(2,3)=1
400 Coef(3,1)=X3^2
410 Coef(3,2)=X3
420 Coef(3,3)=1
430 B(1)=Y1
440 B(2)=Y2
450 B(3)=Y3
460 MAT Inv=INV(Coef)
470 MAT Abc=Inv*B
480 Fit(L,K)=Abc(1)*X^2+Abc(2)*X+Abc(3)
490 IF Fit(L,K)>Max THEN Max=Fit(L,K)
500 X=X+1
510 K=K+1
520 IF X<X2 THEN 480
530 GOTO 860
540 IF Type<>2 THEN 770
550 MAT Coef=IDN
560 Coef(1,1)=2*(X2-X1)
570 Coef(1,2)=2*(Y2-Y1)
580 Coef(2,1)=2*(X2-X3)
590 Coef(2,2)=2*(Y2-Y3)
600 B(1)=X2^2+Y2^2-X1^2-Y1^2
610 B(2)=X2^2+Y2^2-X3^2-Y3^2
620 B(3)=0
630 MAT Inv=INV(Coef)
640 MAT Abc=Inv*B
650 C2=(X1-Abc(1))^2+(Y1-Abc(2))^2
660 Sign=1
670 Slop12=(Y1-Y2)/(X1-X2)
680 Cons12=(X1*Y2-X2*Y1)/(X1-X2)
690 Y3prim=Slop12*X3+Cons12

```

! CIRCULAR SMOOTHING!

```

700 IF Y3-Y3prim>0 THEN Sign=-1
710 Fit(L,K)=Abc(2)+Sign*SQR(C2-(X-Abc(1))^2)
720 IF Fit(L,K)>Max THEN Max=Fit(L,K)
730 X=X+1
740 K=K+1
750 IF X<X2 THEN 710
760 GOTO 860
770 IF Type<>3 THEN 860
780 Slope=(Y1-Y2)/(X1-X2)
790 Const=(X1*Y2-X2*Y1)/(X1-X2)
800 Fit(L,K)=Slope*X+Const
810 IF Fit(L,K)>Max THEN Max=Fit(L,K)
820 X=X+1
830 K=K+1
840 IF X<X2 THEN 800
850 GOTO 860
860 NEXT J
870 IF Type<>1 THEN 930
880 Fit(L,K)=Abc(1)*X^2+Abc(2)*X+Abc(3)
890 IF Fit(L,K)>Max THEN Max=Fit(L,K)
900 X=X+1
910 K=K+1
920 IF K<=180 THEN 880
930 IF Type<>2 THEN 990
940 Fit(L,K)=Abc(2)+Sign*SQR(C2-(X-Abc(1))^2)
950 IF Fit(L,K)>Max THEN Max=Fit(L,K)
960 X=X+1
970 K=K+1
980 IF K<=180 THEN 940
990 IF Type<>3 THEN 1050
1000 Fit(L,K)=Slope*X+Const
1010 IF Fit(L,K)>Max THEN Max=Fit(L,K)
1020 X=X+1
1030 K=K+1

```

! LINEAR SMOOTHING !

```

1040 IF K<=180 THEN 1000
1050 NEXT I .
1060 ! !
1070 ! THE COLUMNS ARE EXPANDED INTO 180 COLUMNS; NOW WE EXPAND THE ROWS !
1080 !
1090 FOR J=1 TO 180
1100 PRINT USING 1110;J
1110 IMAGE "WE ARE ON COLUMN ",DDD
1120 X=180
1130 K=1
1140 FOR I=1 TO M-2
1150 L=(I-1)*179/(M-1)+1
1160 L1=I*179/(M-1)+1
1170 L2=(I+1)*179/(M-1)+1
1180 X1=181-L
1190 X2=181-L1
1200 X3=181-L2
1210 Y1=Fit(L,J)
1220 Y2=Fit(L1,J)
1230 Y3=Fit(L2,J)
1240 IF Type<>1 THEN 1450
1250 Coef(1,1)=X1^2
1260 Coef(1,2)=X1
1270 Coef(1,3)=1
1280 Coef(2,1)=X2^2
1290 Coef(2,2)=X2
1300 Coef(2,3)=1
1310 Coef(3,1)=X3^2
1320 Coef(3,2)=X3
1330 Coef(3,3)=1
1340 B(1)=Y1
1350 B(2)=Y2
1360 B(3)=Y3
1370 MAT Inv=INV(Coef)
1380 MAT Abc=Inv*B

```

! PARABOLIC SMOOTHING !

```

1390 Fit(K,J)=Abc(1)*X^2+Abc(2)*X+Abc(3)
1400 IF Fit(K,J)>Max THEN Max=Fit(K,J)
1410 X=X-1
1420 K=K+1
1430 IF X2<X THEN 1390
1440 GOTO 1770
1450 IF Type<>2 THEN 1600
1460 MAT Coef=IDN
1470 Coef(1,1)=2*(X2-X1)
1480 Coef(1,2)=2*(Y2-Y1)
1490 Coef(2,1)=2*(X2-X3)
1500 Coef(2,2)=2*(Y2-Y3)
1510 B(1)=X2^2+Y2^2-X1^2-Y1^2
1520 B(2)=X2^2+Y2^2-X3^2-Y3^2
1530 B(3)=0
1540 MAT Inv=INV(Coef)
1550 MAT Abc=Inv*B
1560 C2=(X1-Abc(1))^2+(Y1-Abc(2))^2
1570 Sign=1
1580 Slop12=(Y1-Y2)/(X1-X2)
1590 Cons12=(X1*Y2-X2*Y1)/(X1-X2)
1600 Y3prin=Slop12*X3+Cons12
1610 IF Y3-Y3prin>0 THEN Sign=-1
1620 Fit(K,J)=Abc(2)+Sign*SQR(C2-(X-Abc(1))^2)
1630 IF Fit(K,J)>Max THEN Max=Fit(K,J)
1640 X=X-1
1650 K=K+1
1660 IF X2<X THEN 1620
1670 GOTO 1770
1680 IF Type<>3 THEN 1770
1690 Slope=(Y1-Y2)/(X1-X2)
1700 Const=(X1*Y2-X2*Y1)/(X1-X2)
1710 Fit(K,J)=Slope*X+Const
1720 IF Fit(K,J)>Max THEN Max=Fit(K,J)

```

I CIRCULAR SMOOTHING I

I LINEAR SMOOTHING I

```

1730 X=X-1
1740 K=K+1
1750 IF X2<X THEN 1710
1760 GOTO 1770
1770 NEXT I
1780 IF Type<>1 THEN 1840
1790 Fit(K,J)=Abc(1)*X^2+Abc(2)*X+Abc(3)
1800 IF Fit(K,J)>Max THEN Max=Fit(K,J)
1810 X=X-1
1820 K=K+1
1830 IF K<=100 THEN 1790
1840 IF Type<>2 THEN 1900
1850 Fit(K,J)=Abc(2)+Sign*SQR(C2-(X-Abc(1))^2)
1860 IF Fit(K,J)>Max THEN Max=Fit(K,J)
1870 X=X-1
1880 K=K+1
1890 IF K<=100 THEN 1850
1900 IF Type<>3 THEN 1950
1910 Fit(K,J)=Slope*X+Const
1920 X=X-1
1930 K=K+1
1940 IF K<=100 THEN 1910
1950 NEXT J
1960 GCLEAR
1970 GRAPHICS
1980 LINE TYPE 1
1990 K=10+Ratio*90
2000 IF Ratio>=1 THEN 2030
2010 LOCATE 10,100,10,K
2020 GOTO 2040
2030 LOCATE 10,K,10,100
2040 SCALE 1,100,1,100
2050 FRAME
2060 LINE TYPE 2

```

```

2070 FOR I=2 TO 179
2080 FOR J=2 TO 179
2090 Center=10*Fit(I,J)/Max
2100 Up=10*Fit(I-1,J)/Max
2110 Down=10*Fit(I+1,J)/Max
2120 Left=10*Fit(I,J-1)/Max
2130 Right=10*Fit(I,J+1)/Max
2140 IF Center<>Left THEN DRAW J-1,181.5-I
2150 IF Center<>Up THEN DRAW J-.5,182-I
2160 IF Center<>Right THEN DRAW J,181.5-I
2170 IF Center<>Down THEN DRAW J-.5,181-I
2180 NEXT J
2190 NEXT I
2200 BEEP
2210 LINE TYPE 1
2220 LETTER
2230 PAUSE
2240 GOTO 190
2250 STOP

```

## APPENDIX I

## COMPUTER PROGRAM

The name of this program is "EPSLON". It calculates the per cent of reflected to incident power and plots it versus relative permittivity for the layer. The input variables are the number of layers, the maximum permittivity to be considered, the incident frequency, the incident angle, and the measured reflectivity.

```

10  ! THE NAME OF THIS PROGRAM IS 'EPSILON' !
20  ! IT CALCULATES THE PER CENT OF REFLECTED POWER TO INCIDENT POWER AND
    PLOTS IT VERSUS RELATIVE EPSILON!
30  INTEGER I,J,K,L,M,N,O,P,Q,R,Lp,Np
40  DIM Beta(11,2),Z(11),Cothd(12,2),Sigma(10),Mu(12),Epsilon(12),Para(22,22,2
    ),Perp(22,22,2),Paraex(44,44),Perpex(44,44),Sithd(12,2),Betcos(10,2)
50  DIM Parabx(44),Perpbx(44),Epara(44),Eperp(44),Dum(44,44),Epsiln(102),Percn
    t(102)
60  INPUT "Enter the Number of Layers not to Exceed 10.",N
70  INPUT "Enter Relative Epsilon Max.",Epsmax
80  INPUT "Enter the Incident Frequency in Gigahertz.",F
90  INPUT "Enter Theda.",Theda
100 INPUT "Enter the Measured Reflectivity (%)",Pin
110 Power=10
120 Omega=2*PI*F*1E9
130 Beta0=Omega/2.998E8
140 Beta02=Beta0^2
150 Power=10*Power
160 FOR I=1 TO N
170 DISP "Sigma(";I;")";
180 INPUT Sigma(I)
190 IF Sigma(I)=0 THEN Sigma(I)=1E-12
200 DISP "Mu(";I;")";
210 INPUT Mu
220 Mu(I)=Mu*4*PI*1E-7
230 IF I=1 THEN 270
240 DISP "Epsilon(";I;")";
250 INPUT Epsilon
260 Epsilon(I)=Epsilon*8.8542E-12
270 DISP "Thickness(";I;")";
280 INPUT Thick
290 Delta=SOR(2/(Omega*Mu(I)*Sigma(I)))
300 IF Thick<23*Delta THEN 370
310 Thick=23*Delta
320 N=I

```

!ANGULAR FREQUENCY IS CALCULATED!  
 !FREE SPACE WAVE VECTOR IS CALCULATED!  
 !THE WAVE VECTOR IS SQUARED!  
 !CONVERTS TO WATT/METER^2!  
 !ELEC. PROPERTIES OF LAYERS IS INSERTED!  
 !ELECTRICAL CONDUCTIVITY IN MHOS!  
 !RELATIVE MAGNETIC PERMEABILITY!  
 !RELATIVE ELECTRIC PERMITTIVITY!  
 !EACH LAYER THICKNESS IN METERS!

```

330 Key=1
340 PRINT USING 350;I,I,I,Thick
350 IMAGE "LAYER ",DD," WAS THICKER THAN 23 SKIN DEPTHS. THE PROBLEM IS TRUNCA
    TED AT ",DD," LAYERS, WITH LAYER ",DD," ",D.DDE," METERS THICK."
360 PRINT
370 Z(I)=Z(I-1)+Thick      !Z(n) IS CALCULATED FROM THICKNESSES!
380 IF I=1 THEN 430
390 Coef=0omega*SQR(Mu(I)*Epsilon(I)/2)
400 Sqrroot=SQR(1+(Sigma(I)/(Omega*Epsilon(I))^2)
410 Beta(I,1)=Coef*SQR(1+Sqrroot)      !REAL WAVE VECTOR (Alpha) IS CALC.!
420 Beta(I,2)=Coef*SQR(Sqrroot-1)      !IMAG WAVE VECTOR (Gamma) IS CALC.!
430 NEXT I
440 IF Key<>1 THEN 490
450 Shift=Z(N-1)
460 FOR I=0 TO N
470 Z(I)=Z(I)-Shift
480 NEXT I
490 Count=1
500 FOR Eps=1 TO Epsmax STEP (Epsmax-1)/100
510 PRINT Eps
520 Epsilon(1)=Eps*8.8542E-12
530 Coef=0omega*SQR(Mu(1)*Epsilon(1)/2)
540 Sqrroot=SQR(1+(Sigma(1)/(Omega*Epsilon(1))^2)
550 Beta(1,1)=Coef*SQR(1+Sqrroot)      !REAL WAVE VECTOR (Alpha) IS CALC.!
560 Beta(1,2)=Coef*SQR(Sqrroot-1)      !IMAG WAVE VECTOR (Gamma) IS CALC.!
570 Np=N+1
580 L=4*Np
590 Lp=L+1
600 Mu(0)=4*PI*1E-7
610 Epsilon(0)=8.8542E-12
620 Mu(Np)=4*PI*1E-7
630 Epsilon(Np)=8.8542E-12
640 Beta(0,1)=Beta0
650 Beta(0,2)=0
660 Beta(Np,1)=Beta0
    !ELEC. CHARAC. EA. SIDE OF LAYERS!
    !REAL Beta 0!
    !IMAGINARY Beta 0!

```

```

670 Beta(Np,2)=0
680 E1=(Mu(0)/Epsilon(0))^.25*SQR(2*Power)
690 E12=E1^2
700 Deg=P1/180
710 ! !
720 ! ! ! ! ! NOW WE START ! ! ! ! !
730 ! !
740 X=COS(Theda*Deg)
750 Y=SIN(Theda*Deg)
760 IF X=0 THEN X=1E-5
770 IF Y=1 THEN Y=.9999999999999
780 Sin2=Y^2
790 H1perp=H1para*X
800 Cothed(Np,1)=X
810 Cothed(Np,2)=0
820 Cothed(0,1)=X
830 Cothed(0,2)=0
840 S1thed(Np,1)=Y
850 S1thed(Np,2)=0
860 S1thed(0,1)=Y
870 S1thed(0,2)=0
880 ! !
890 ! WE CALCULATE REAL AND IMAGINARY COS(Theda) AND SIN(Theda) !
900 ! !
910 FOR I=1 TO N
920 Denom=(Beta(I,1)^2+Beta(I,2)^2)^2
930 Pee=.5*(1-Beta02*SIN2*(Beta(I,1)^2-Beta(I,2)^2)/Denom)
940 Que=Beta02*SIN2*Beta(I,1)*Beta(I,2)/Denom
950 X=SQR(Pee^2+Que^2)
960 Cothed(I,1)=SQR(Pee+X)
970 Cothed(I,2)=SQR(ABS(X-Pee))
980 S1thed(I,1)=Beta(0,1)*Y+Beta(I,1)/(Beta(I,1)^2+Beta(I,2)^2)
990 S1thed(I,2)=-Beta(0,1)*Y+Beta(I,2)/(Beta(I,1)^2+Beta(I,2)^2)
1000 Betcos(I,1)=Beta(I,1)*Cothed(I,1)-Beta(I,2)*Cothed(I,2) !REAL Beta x Cos(
Theda)!

```

```

1010 Betcos(I,2)=Beta(I,1)*Cothed(I,2)+Beta(I,1)*Cothed(I,1) !IMAG Beta x Cos(
Theda)!
1020 IF Betcos(I,1)*Z(I)>75 THEN Betcos(I,1)=75/Z(I)
1030 IF Betcos(I,2)*Z(I)>75 THEN Betcos(I,2)=75/Z(I)
1040 NEXT I
1050 ! !
1060 ! WE BEGIN TO CALCULATE THE COMPLEX MATRIX!
1070 ! !
1080 FOR I=1 TO 2*(N-Key)+1 STEP 2 ! WE ENTER ROWS BY BOUNDARY, 2 PER
BOUNDARY !
1090 K=(I-1)/2
1100 M=I-1
1110 R=I+1
1120 O=I+2
1130 X=-Z(K)*(Beta(K,1)*Cothed(K,2)+Beta(K,2)*Cothed(K,1))
1140 Y=Z(K)*(Beta(K,1)*Cothed(K,1)-Beta(K,2)*Cothed(K,2))
1150 P=K+1
1160 Xx=-Z(K)*(Beta(P,1)*Cothed(P,2)+Beta(P,2)*Cothed(P,1))
1170 Yy=Z(K)*(Beta(P,1)*Cothed(P,1)-Beta(P,2)*Cothed(P,2))
1180 IF X>170 THEN X=170 !X>170 IMPLIES A LAYER THICKNESS >170 SKIN DEPTHS!
1190 IF Xx>170 THEN Xx=170 !Xx>170 IMPLIES A LAYER THICKNESS >170 SKIN DEPTHS!
1200 ExpX=EXP(X)
1210 ExpXX=EXP(Xx)
1220 IF X<-170 THEN X=-170
1230 IF Xx<-170 THEN Xx=-170
1240 ExpXX=EXP(-X)
1250 ExpXX=EXP(-Xx)
1260 CosY=COS(Y)
1270 Siny=SIN(Y)
1280 Cosyy=COS(Yy)
1290 Sinyy=SIN(Yy)
1300 Expr=ExpX*CosY
1310 Expi=ExpX*Siny
1320 Bcr=Beta(K,1)*Cothed(K,1)-Beta(K,2)*Cothed(K,2)
1330 Bci=Beta(K,1)*Cothed(K,2)+Beta(K,2)*Cothed(K,1)
!Bcr IMPLIES THE REAL PART OF Beta*cos(Theda)!
!Bci IMPLIES THE IMAG PART OF Beta*cos(Theda)!

```

```

1340 ! !
1350 ! WE CALCULATE THE <I,I-1> AND <I+1,I-1> COMPLEX MATRIX ELEMENTS!
1360 ! !
1370 IF I=1 THEN 1430
1380 Perp(I,M,1)=Expr
1390 Perp(I,M,2)=Expi
1400 Perp(R,M,1)=(Bcr*Expr-Bci*Expi)/Mu(K)
1410 Perp(R,M,2)=(Bcr*Expi+Bci*Expr)/Mu(K)
1420 ! !
1430 ! WE CALCULATE THE <I,I> AND <I+1,I> COMPLEX MATRIX ELEMENTS!
1440 ! !
1450 Expr=ExpmxxCosy
1460 Expi=-ExpmxxSiny
1470 Perp(I,I,1)=Expr
1480 Perp(I,I,2)=Expi
1490 Perp(R,I,1)=-(Bcr*Expr-Bci*Expi)/Mu(K)
1500 Perp(R,I,2)=-(Bcr*Expi+Bci*Expr)/Mu(K)
1510 ! !
1520 ! WE CALCULATE THE <I,I+1> AND <I+1,I+1> COMPLEX MATRIX ELEMENTS!
1530 ! !
1540 Expr=ExpxxxCosyy
1550 Expi=ExpxxSinyy
1560 Bcr=Beta(P,1)*Cothed(P,1)-Beta(P,2)*Cothed(P,2)
1570 Bci=Beta(P,1)*Cothed(P,2)+Beta(P,2)*Cothed(P,1)
1580 Perp(I,R,1)=Expr
1590 Perp(I,R,2)=-Expi
1600 Perp(R,R,1)=-(Bcr*Expr-Bci*Expi)/Mu(P)
1610 Perp(R,R,2)=-(Bcr*Expi+Bci*Expr)/Mu(P)
1620 ! !
1630 ! WE CALCULATE THE <I,I+2> AND <I+1,I+2> COMPLEX MATRIX ELEMENTS!
1640 ! !
1650 Expr=ExpmxxCosyy
1660 Expi=-ExpmxxSinyy
1670 IF I=2*N+1 THEN 1720
1680 Perp(I,0,1)=Expr
1690 Perp(I,0,2)=-Expi
1700 Perp(R,0,1)=(Bcr*Expr-Bci*Expi)/Mu(P)

```

```

1710 Perp(R,0,2)=(Bcr*Expi+Bci*Expr)/Mu(P)
1720 NEXT I
1730 ! !
1740 ! COMPLEX MATRICES ARE EXPANDED INTO REAL MATRICES!
1750 ! !
1760 MAT Perpex=IDN(L,L)
1770 FOR I=1 TO L/2-2*Key
1780 FOR J=I-2 TO I+2
1790 IF J<1 THEN 1890
1800 IF J>L/2-2*Key THEN 1890
1810 M=2*I
1820 R=2*J
1830 O=M-1
1840 P=R-1
1850 Perpex(O,P)=Perp(I,J,1)
1860 Perpex(M,R)=Perp(I,J,1)
1870 Perpex(M,P)=Perp(I,J,2)
1880 Perpex(O,R)=-Perp(I,J,2)
1890 NEXT J
1900 NEXT I
1910 Perpbx(1)=-E1
1920 Perpbx(3)=-E1*Cothd(0,1)*(Beta0/Mu(0))
1930 ! !
1940 ! AT THIS POINT WE ARE READY FOR THE MATRIX SOLUTION!
1950 ! !
1960 MAT Dum=INV(Perpex)
1970 FOR I=1 TO L
1980 Eperp(I)=Dum(I,1)*Perpbx(1)+Dum(I,3)*Perpbx(3)
1990 NEXT I
2000 ! !
2010 ! THE MAG. OF THE ELECTRIC FIELDS ARE NOW CALCULATED IN Epara AND Eperp !
2020 ! !
2030 Epsiln(Count)=Eps
2040 Percent(Count)=(Eperp(1)^2+Eperp(2)^2)/E1^2*100

```

```

2050 IF (Percent(Count)>Pin-.5) AND (Percent(Count)<Pin+.5) THEN Xxx=Eps
2060 IF (Percent(Count)>Pin-.5) AND (Percent(Count)<Pin+.5) THEN Yyy=Percent(Count
)
2070 Count=Count+1
2080 NEXT Eps
2090 ! !
2100 ! WE BEGIN THE GRAPHICS PORTION HERE !
2110 ! !
2120 GRAPHICS
2130 CSIZE 2.5,9/15,0
2140 LINE TYPE 1
2150 LOCATE 15,115,15,95
2160 SCALE 1,Epsmax,0,100
2170 LOCATE 14,115,14,95
2180 Xtick=(Epsmax-1)/100
2190 AXES Xtick,1,1,0,10,10
2200 MOVE Epslin(1),Percent(1)
2210 FOR I=1 TO 100
2220 DRAW Epslin(I),Percent(I)
2230 NEXT I
2240 LINE TYPE 3
2250 MOVE 1,Pin
2260 DRAW Epsmax,Pin
2270 LINE TYPE 1
2280 ! !
2290 ! PLOTS ARE DRAWN NOW LABELING IS INSERTED !
2300 ! !
2310 MOVE .35*(Epsmax-1)+1,-7.5
2320 CSIZE 3,9/15,0
2330 LABEL "Sample Epsilon (relative)"
2340 MOVE 1-.1*(Epsmax-1),10
2350 LDIR PI/2
2360 LABEL "Reflectivity in Per Cent"
2370 LDIR 0
2380 MOVE 1-.06*(Epsmax-1),-1.5

```

```

2390 LABEL 0
2400 FOR I=0 TO 100 STEP 10
2410 IF I=100 THEN 2470
2420 MOVE 1-.06*(Epsmax-1),8.5+I
2430 LABEL USING 2440;10+I
2440 IMAGE DDD
2450 J=I/20-.1
2460 IF I/20-J>0 THEN 2520
2470 MOVE 1+I/100*(Epsmax-1),-2
2480 LOG 6
2490 LABEL USING 2500;I/100*(Epsmax-1)+1
2500 IMAGE DD.D
2510 LOG 1
2520 NEXT I
2530 CSIZE 4.2,9/15,0
2540 MOVE 1,-14
2550 LABEL USING 2560;N
2560 IMAGE DD,"-LAYER ELECTROMAGNETIC WAVE INTERACTION "
2570 CSIZE 3,9/15,0
2580 LETTER
2590 EXIT GRAPHICS
2600 STOP

```

!LABEL Y AXIS!

!LABEL X AXIS!



END

DATE  
FILMED

8-83

DT